AN ABSTRACT OF THE DISSERTATION OF

Dojung Kim for the degree of Doctor of Philosophy in Pharmacy presented on March 2, 2004.

Title: Studies on Isoprenoid Biosynthesis in *Euglena gracilis*

Redacted for privacy

Abstract approved:_____

Philip J. Proteau

This dissertation describes studies of isoprenoid biosynthesis in the phytoflagellate *Euglena gracilis*. Elucidation of a novel isoprenoid pathway, the 2-*C*-methyl-D-erythritol-4-phosphate (MEP) pathway, in addition to the generally known mevalonate (MVA) pathway, led to extensive exploration of the distribution of both pathways in a variety of organisms. To date, photosynthetic eukaryotes have been known to possess both pathways in separate compartments, such as the cytosol and chloroplasts. They are able to utilize the MVA pathway to produce cytosolic isoprenoids such as sterols and the MEP pathway to synthesize phytol and carotenoids in the chloroplasts. *Euglena gracilis*, however, was regarded as the only photosynthetic eukaryote in which the MEP pathway was not detected.

In this dissertation, isoprenoid biosynthesis in *E. gracilis* strain *Z* was investigated using incubation experiments with the labeled precursors [1-^{13}C]-glucose, [5-$^{2}H_2$]-deoxy-D-xylulose, [U-$^{13}C_6$]-glucose, [1,2-$^{13}C_2$]-acetate, [methyl-^{13}C]-methionine, [2-^{13}C]-leucine, [1-^{13}C]-butyric acid, [1,2,3,4-$^{13}C_4$]-acetoacetyl-*N*-acetylcysteamine, [1,2,3,4-$^{13}C_4$]-dimethylacrylic acid, 3-[methyl-$^{2}H_3$]-3-butenoic acid, 3-[methyl-$^{2}H_3$]-3-butenoyl-*N*-acetylcysteamine, [2-^{13}C]-malonic acid, [1-^{13}C-2-$^{2}H_3$]-acetate, and [2-^{13}C-2-$^{2}H_3$]-acetate. Several isoprenoid compounds were analyzed, such as carotenoids (β-carotene and diadinoxanthin), phytol, α-tocopherol and ergosterol. These experiments provided new findings in contrast to previous results, which are: (1) *E. gracilis* does indeed possess the MEP pathway and utilizes both the MVA and the

MEP pathways to produce isoprenoid compounds, especially carotenoids, and (2) phytol appears to be synthesized by a polyketide-type pathway, rather than an isoprenoid pathway.

Therefore, the existence of the MEP pathway to isoprenoids in *E. gracilis* is first described in this dissertation. Also strong evidence is provided that phytol biosynthesis in *E. gracilis* is not via an isoprenoid pathway, but rather by a polyketide-type pathway. Further studies will be necessary to explore the details of this unprecedented route to phytol.

Studies on Isoprenoid Biosynthesis in *Euglena gracilis*

by
Dojung Kim

A DISSERTATION

submitted to

Oregon State University

in partial fulfillment of
the requirements for the
degree of

Doctor of Philosophy

Presented March 2, 2004
Commencement June 2004

Doctor of Philosophy dissertation of Dojung Kim presented on March 2, 2004.

APPROVED:

Redacted for privacy

Major Professor, representing Pharmacy

Redacted for privacy

Dean of the College of Pharmacy

Redacted for privacy

Dean of the Graduate School

I understand that my dissertation will become part of the permanent collection of Oregon State University libraries. My signature below authorizes release of my dissertation to any reader upon request.

Redacted for privacy

Dojung Kim, Author

ACKNOWLEGEMENTS

I would like to sincerely thank my major Professor, Philip J. Proteau, for his support, guidance, and patience throughout my graduate career. I would also like to express my gratitude to my committee members, Dr. Mark Zabriskie, Dr. William Gerwick, Dr. Victor Hsu, and Dr. David Williams for their support and academic guidance in helping me to complete this dissertation. I am grateful to Brian Arbogast and Jeff Morre for their assistance on MS analysis and Roger Kohnert for his assistance on the NMR work.

I would like to acknowledge past and present colleagues, Chanokporn Phaosiri, Roberta Fernandes, Qingmei Yao, and Dr. Younhi Woo of the Proteau group, David Blanchard, Laura Grochowski, and Tracy Han of the Zabriskie group, and Dr. Xihou Yin for their friendship and useful discussion.

I thank the past and present members of Korean Presbyterian Church of Corvallis for their friendship, care, and encouragement.

Finally, I would like to give my special thanks to my parents, Sukchan Kim and Hyesook Lee, my sister Doshin Kim, and my sister Dohyang Kim and her family.

CONTRIBUTION OF AUTHORS

Mike Filtz performed the NMR assignments of diadinoxanthin discussed in Chapter Two and [U-$^{13}C_6$]-glucose and [1,2-$^{13}C_2$]-acetate incubation experiments in Chapter Three. Dr. Brian Marquez ran the ^{1}H- and ^{2}H-decoupled ^{13}C-NMR experiment described in Chapter Three.

TABLE OF CONTENTS

TABLE OF CONTENTS (Continued)

LIST OF FIGURES

LIST OF FIGURES (Continued)

LIST OF FIGURES (Continued)

LIST OF FIGURES (Continued)

LIST OF TABLES

LIST OF APPENDICES

LIST OF APPENDIX FIGURES

LIST OF ABBREVIATIONS

ACP	Acyl carrier protein
AT	Acyl transferase
ATP	Adenosine 5'-triphosphate
CDP-ME	4-(Cytidine 5'-diphospho)-2-*C*-methyl-D-erythritol
CDP-ME2P	2-Phospho-4-(cytidine 5'-diphospho)-2-*C*-methyl-D-erythritol
Chl/Chl_P	Chlorophylls
Chl_{DHGG}	Dihydrogeranylgeranyl chlorophyll
Chl_{GG}	Geranylgeranyl chlorophyll
Chlide	Chlorophyllides
Chl_{THGG}	Tetrahydrogeranylgeranyl chlorophyll
CI	Chemical ionization
CoA	Coenzyme A
CDP	Cytidine diphosphate
CTP	Cytidine triphosphate
d	doublet
DCC	1,3-Dicyclohexyl carbodiimide
DH	Dehydratase
DMAP	4-Dimethyl aminopyridine
DMAPP	Dimethylallyl diphosphate
DMSO	Dimethyl sulfoxide
DX	1-Deoxy-D-xylulose
DXP	1-Deoxy-D-xylulose-5-phosphate
DXR	DXP reductoisomerase
ER	Enoyl reductase
EtOAc	Ethyl acetate
FAB	Fast atom bombardment
FAD	Flavin adenine dinucleotide
FMN	Flavin mononucleotide
FPP	Farnesyl diphosphate
GAP	Glyceraldehyde 3-phosphate
GGPP	Geranylgeranyl diphosphate

LIST OF ABBREVIATIONS (CONTINUED)

GPP	Geranyl diphosphate
HMBC	Heteronuclear multiple bond connectivity
HMBDP	1-Hydroxy-2-methyl-2-(*E*)-butenyl 4-diphosphate
HMG-CoA	3-Hydroxy-3-methylglutaryl-CoA
IPP	Isopentenyl diphosphate
J	Coupling constants
KR	Ketoreductase
KS	β-Ketoacyl synthase
LAD	Lithium aluminum deuteride
m	multiplet
MECDP	2-*C*-Methyl-D-erythritol-2,4-cyclodiphosphate
MEP	2-*C*-Methyl-D-erythritol-4-phosphate
MS	Mass spectrometry
MVA	Mevalonic acid/ Mevalonate
NAC	N-Acetyl cysteamine
NADPH	Reduced nicotinamide adenine dinucleotide phosphate
NMO	4-Methyl morpholine *N*-oxide
NMR	Nuclear magnetic resonance
Phy-PP/PDP	Phytyl diphosphate
PK	Polyketide
PKS	PK synthase
prep-TLC	preparative TLC
q	quartet
RP	Reversed phase
s	singlet
SAM	*S*-Adenosyl methionine
t	triplet
TEA	Triethylamine
TLC	Thin layer chromatography
TPAP	Tetrapropyl ammonium perruthenate
TPP	Thiamine diphosphate

Studies on the Biosynthesis of Isoprenoids in *Euglena gracilis*

CHAPTER ONE

General Introduction

Isoprenoid compounds

Isoprenoids are a large family of natural products based on the biological five carbon precursors, isopentenyl diphosphate (IPP) and dimethylallyl diphosphate (DMAPP) which are the active isoprene units proposed by Ruzicka in 1953.[1] An integral number of isoprene units are joined together head-to-tail fashion to give the isoprenoid precursors, geranyl diphosphate (GPP), farnesyl diphosphate (FPP), geranylgeranyl diphosphate (GGPP), and polyprenyl diphosphate (Fig.1.1). Isoprenoids are also known as terpenes.

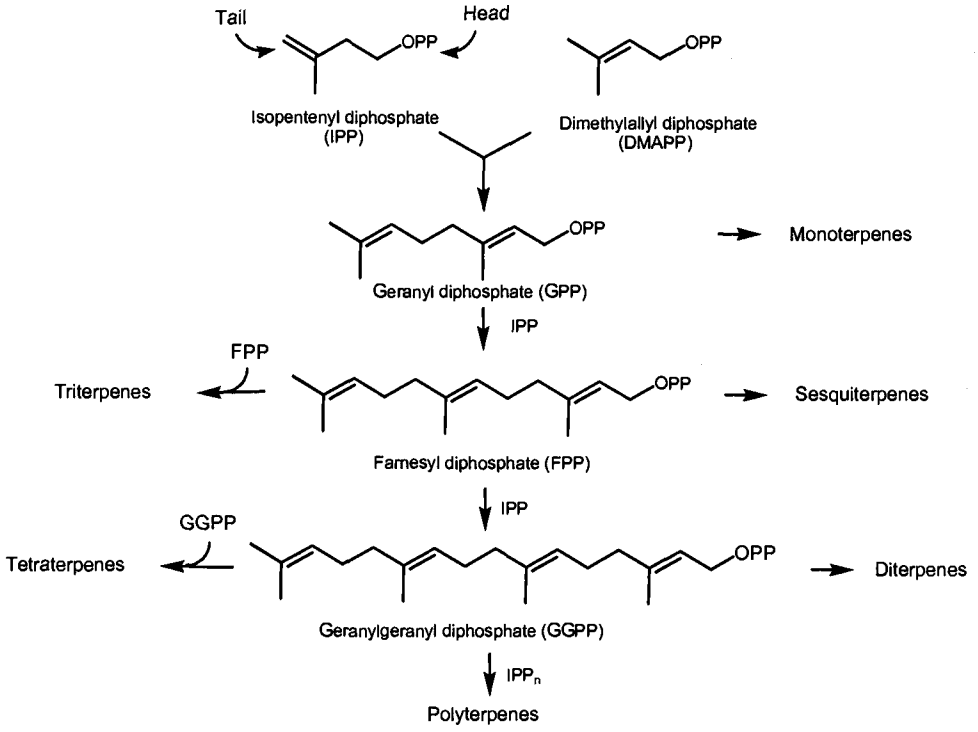

Fig.1.1. Outline of isoprenoid metabolism.

Condensation of two FPP moieties in a head-to-head fashion forms the precursor to the triterpenoids, and head-to-head condensation of two GGPP units produces the C_{40} isoprenoid precursor.[2,3] Further modifications of isoprenoid precursors, such as cyclization reactions, rearrangements, and oxidations, lead to the diverse structures of isoprenoids which have important roles in organisms as well as being profitable goods in industry (Fig.1.2).[4]

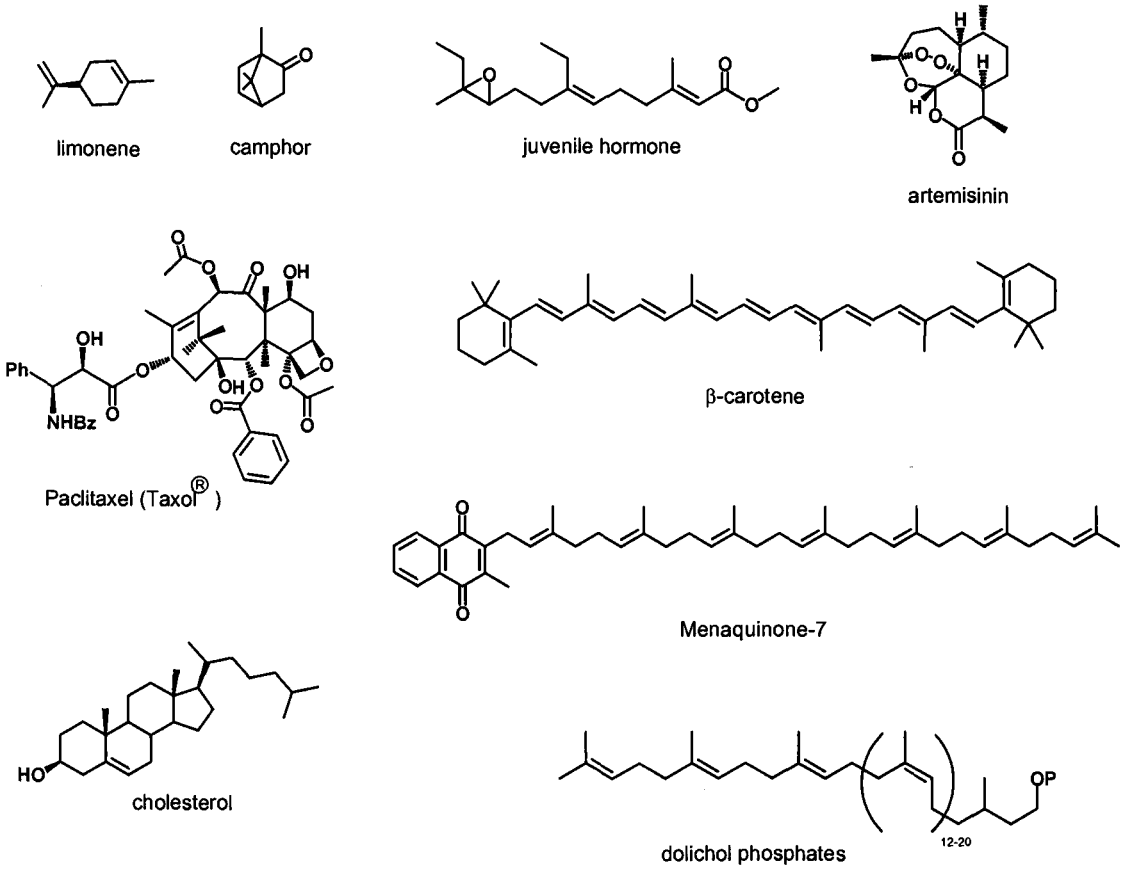

Fig.1.2. Various structures of isoprenoids.

More than 30,000 isoprenoids have been reported, even though only a small portion have known physiological functions.[5] For example, triterpenoids are essential metabolites in many organisms. Sterols, such as cholesterol in mammals, ergosterol in fungi, and sitosterol in plants, and sterol-like hopanoids in bacteria, act as constituents of cell membranes helping to maintain structural integrity and to control permeability. Many hormones, such as sex hormones, juvenile hormones, and molting hormones, are classified as triterpenoids and sesquiterpenoids. Tetraterpenoid carotenoids are essential pigments in photosynthetic organisms and serve to protect organisms from photooxidation during photosynthesis. Dolichol phosphates, having chains of repeating isoprene units, play a key role in cell wall formation and glycoprotein biosynthesis. Quinones, such as menaquinones and ubiquinones, with a variable length isoprenoid sidechain, function in electron transport and are important components of the blood coagulation system in mammals.

In addition to the known physiological functions, numerous isoprenoids are used as pharmaceuticals or as important items of commerce. Most of the mono- and bicyclic monoterpenoids such as pinene, carvone, camphor, and limonene have favorable aromas which have attracted attention of the flavor industry, while latex rubber is an example of a commercially important polyterpenoid.[6] For medical treatment, the diterpenoid paclitaxel (Taxol®) is prescribed for anticancer treatment, showing extremely potent activity.[7] The sesquiterpenoid artemisinin is isolated from the Chinese medicinal herb, *Artemisia annua L.*, and has been used for the prevention and treatment of malaria for at least 2000 years in China.[8,9] A synthetic analog of artemisinin has recently been approved as a drug.[9]

The physiological and commercial importance of isoprenoids have driven many studies to discover the biosynthetic pathway to isoprenoids because information on this pathway may be applied to the biotechnological production of commercially interesting isoprenoids and the development of new drugs. Early investigations of the biosynthetic pathway to isoprenoids resulted in identification of the first specific isoprenoid precursor, mevalonic acid (MVA), in 1957.[10] Incorporation studies with labeled mevalonic acid were performed by Gibbs *et al.*,[11,12] Cornforth *et al.*,[13] and Goodwin *et al.*,[14] and the results indicated the intact incorporation of [2-^{14}C]-MVA into cholesterol and other isoprenoid metabolites. Shortly after the discovery of MVA itself, the complete mevalonate pathway (MVA pathway) to isoprenoids was

determined through studies on the biosynthesis of cholesterol in yeast cells and mammalian liver extracts (Fig.1.3).[15,16]

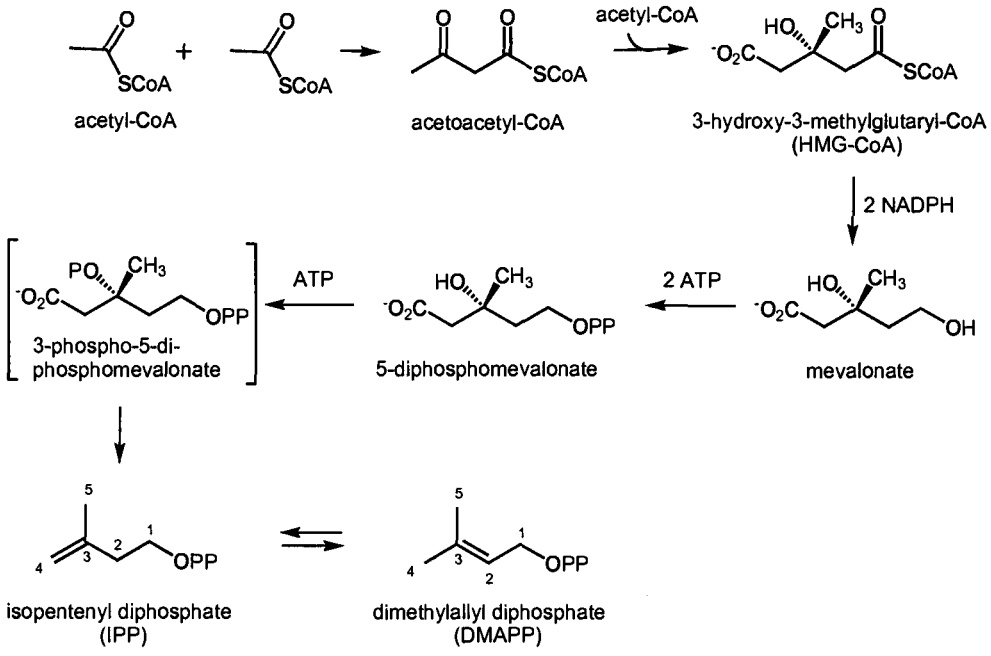

Fig.1.3. MVA pathway for isoprenoid biosynthesis.

The first step in the formation of MVA is the Claisen-type condensation of two molecules of acetyl-CoA catalyzed by the enzyme acetoacetyl-CoA thiolase (EC 2.3.1.9) to produce acetoacetyl-CoA. In the second step, 3-hydroxy-3-methylglutaryl-CoA (HMG-CoA) synthase (EC 4.1.3.5) mediates the aldol reaction between acetoacetyl-CoA and another acetyl-CoA to form (*S*)-HMG-CoA, which is subsequently transformed to (*R*)-MVA by HMG-CoA reductase (EC 1.1.1.34), consuming two moles of NADPH. The (*R*)-MVA undergoes a phosphorylation reaction catalyzed by the ATP-dependent MVA kinase (EC 2.7.1.36) to form 5-phosphomevalonate. A second kinase, 5-phosphomevalonate phosphotransferase (EC 2.7.4.2), converts 5-phosphomevalonate to 5-diphosphomevalonate, requiring ATP. The activity of 5-diphosphomevalonate phosphotransferase (EC 4.1.1.33), coupled with a decarboxylation reaction, gives rise to IPP via 3-phospho-5-

diphosphomevalonate. The conversion of IPP to DMAPP is accomplished by IPP isomerase (EC 5.3.3.2).[17]

The rate-limiting step in the formation of IPP by this route is the two-step reduction catalyzed by HMG-CoA reductase forming (*R*)-MVA from (*S*)-HMG-CoA. The activity of HMG-CoA reductase is able to regulate the whole biosynthesis of isoprenoids via the MVA pathway.[18] This enzyme, therefore, is considered as a critical target to control cholesterol biosynthesis in mammals. Mevinolin, an HMG-CoA reductase inhibitor isolated from *Aspergillus terreus*, functions by strong inhibition of sterol biosynthesis.[19] Mevinolin, also known as Lovastatin®, as well as other statins, such as simvastatin (Zocor®), structurally resemble HMG-CoA, and are broadly used to treat hypercholesterolemia.[20]

Besides the route utilizing acetate as a starting unit, MVA can also be formed from a bypass pathway in some green plants and red yeasts.[21] This discovery was inspired by the finding that the production of β-carotene in a fungus, *Phycomyces blakesleeanus,* was stimulated in medium containing L-leucine.[22] Consecutive incubation experiments with labeled leucine and $^{14}CO_2$ revealed the contribution of leucine, through HMG-CoA, to MVA production for isoprenoid biosynthesis (Fig. I.4).[23-25]

According to the leucine catabolic pathway, leucine is transformed to α-ketoisocaproic acid, which undergoes decarboxylation and reduction reactions to form dimethylacrylyl-CoA. Fixation of CO_2 into dimethylacrylyl-CoA gives rise to 3-methylglutaconyl-CoA, which is converted to HMG-CoA. Subsequent steps from HMG-CoA can go through two routes. One is a cleavage of HMG-CoA to form acetyl-CoA and acetoacetate which are reutilized to produce HMG-CoA. When HMG-CoA is resynthesized, the acetate unit is diluted by an endogenous acetate pool, while the intact acetoacetate is readily incorporated into HMG-CoA without further breakdown to acetate.[26] The other route is the direct conversion of HMG-CoA into MVA, which was discovered in a parasitic trypanosomatid, *Leishmania mexicana* in the late 1990's.[27] Several *Leishmania* species, such as *L. adleri* and *L. panamamensis,* and the related trypanosomatid *Endotrypanum monterogeii* were also reported to efficiently produce sterols from leucine rather than acetate.[28,29]

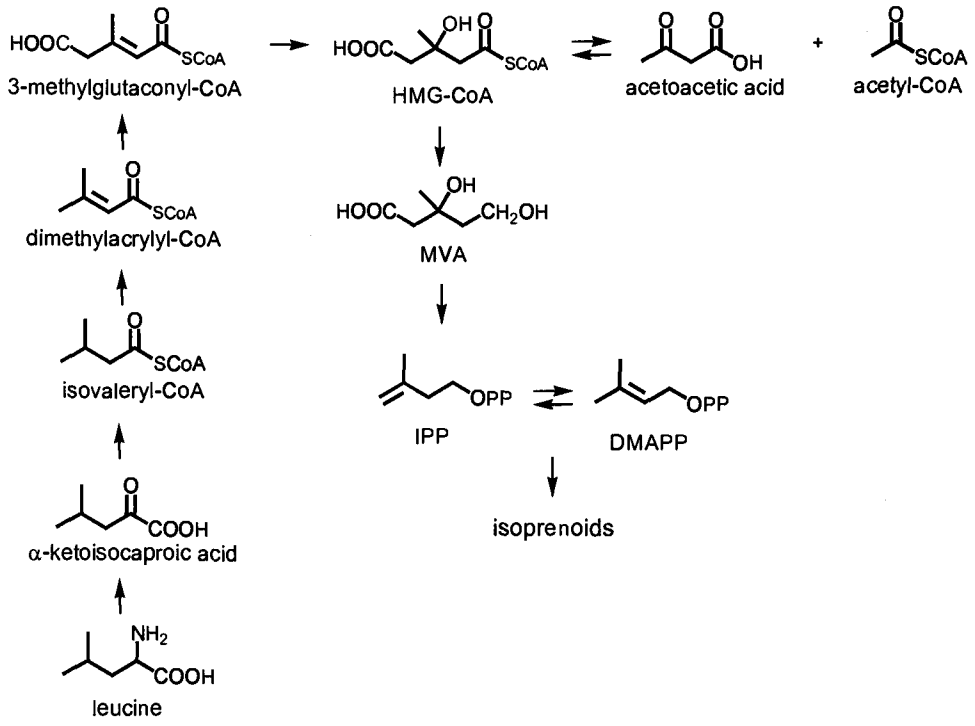

Fig.1.4. Leucine catabolic pathway to form IPP.

Until the late 1980's, the MVA pathway was the unquestioned pathway to biosynthesize isoprenoids in all organisms. A contradictory proposal against the universal MVA pathway was reported by Flesch and Rohmer in 1988.[30] Through incorporation experiments with ^{13}C-labeled acetate and glucose into prokaryotic hopanoids, they found that isoprene units are not directly synthesized via the simple acetyl-CoA of the starting C_2 unit in the MVA pathway.[31] These results drove them to think of different pools of C_2 unit precursors derived from the glyoxylate cycle, the Entner-Doudoroff pathway of glucose catabolism, and even an unknown pathway.[30,31] Successive studies with *Zymomonas mobilis* and *Escherichia coli* led to the proposal in 1993 that a new pathway had been discovered in which the five carbons of the isoprene unit derived from glucose, one as a two carbon unit and one as a three-carbon unit. Further studies with *E. coli* published in 1996 identified that pyruvate and glyceraldehyde 3-phosphate (GAP) might be the carbon sources for the isoprene unit,

instead of three molecules of acetate for the isoprene unit, and constitute C3-5 and C1-2-4 of IPP, respectively.[32,33]

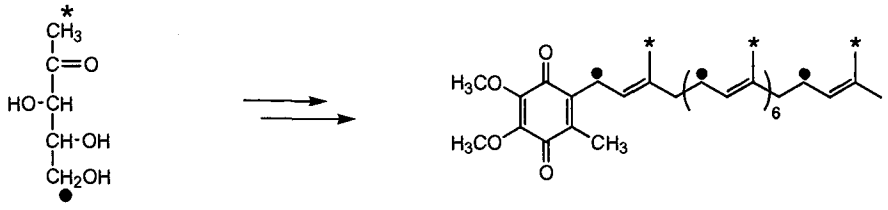

1-deoxy-D-xylulose ubiquinone-8

Fig.1.5. Labeling pattern of ubiquinone-8 from [5,5-$^2H_2$]-DX (•) and [1-^2H]-DX (*) in *E. coli*.

The identification of the C_5 precursor in this new pathway was revealed by Broers and Schwarz in 1994 (Fig.1.5).[34,35] Through incubation experiments using ^{13}C-labeled glucose with *E. coli* and *Ginkgo biloba*, they proposed either 1-deoxy-D-xylulose-5-phosphate (DXP) or 1-deoxy-D-xylulose (DX) itself as the intermediate in a novel pathway. In order to confirm this proposal, experiments were performed with deuterium-labeled DX, anticipating incorporation into the isoprenoid sidechain of ubiquinone-8 in *E. coli* (Fig.1.5).[34]

Based on the intact incorporation of DX into *E. coli* ubiquinone, they confirmed that DX, most likely as its 5-phosphate, is a key precursor of a novel isoprenoid biosynthetic pathway. Later, further incubation experiments with deuterium-labeled DX were applied to algae and higher plants resulting in the intact incorporation of DX into isoprenoids, as was observed with *E. coli*.[36-38] Additionally, these discoveries provided an explanation for the unexpected survival of *E. coli*, and the differential inhibition between the plastidial pigments and sterols of plants, when grown in media containing HMG-CoA reductase inhibitors.[19,39]

This novel isoprenoid pathway has been called several names, such as the non-mevalonate pathway, the deoxyxylulose phosphate pathway, the pyruvate/triose phosphate pathway, and the mevalonate-independent pathway. However, as will be described shortly, 2-*C*-methyl-D-erythritol 4-phosphate (MEP) is the committed intermediate to this biosynthetic route, so the MEP pathway is the name that will be used throughout the dissertation. The MEP pathway is also the name recommended

at the Fourth European Symposium on Plant Isoprenoids held in Barcelona, Spain in 1999.

After the MEP pathway was discovered in the early 1990's, intense investigations were triggered to elucidate all of the steps in the MEP pathway. By 2002, all of the steps of the pathway had been identified (Fig.1.6).[40-42] The first step of the MEP pathway is the formation of DXP through condensation of pyruvate and GAP accompanied by decarboxylation. This reaction is catalyzed by DXP synthase (EC 2.7.1.17) which requires thiamine-diphosphate (TPP) and a divalent cation, Mg^{2+} or Mn^{2+}, as cofactors for enzyme activity. In fact, the formation of DX or DXP from pyruvate and GAP is not a reaction specific to the MEP pathway. In 1978, White *et al.* postulated this C_5 precursor for the thiazole structure in thiamine[43], and further experiments with deuterium-labeled DX in *E. coli* revealed that DXP is a precursor to thiamine and pyridoxal.[44,45] After DXP was demonstrated as a precursor in the MEP pathway, the gene encoding DXP synthase was cloned and overexpressed in *E. coli* by Sprenger *et al.*[46]

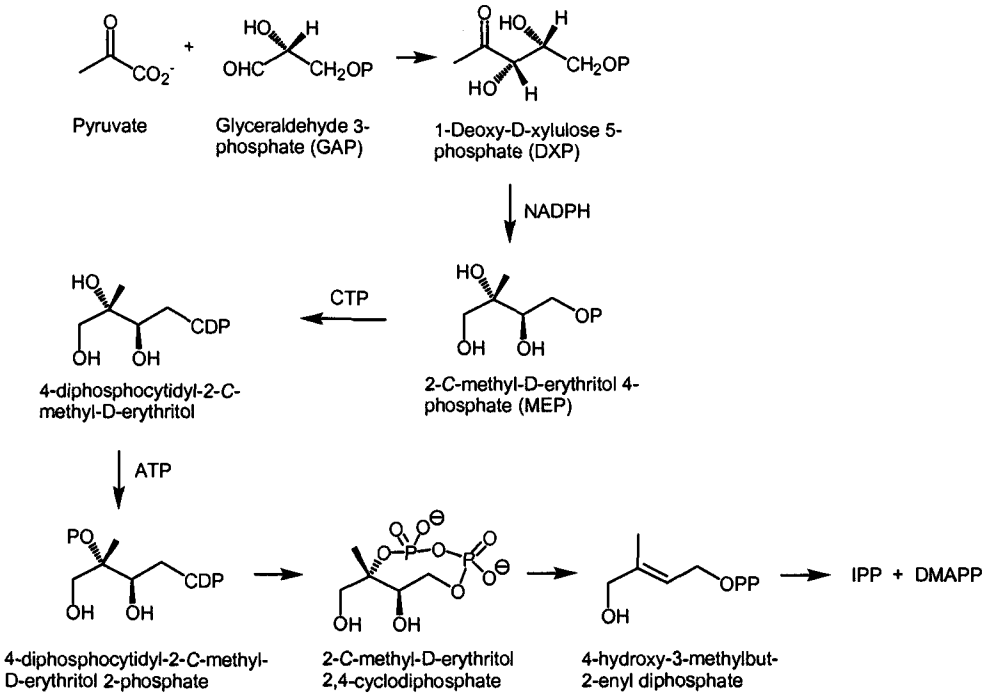

Fig.1.6. MEP pathway for isoprenoid biosynthesis.

In the second step, two consecutive reactions, a rearrangement and a subsequent reduction, result in the formation of MEP from DXP, a conversion catalyzed by DXP reductoisomerase (DXR) (EC 1.1.1.267) (Fig.1.7). The nature of the rearrangement was proposed through the differential ^{13}C incorporation from [1-^{13}C]-glucose and then proved by the analysis of long-range couplings between C4 and C1-C2 of IPP units derived from [U-$^{13}C_6$]-glucose, reflecting the intact GAP starting unit.[47] Because GAP is fragmented in the formation of MEP, long-range C4-C1 ($^{3}J_{C\text{-}C}$ = 2.0-2.6 Hz) and C4-C2 ($^{2}J_{C\text{-}C}$ = 3.6-4.0 Hz) couplings in the isoprene units of a variety of isoprenoids can be clearly observed by using modified two dimensional NMR techniques.[36,48-50]

The rearranged intermediate was assumed to be 2-C-methyl-D-erythrose-4-phosphate on the basis of a similar reaction mechanism to ketol acid reductoisomerase (EC 1.1.1.86), a functionally related enzyme which converts 2-acetolactate to 2,3-dihydroxyisovalerate in the valine and leucine biosyntheses (Fig.1.7).[37,38,51] This enzyme carries out a rearrangement of acetolactate to form 2-oxo-3-hydroxyisovalerate, a bound intermediate, followed by a reduction in the presence of NADPH to provide 2,3-dihydroxyisovalerate.

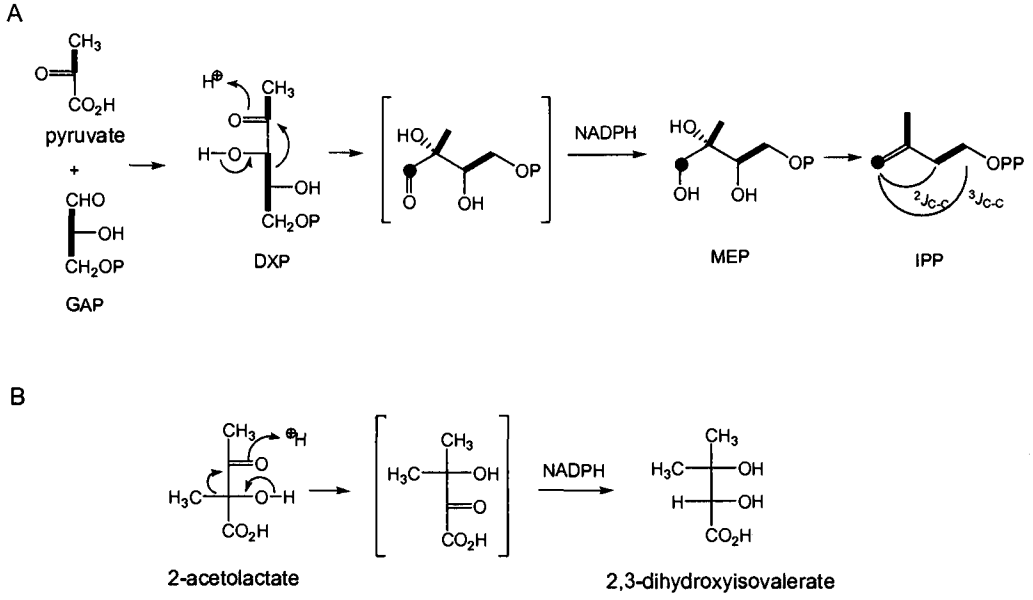

Fig.1.7. Reduction step of DXR (A) and ketol acid reductoisomerase (B). Bold lines indicate sequential ^{13}C enriched positions, and filled circles indicate enhanced ^{13}C positions. *J* indicates the coupling constant between carbons two and three-bonds away in isoprene units.

The discovery of MEP, a rearranged intermediate, was inspired from studies on the accumulated 2-*C*-methyl-D-erythritol-2,4-cyclodiphosphate (MECDP) in *Desulfovibrio desulfuricans* and *Corynebaterium ammoniagenes* by Rohmer *et al.*[50] The ^{13}C-NMR spectra of dihydromenaquinone and 2-*C*-methyl-D-erythritol (prepared by phosphatase treatment of MECDP) obtained after the incorporation of [U-$^{13}C_6$]-glucose in *C. ammoniagenes* were consistent with biosynthesis from GAP and pyruvate.[50] The intact incorporation of deuterated 2-*C*-methyl-D-erythritol into ubiquinone and menaquinone of *E. coli* confirmed the likely role of 2-*C*-methyl-D-erythritol or its 4-phosphate in the novel pathway.[52] Further evidence for this proposal was provided by preparing and selecting *E. coli* mutants which were unable to transform DXP to MEP, consequently requiring 2-*C*-methyl-D-erythritol for their growth and survival.[53,54] The enzyme corresponding to the defective DNA fragment in the mutant was characterized and it turned out to be the key enzyme for the transformation of DXP, designated DXR. Incubation of DXR with DXP resulted in the formation of MEP. The enzyme DXR requires NADPH and Mn^{2+} or Mg^{2+} as cofactors. The reduction step of DXR is stereospecific, delivering the *pro S*-hydride from NADPH to the substrate, which classifies DXR as a class B dehydrogenase.[55,56] Three X-ray crystal structures of the *E. coli* DXR have been reported, indicating three domains, including binding regions for NADPH and DXP, and a C-terminal α-helical domain.[57,58]

Identification of DXR provided an explanation for the biological activity of fosmidomycin, an antibiotic compound whose mechanism of action had remained unsolved since it was isolated from *Streptomyces lavendulae* in 1980.[59] In the late 1980's, experiments showed fosmidomycin blocked isoprenoid synthesis, but no particular step was identified.[60] Now fosmidomycin is known to inhibit DXR activity by competitively binding at the active site due to structural similarity to DXP.[61]

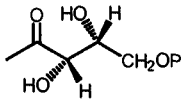

1-deoxy-D-xylulose 5-phosphate (DXP)

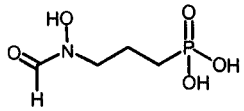

fosmidomycin

The conversion of MEP to IPP is accomplished through five additional steps (Fig.1.8). Once MEP was established as an intermediate of the MEP pathway, enzymes, such as IspD (YgbP), IspE (YchB), and IspF (YgbB) involved in the downstream steps, were consecutively determined. The *ispD* (*ygbP*), *ispE* (*ychB*), and *ispF* (*ygbB*) genes were found in *E. coli* through genomic approaches and the corresponding enzymes were biochemically characterized as being involved in the MEP pathway.[62-64] Another approach to elucidate the reaction steps was performed by screening *E. coli* mutants whose pathway leading to IPP from MEP was disrupted.[65-67] From this screening, several uncharacterized genes, *ispD, ispE,* and *ispF* were identified and tested for their functions in the MEP pathway. The *ispD* gene product encodes MEP cytidyltransferase (EC 2.7.7.60), which converts MEP to 4-(cytidine 5'-diphospho)-2-*C*-methyl-D-erythritol (CDP-ME) in the presence of cytidine triphosphate (CTP). The *ispE* gene encodes CDP-ME kinase (EC 2.7.1.148) which is an ATP-dependent enzyme which delivers a phosphate group to the 2-hydroxyl group. The next step is the cyclization reaction, catalyzed by IspF (MECDP synthase, EC 4.6.1.12), which transforms 2-phospho-4-(cytidine 5'-diphospho)-2-*C*-methyl-D-erythritol (CDP-ME2P) into MECDP. The recent crystal structure of MECDP synthase from *E. coli* revealed a Mg^{2+}/Mn^{2+}-dependent catalytic mechanism showing a tetragonal coordination complex containing cytidine monophosphate (CMP), MECDP, and a metal cation.[68]

A bioinformatics approach led to identification of the *ispG (gcpE)* gene whose distribution was correlated with the occurrence of DXR, *ispD*, *ispE*, and *ispF*.[69,70] The activity of the *ispG* gene product was tested in a recombinant *E. coli* strain with or without the additionally expressed *ispG* gene.[71] Incubation of the recombinant with the extra *ispG* gene and labeled DX resulted in the accumulation of labeled 1-hydroxy-2-methyl-2-(*E*)-butenyl-4-diphosphate (HMBDP), whereas the *ispG* gene-deficient *E. coli* mutant produced a high level of MECDP. Further studies characterized the IspG protein as an oxygen-sensitive iron-sulfur protein requiring flavin adenine dinucleotide (FAD) and /or NADPH as a cofactor(s) to convert MECDP to HMBDP.[72,73] The reaction catalyzed by the IspG protein results in the exclusive formation of the (*E*)-isomer.[42]

The role of the *ispH* (*lytB*) gene was found by a similar approach to that used to discover the *ispG* gene function, showing an accumulation of IPP and DMAPP

when *ispH* was overexpressed in *E. coli* grown in the presence of labeled DX and the accumulation of HMBDP with the *ispH*-deficient *E. coli* mutant.[74,75] Like the IspG protein, the IspH protein requires a $[4Fe\text{-}4S]^{2+}$ cluster and NADPH for activity, leading to the independent formation of IPP and DMAPP in a 4:1 to 6:1 mixture.[41,42]

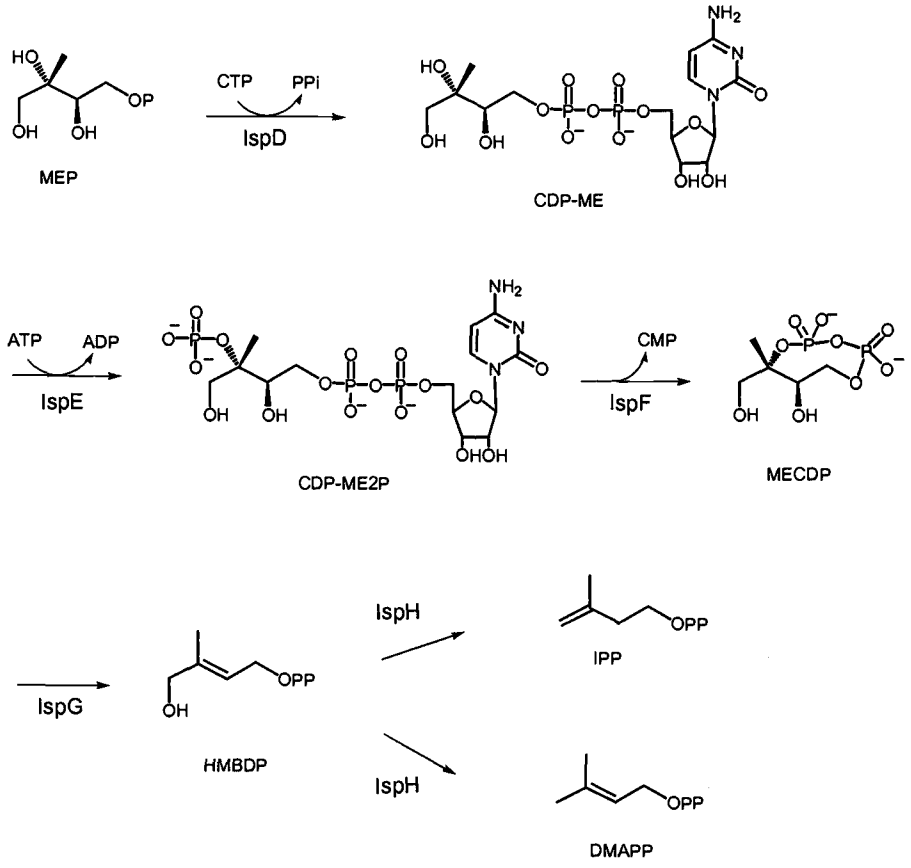

Fig.1.8. Enzymes in the MEP pathway.

Distribution of the two isoprenoid biosynthetic pathways

Besides the elucidation of the individual steps of the MEP pathway, the distribution of both pathways in organisms became another area of interest to many researchers. Based on the studies in *E. coli*, the presence of the MEP pathway was widely investigated in prokaryotes.[76-78] In Gram-(-) bacteria, all of the *Burkholderia*, *Enterobacteriaceae, Pseudomonas, Rhodopseudomonas,* and *Methylobacterium*

species examined were reported to utilize only the MEP pathway.[79] *Acinetobacter calcoaceticus* and the cyanobacteria, *Synechocystis* species, also rely on the MEP pathway to biosynthesize isoprenoid compounds,[79,80] and Gram-(+) bacteria, such as *Mycobacterium phlei*, *Bacillus subtilis*, *Alicyclobacillus acidoterrestris*, and *C. ammoniagenes* only have genes corresponding to the MEP pathway.[79] In fact, the MEP pathway is apparently widespread in bacteria, including pathogens as well as innocuous species.

However, not all bacteria possess the MEP pathway. Gene clusters for the MVA pathway were found in some eubacteria, including *Staphylococcus carnosus*, *Myxococcus fulvus*, *Flavobacterium* species and *Chloroflexus aurantiacus,* which utilize only the MVA pathway for isoprenoid compounds. Besides the above eubacteria, Archaea, such as *Caldariella acidophila*, *Halobacterium halobium*, *Halobacterium cutirubum*, and *Halobacterium japonica,* are believed to possess only the MVA pathway.[40]

Prior to the discovery of the MEP pathway, the sesquiterpenoid pentalenolactone from *Streptomyces* UC5319 was found to not incorporate labeled acetate in a manner consistent with the MVA pathway.[81] Once the MEP pathway was identified, it was clear that the labeling pattern observed for pentalenolactone biosynthesis was consistent with the new pathway. Based on this observation, many *Streptomyces* species, well-known to produce various antibiotics as secondary metabolites, were reinvestigated for the distribution of the two pathways relative to the production of mono-, sesqui-, and diterpenoids.[40] Although most *Streptomyces* species utilize the MEP pathway for isoprenoid biosynthesis, some species maintain both pathways. For example, *Streptomyces aeriouvifer* can produce tetrahydromenaquinone-9 as a primary metabolite via the MEP pathway during the exponential growth phase, whereas the monoterpene moiety of the secondary metabolite naphterpin, is assembled via the MVA pathway during the stationary growth phase (Fig.1.9).[48] A similar situation occurs in *Actinoplanes* species which utilizes the MEP pathway for the formation of tetrahydromenaquinone-9 and the MVA pathway for the formation of the isoprenoid moiety of antibiotic BE-40644.[82] *Streptomyces* species CL190, another naphterpin producer, was also reported to utilize the MEP pathway for the formation of the primary metabolite and then switches to the MVA pathway for the production of the secondary metabolite.[83]

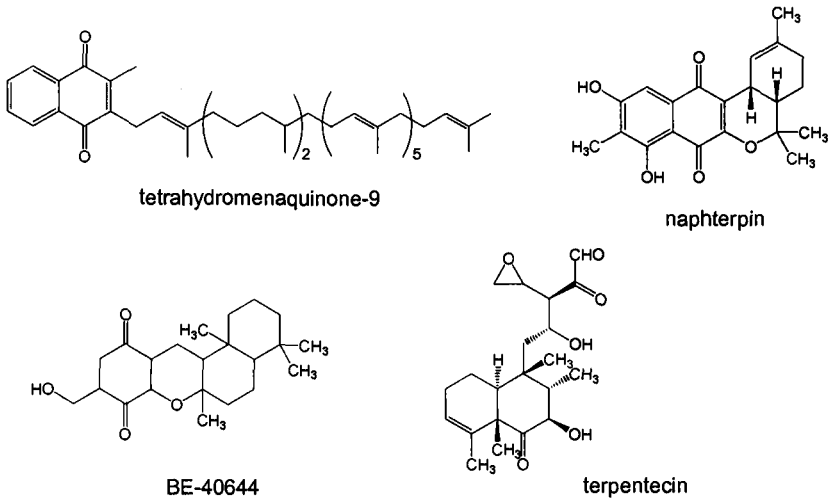

Fig.1.9. Isoprenoid compounds in *Streptomyces* species.

All investigated *Streptomyces* species except for the above organisms have been reported to exclusively utilize the MEP pathway for secondary metabolites such as carquinostatin A, novobiocin, longestin, moenomycin, and pentalenolactone.[81,84-86] On the basis of these findings, all *Streptomyces* species are indeed equipped with the MEP pathway for the formation of essential primary terpenoids, while some species are supported with the addition of the MVA pathway for the formation of secondary terpenoids. In fact, a gene cluster for the MVA pathway adjacent to GGPP synthase and diterpene cyclase genes was found in *Streptomyces griseolosporeus* strain MF730-N6, the terpentecin producer.[87]

As for the distribution of the two pathways in photosynthetic organisms, there are apparently two classes. One is the green algae, including *Scendesmus obliquus*, *Chlamydomonas reinhardtii*, and *Chlorella fusca,* with no evidence for the presence of the MVA pathway.[88] The other class includes red algae and higher plants, which show the functioning of both pathways simultaneously.[76,89] In order to explain the existence of both pathways in red algae and higher plants, Lichtenthaler cited a proposal on compartmentation of isoprenoid biosynthesis which was first reviewed by Kleinig in 1989 (Fig.1.10).[89,90]

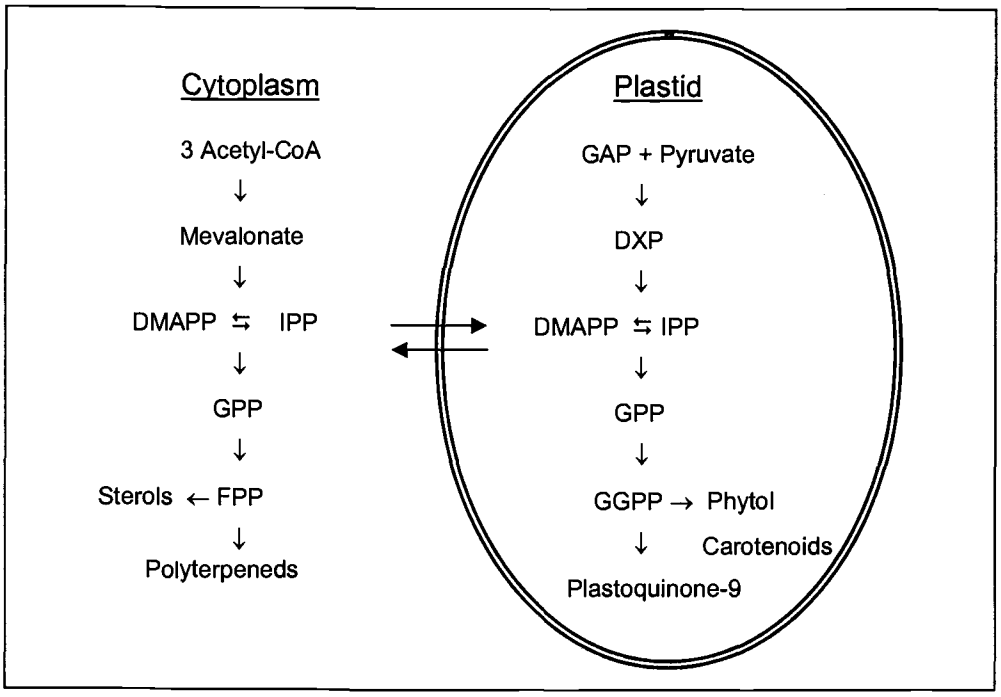

Fig.1.10. Proposed compartmentation of isoprenoid biosynthesis.[89]

Based on this proposal, it was suggested that red algae and higher plants have the MVA and the MEP pathways in different compartments, such as the chloroplasts and cytosol in the cell. The MVA pathway operates for the formation of cytosolic isoprenoids such as sterols, and the MEP pathway for plastidic isoprenoids such as carotenoids and the phytyl sidechain of chlorophyll. This proposal has been generally accepted, especially considering that the chloroplasts of higher plants are proposed to originate from prokaryotic cyanobacteria during an endosymbiotic process.[5,76,91] Cyanobacteria use the MEP pathway exclusively.

Many volatile mono- and sesquiterpenoids are produced via the MEP pathway in leaves and flowers of higher plants, such as *Phaseolus lunatus*, *Nicotiana plombaginifolia*, and *Eucalyptus globulces.*[92] Diterpenoids in cell cultures of liverworts and higher plants were also reported to be formed via the MEP pathway. Although the formation of such mono-, sesqui-, and diterpenoids is not well clarified, these isoprenoids are thought to originate in plastids or plastid-related organelles.[76]

However, all photosynthetic organisms may not display complete compartmentation for both pathways. The diterpenoid ginkgolide from *Ginkgo biloba* embryos was reported to be formed 98-99 % from plastid GGPP via the MEP pathway in the chloroplasts and 1-2 % of a mixed origin.[35] IPP and FPP derived from the MVA pathway was assimilated into GGPP, which leads to the differential incorporation of IPP and FPP moieties into the ginkgolide of mixed origin. The liverworts *Heteroscyphus planus* and *Lophocolea heterophylla*, and the hornwort, *Anthoceros punctatus* also produce diterpenoids (phytol and heteroscyphic acid) and the tetraterpenoid β-carotene with a mixed origin of FPP imported from the cytoplasm and IPP from the chloroplasts.[93,94] In plant cell cultures of *Catharanthus roseus*, a minor contribution of the MVA pathway in the formation of carotenoids, as well as a minor contribution of the MEP pathway to sitosterol biosynthesis were detected.[36] These findings imply that common metabolites at the level of IPP, GPP, and FPP are able to be exchanged to a small extent between the cytoplasm and the chloroplasts. In contrast with photosynthetic eukaryotes, fungi, yeasts, and animals have been reported to exclusively rely on the MVA pathway to biosynthesize isoprenoid compounds. (Table 1).[5,40,77,89]

Table 1.1. Examples of the distribution of the MVA and the MEP pathways in various organisms.

MVA Pathway only	MEP Pathway only	Both Pathways
Animals	Cyanobacteria	Higher plants
Fungi	*Synechocystis* spp.	Red algae
Staphylococcus sp.	Gram-(-) Bacteria	Liverworts
Archaea	*E. coli*	Some *Streptomyces*
	Z. mobilis	
	P. aeruginosa	
	Gram-(+) Bacteria	
	B. subtilis	
	Chlorophyta	
	Plasmodium falciparum	

Although the complete distribution of the two pathways may not be fully clarified yet, the fact that the MEP pathway is an important pathway in plants and in pathogenic organisms, such as *Pseudomonas* species and *Mycobacterium* species, but is absent in animals, including humans, provides a new opportunity to develop antibiotics and herbicides.[95,96] Additionally, the malaria parasite *Plasmodium falciparum* has been reported to rely exclusively on the MEP pathway which provides an ideal target for the development of novel anti-malarial agents.[97] Currently, fosmidomycin, an inhibitor of DXR, is being tested as a potential antimalarial agent, showing activity against *P. falciparum*, the deadliest of the four *Plasmodium* species that cause malaria. In Gabon and Thailand, clinical studies with fosmidomycin have been conducted in malaria-infected humans, and the treatment resulted in pharmacological efficacy of the drug, showing low toxicity and high tolerence.[98,99]

In this dissertation, *Euglena* species, unicellular flagellates which have both plant and animal characteristics, were examined using isotope incorporation experiments to understand the distribution of the MVA and the MEP pathways. Interestingly, *E. gracilis* was reported to be the only photosynthetic eukaryote with no evidence for the presence of the MEP pathway.[100,101] Studies on carotenoid biosynthesis and possible precursors to isoprenoids in *E. gracilis* are described in Chapter Two. Chapter Three details the finding that phytol is produced via an alternate pathway instead of the known isoprenoid pathways. Based on the unusual phytol pathway described in Chapter Three, the isoprenoid and phytol pathways were explored in other *Euglena* strains. The results of these studies are presented in Chapter Four. Chapter Five provides a summary of the overall research described in the dissertation.

References

(1) Ruzicka, L. The isoprene rule and the biogenesis of terpenic compounds. *Experientia* **1953**, *9*, 357-367.

(2) Cane, D. E. In *Comprehensive Natural Product Chemistry*; Cane, D. E., Ed.; Elsevier: New York, 1999; Vol. 2, pp. 1-13.

(3) Porter, J. W.; Spurgeon, S. L. *Biosynthesis of Isoprenoid Compounds*; Wiley, New York, 1981.

(4) Sacchettini, J. C.; Poulter, C. D. Creating isoprenoid diversity. *Science* **1997**, *277*, 1788-1789.

(5) Lange, B. M.; Rujan, T.; Martin, W.; Croteau, R. Isoprenoid biosynthesis: the evolution of two ancient and distinct pathways across genomes. *Proc. Natl. Acad. Sci. U S A* **2000**, *97*, 13172-13177.

(6) Wise, M. L.; Croteau, R. In *Comprehensive Natural Product Chemistry*; Elsevier: New York, 1999; Vol. 2, pp. 97-153.

(7) Alexander, R. W. Teasing apart the taxol pathway. *Trends Biochem. Sci.* **2001**, *26*, 152.

(8) Mann, J. *Chemical Aspects of Biosynthesis*; Oxford University Press, 1994.

(9) Wang, D.-Y.; Wu, Y.; Wu, Y.-L.; Li, Y.; Shan, F. Synthesis, iron(II)-induced cleavage and *in vivo* antimalarial efficacy of 10-(2-hydroxy-1-naphthyl)-deoxoqinghaosu. *J. Chem. Soc., Perkin Trans. 1* **1999**, 1827-1831.

(10) Wolf, D. E.; Hoffman, C. H.; Aldrich, P. E.; Skeggs, H. R.; Wright, L. D.; Folkers, K. Determination of structure of β,γ-dihydroxy-β-methylvaleric acid. *J. Am. Chem. Soc.* **1957**, *79*, 1486-1487.

(11) Tavormina, P. A.; Gibbs, M. H. The metabolism of β,γ-hydroxy-β-methylvaleric acid by liver homogenates. *J. Am. Chem. Soc.* **1956**, *78*, 6210.

(12) Tavormina, P. A.; Gibbs, M. H.; Huff, J. W. The utilization of β-hydroxy-β-methyl-γ-valerolactone in cholesterol biosynthesis. *J. Am. Chem. Soc.* **1956**, *78*, 4498-4499.

(13) Cornforth, J. W.; Cornforth, R. H.; Popjak, G.; Youhotsky-Gore, I. Biosynthesis of squalene and cholesterol from DL-β-hydroxy-β-methyl-γ-[2-^{14}C]-valerolactone. *Biochem. J.* **1957**, *66*, 10p.

(14) Braithwaite, G. D.; Goodwin, T. W. Biosynthesis of β-carotene from DL-β-Hydroxy-β-methyl-γ-[2-14C]valerolactone by Phycomyces blakesleeanus and Carrot Slices. *Biochem. J.* **1957**, *67*, 13p-14p.

(15) Bloch, K.; Chaykin, S.; Phillips, J. W.; deWaard, A. Mevalonic acid pyrophosphate and isopentenylpyrophosphate. *J. Biol. Chem.* **1959**, *234*, 2595-2604.

(16) Witting, L. A.; Porter, J. W. Intermediates in the conversion of melaonic acid to squalene by a rat liver enzyme system. *J. Biol. Chem.* **1959**, *234*, 2841-2846.

(17) Anderson, M. S.; Muehlbacher, M.; Street, I. P.; Proffitt, J.; Poulter, C. D. Isopentenyl diphosphate:dimethylallyl diphosphate isomerase. An improved purification of the enzyme and isolation of the gene from *Saccharomyces cerevisiae*. *J. Biol. Chem.* **1989**, *264*, 19169-19175.

(18) Bochar, D. A.; Friesen, J. A.; Stauffacher, C. V.; Rodwell, V. W. In *Comprehensive Natural Product Chemistry*; Cane, D. E., Ed.; Elsevier: New York, 1999; Vol. 2, pp. 15-44.

(19) Bach, T. J.; Lichtenthaler, H. K. Plant growth regulation by mevinolin and other sterol biosynthesis inhibitors. *Am. Chem. Soc. Symp. Series* **1987**, *325*, 109-139.

(20) Endo, A. The discovery and development of HMG-CoA reductase inhibitor. *J. Lipid Res.* **1992**, *33*, 1569-1582.

(21) Britton, G. In *Carotenoids*; Britton, G., Liaaen-Jensen, S., Pfander, H., Eds.; Birkhäuser: Basel, 1998; Vol. 3, pp. 13-147.

(22) Goodwin, T. W.; Griffiths, L. A. Studies in carotenogenesis. V. Carotene production by various mutants of *Phycomyces blakesleeanus* and by *Phycomyces nitens*. *Biochem. J.* **1952**, *52*, 499-501.

(23) Chichester, C. O.; Yokoyama, H.; Nakayama, T. O.; Lukton, A.; Mackinney, G. Leucine metabolism and carotene biosynthesis. *J. Biol. Chem.* **1959**, *234*, 598-602.

(24) Braithwaite, G. D.; Goodwin, T. W. Studies in carotenogenesis. 27. Incorporation of [2-^{14}C] acetate, DL-[2-^{14}C] mevalonate and ^{14}C-labelled carbon dioxide into carrotroot preparations. *Biochem. J.* **1960**, *76*, 194-197.

(25) Braithwaite, G. D.; Goodwin, T. W. Studies in carotenogenesis. 25. The incorporation of [1-^{14}C] acetate, [2-^{14}C] acetate and ^{14}C-labelled carbon dioxide into lycopene by tomato slices. *Biochem. J.* **1960**, *76*, 1-5.

(26) Nes, W. D.; Bach, T. J. Evidence for a mevalonate shunt in a tracheophyte. *Proc. R. Soc. Lond. B* **1985**, *225*, 425-444.

(27) Ginger, M. L.; Chance, M. L.; Goad, L. J. Elucidation of carbon sources used for the biosynthesis of fatty acids and sterols in the trypanosomatid Leishmanis mexicana. *Biochem. J.* **1999**, *342*, 397-405.

(28) Ginger, M. L.; Chance, M. L.; Sadler, I. H.; Goad, L. J. The biosynthetic incorporation of the intact leucine skeleton into sterol by the trypanosomatid Leishmania mexicana. *J. Biol. Chem.* **2001**, *276*, 11674-11682.

(29) Ginger, M. L.; Prescott, M. C.; Reymonds, D. G.; Chance, M. L.; Goad, L. J. Utilization of leucine and acetate as carbon souces for sterol and fatty acid biosynthesis by old and new world *Leishmanis* species, *Endotrypanum monterogeii* and *Trypanosoma cruzi. Eur. J. Biochem.* **2000**, *267*, 2555-2566.

(30) Flesch, G.; Rohmer, M. Prokaryotic hopanoids: the biosynthesis of the bacteriohopane skeleton. Formation of isoprenic units from two distinct acetate pools and a novel type of carbon/carbon linkage between a triterpene and D-ribose. *Eur. J. Biochem.* **1988**, *175*, 405-411.

(31) Rohmer, M.; Sutter, B.; Sahm, H. Bacterial sterol surrogates. Biosynthesis of the side-chain of bacteriohopanetetrol and of a carbocyclic pseudopentose from ^{13}C-labelled glucose in *Zymomonas mobilis. J. Chem. Soc., Chem. Commun.* **1989**, *19*, 1471-1472.

(32) Rohmer, M.; Knani, M.; Simonin, P.; Sutter, B.; Sahm, H. Isoprenoid biosynthesis in bacteria: a novel pathway for the early steps leading to isopentenyl diphosphate. *Biochem. J.* **1993**, *295*, 517-524.

(33) Rohmer, M.; Seemann, M.; Horbach, S.; Bringer-Meyer, S.; Sahm, H. Glyceraldehyle 3-phosphate and pyruvate as precursors of isoprenic units in an alternative non-mevalonate pathway for terpenoids biosynthesis. *J. Am. Chem. Soc.* **1996**, *118*, 2564-2566.

(34) Broers, S. T. J. Ph. D. Dissertation, Eidgenössische Technische Hochschule, Zürich, 1994.

(35) Schwarz, M. K. Ph.D. Dissertation, Eidgenössische Technische Hochschule, Zürich, 1994.

(36) Arigoni, D.; Sagner, S.; Latzel, C.; Eisenreich, W.; Bacher, A.; Zenk, M. H. Terpenoid biosynthesis from 1-deoxy-D-xylulose in higher plants by intramolecular skeletal rearrangement. *Proc. Natl. Acad. Sci. U S A* **1997**, *94*, 10600-10605.

(37) Schwender, J.; Zeidler, J.; Groner, R.; Muller, C.; Focke, M.; Braun, S.; Lichtenthaler, F. W.; Lichtenthaler, H. K. Incorporation of 1-deoxy-D-xylulose into isoprene and phytol by higher plants and algae. *FEBS Lett.* **1997**, *414*, 129-134.

(38) Zeidler, J. G.; Lichtenthaler, H. K.; May, H. U.; Lichtenthaler, F. W. Is isoprene emitted by plants synthesized via the novel isopentenyl pyrophosphate pathway? *Z. Naturforsch,* **1997**, *52C*, 15-23.

(39) Zhou, D.; White, R. H. Early steps of isoprenoid biosynthesis in *Escherichia coli. Biochem. J.* **1991**, *273*, 627-634.

(40) Kuzuyama, T.; Seto, H. Diversity of the biosynthesis of the isoprene units. *Nat. Prod. Rep.* **2003**, *20*, 171-183.

(41) Wolff, M.; Seemann, M.; Tse Sum Bui, B.; Frapart, Y.; Tritsch, D.; Estrabot, A. G.; Rodriguez-Concepcion, M.; Boronat, A.; Marquet, A.; Rohmer, M. Isoprenoid biosynthesis via the methylerythritol phosphate pathway: the (E)-4-hydroxy-3-methylbut-2-enyl diphosphate reductase (LytB/IspH) from *Escherichia coli* is a [4Fe-4S] protein. *FEBS Lett.* **2003**, *541*, 115-120.

(42) Rohdich, F.; Zepeck, F.; Adam, P.; Hecht, S.; Kaiser, J.; Laupitz, R.; Grawert, T.; Amslinger, S.; Eisenreich, W.; Bacher, A.; Arigoni, D. The deoxyxylulose phosphate pathway of isoprenoid biosynthesis: studies on the mechanisms of the reactions catalyzed by IspG and IspH protein. *Proc. Natl. Acad. Sci. U S A* **2003**, *100*, 1586-1591.

(43) White, R. H. Stable isotope studies on the biosynthesis of the thiazole moiety of thiamin in *Escherichia coli. Biochemistry* **1978**, *17*, 3833-3840.

(44) Himmeldirk, K.; Kennedy, I. A.; Hill, R. E.; Sayer, B. G.; Spenser, I. D. Biosynthesis of vitamin B_1 and B_6 in Escherichia coli: consurrent incorporation of 1-deoxy-D-xylulose into thiamin (B_1) and pyridoxol (B_6). *J. Chem. Soc., Chem. Commun.* **1996**, 1187-1188.

(45) Therisod, M.; Fischer, J. C.; Estramareix, B. The origin of the carbon chain in the thiazole moiety of thiamine in Escherichia coli: incorporation of deuterated

1-deoxy-D-threo-2-pentulose. *Biochem. Biophys. Res. Commun.* **1981**, *98*, 374-379.

(46) Sprenger, G. A.; Schörken, U.; Wiegert, T.; Grolle, S.; Graaf, A. A. D.; Taylor, S. V.; Begley, T. P.; Bringer-Meyer, S.; Sahm, H. Identification of a thiamin-dependent synthase in *Escherichia coli* required for the formation of the 1-deoxy-D-xylulose 5-phosphate precursor to isoprenoids, thiamin, and pyridoxaol. *Proc. Natl. Acad. Sci. U S A* **1997**, *94*, 12857-12862.

(47) Schwender, J.; Seemann, M.; Lichtenthaler, H. K.; Rohmer, M. Biosynthesis of isoprenoids (carotenoids, sterol, prenyl side-chains of chlorophylls and plastoquinone) via a novel pyruvate.gylceraldehyde 3-phosphate non-mevalonate pathway in the green alga *Scenedesmus Obliquus*. *Biochem. J.* **1996**, *316*, 73-80.

(48) Seto, H.; Watanabe, H.; Furihata, K. Simultaneous operation of the mevalonate and non-mevalonate pathway in the biosynthesis of isopentenyl diphosphate in *Streptomyces aeriouvifer*. *Tetrahedron Lett.* **1996**, *37*, 7979-7982.

(49) Eisenreich, W.; Menhard, B.; Hylands, P. J.; Zenk, M. H.; Bacher, A. Studies on the biosynthesis of taxol: the taxane carbon skeleton is not of mevalonoid origin. *Proc. Natl. Acad. Sci. U S A* **1996**, *93*, 6431-6436.

(50) Duvold, T.; Bravo, J.-M.; Pale-Grosdemange, C.; Rohmer, M. Biosynthsis of 2-C-methyl-D-erythritol, a putative C_5 intermediate in the mevelonate independent pathway for isoprenoid bisynthesis. *Tetrahedron Lett.* **1997**, *38*, 4769-4772.

(51) Lichtenthaler, H. K.; Schwender, J.; Disch, A.; Rohmer, M. Biosynthesis of isoprenoids in higher plant chloroplasts proceeds via a mevalonate-independent pathway. *FEBS Lett.* **1997**, *400*, 271-274.

(52) Duvold, T.; Cali, P.; Bravo, J.-M.; Rohmer, M. Incorporation of 2-C-methyl-D-erythritol, a putative C_5 isoprenoid precursor in the mevelonate-independent pathway, into ubiquinone and menaquinone of *Escherichia coli*. *Tetrahedron Lett.* **1997**, *38*, 6181-6184.

(53) Kuzuyama, T.; Takahashi, S.; Watanabe, H.; Seto, H. Direct Formation of 2-C-methyl-D-erythritol 4-phosphate from 1-deoxy-D-xylulose 5-phosphate by 1-deoxy-D-xylulose 5-phosphate reductoisomerase, a new enzyme in the non-mevalonate pathway to isopentenyl diphosphate. *Tetrahedron Lett.* **1998**, *39*, 4509-4512.

(54) Takahashi, S.; Kuzuyama, T.; Watanabe, H.; Seto, H. A 1-deoxy-D-xylulose 5-phosphate reductoisomerase catalyzing the formation of 2-C-methyl-D-erythritol 4-phosphate in an alternative nonmevalonate pathway for terpenoid biosynthesis. *Proc. Natl. Acad. Sci. U S A* **1998**, *95*, 9879-9884.

(55) Proteau, P. J.; Woo, Y.-H.; Williamson, R. T.; Phaosiri, S. Stereochemistry of the reduction step mediated by recombinant 1-deoxy-D-xylulose 5-phosphate isomeroreductase. *Org. Lett.* **1999**, *1*, 921-923.

(56) Giner, J. L.; Jaun, B.; Arigoni, D. Biosynthesis of isoprenoids in *Escherichia coli*: The fate of the 3-H and 4-H atoms of 1-deoxy-d-xyxyluose. *Chem. Commun.* **1998**, 1857-1858.

(57) Reuter, K.; Sanderbrand, S.; Jomaa, H.; Wiesner, J.; Steinbrecher, I.; Beck, E.; Hintz, M.; Klebe, G.; Stubbs, M. T. Crystal structure of 1-deoxy-D-xylulose-5-phosphate reductoisomerase, a crucial enzyme in the non-mevalonate pathway of isoprenoid biosynthesis. *J. Biol. Chem.* **2002**, *277*, 5378-5384.

(58) Yajima, S.; Nonaka, T.; Kuzuyama, T.; Seto, H. Crystal structure of 1-deoxy-D-xylulose 5-phosphate reductoisomerase complexed with cofactors: Implications of a flexible loop movement upon substrate binding. *J. Biochem.* **2002**, *131*, 313-317.

(59) Okuhara, M.; Kuroda, Y.; Goto, T.; Okamoto, M.; Terano, H.; Kohsaka, M.; Aoki, H.; Imanaka, H. Studies on new phosphonic acid antibiotics. III. Isolation and characterization of FR-31564, FR-32863 and FR-33289. *J. Antibiotics* **1980**, *33*, 24-28.

(60) Shigi, Y. Inhibition of bacterial isoprenoid synthesis by fosmidomycin, a phosphonic acid-containing antibiotic. *J. Antimicrob. Chemother.* **1989**, *24*, 131-145.

(61) Kuzuyama, T.; Shimizu, T.; Takahashi, S.; Seto, H. Fosmidomycin, a specific inhibitor of 1-deoxy-D-xylulose 5-phosphate reductoisomerase in the nonmevalonate pathway for terpenoid biosynthesis. *Tetrahedron Lett.* **1998**, *39*, 7913-7916.

(62) Rohdich, F.; Wungsintaweekul, J.; Fellermeier, M.; Sagner, S.; Herz, S.; Kis, K.; Eisenreich, W.; Bacher, A.; Zenk, M. H. Cytidine 5'-triphosphate-dependent biosynthesis of isoprenoids: YgbP protein of Escherichia coli catalyzes the formation of 4-diphosphocytidyl-2-C-methylerythritol. *Proc. Natl. Acad. Sci. U S A* **1999**, *96*, 11758-11763.

(63) Herz, S.; Wungsintaweekul, J.; Schuhr, C. A.; Hecht, S.; Luttgen, H.; Sagner, S.; Fellermeier, M.; Eisenreich, W.; Zenk, M. H.; Bacher, A.; Rohdich, F.

Biosynthesis of terpenoids: YgbB protein converts 4-diphosphocytidyl-2-C-methyl-D-erythritol 2-phosphate to 2C-methyl-D-erythritol 2,4-cyclodiphosphate. *Proc. Natl. Acad. Sci. U S A* **2000**, *97*, 2486-2490.

(64) Luttgen, H.; Rohdich, F.; Herz, S.; Wungsintaweekul, J.; Hecht, S.; Schuhr, C. A.; Fellermeier, M.; Sagner, S.; Zenk, M. H.; Bacher, A.; Eisenreich, W. Biosynthesis of terpenoids: YchB protein of Escherichia coli phosphorylates the 2-hydroxy group of 4-diphosphocytidyl-2C-methyl-D-erythritol. *Proc. Natl. Acad. Sci. U S A* **2000**, *97*, 1062-1067.

(65) Takagi, M.; Kuzuyama, T.; Kaneda, K.; Watanabe, H.; Dairi, T.; Seto, H. Studies on the nonmevalonate pathway: formation of 2-C-methyl-D-erythritol 2,4-cyclodiphosphate from 2-phospho-4-(cytidine 5'-diphospho)-2-C-methyl-D-erythritol. *Tetrahedron Lett.* **2000**, *41*, 3395-3398.

(66) Kuzuyama, T.; Takagi, M.; Kaneda, K.; Watanabe, H.; Dairi, T.; Seto, H. Studies on the nonmevalonate pathway: conversion of 4-(cytidine 5'-diphospho)-2-C-methyl-D-erythritol to its 2-phospho derivative by 4-(cytidine 5'-diphospho)-2-C-methyl-D-erythritol kinase. *Tetrahedron Lett.* **2000**, *41*, 2925-2928.

(67) Kuzuyama, T.; Takagi, M.; Kaneda, K.; Dairi, T.; Seto, H. Formation of 4-(cytidine 5'-diphospho)-2-C-methyl-D-erythritol from 2-C-methyl-D-erythritol 4-phosphate by 2-C-methyl-D-erythritol 4-phosphate cytidylyltransferase, a new enzyme in the nonmevalonate pathway. *Tetrahedron Lett.* **2000**, *41*, 703-706.

(68) Richard, S. B.; Ferrer, J. L.; Bowman, M. E.; Lillo, A. M.; Tetzlaff, C. N.; Cane, D. E.; Noel, J. P. Structure and mechanism of 2-C-methyl-D-erythritol 2,4-cyclodiphosphate synthase. An enzyme in the mevalonate-independent isoprenoid biosynthetic pathway. *J. Biol. Chem.* **2002**, *277*, 8667-8672.

(69) Altincicek, B.; Kollas, A. K.; Sanderbrand, S.; Wiesner, J.; Hintz, M.; Beck, E.; Jomaa, H. GcpE is involved in the 2-C-methyl-D-erythritol 4-phosphate pathway of isoprenoid biosynthesis in Escherichia coli. *J. Bacteriol.* **2001**, *183*, 2411-2416.

(70) Campos, N.; Rodriguez-Concepcion, M.; Seemann, M.; Rohmer, M.; Boronat, A. Identification of gcpE as a novel gene of the 2-C-methyl-D-erythritol 4-phosphate pathway for isoprenoid biosynthesis in Escherichia coli. *FEBS. Lett.* **2001**, *488*, 170-173.

(71) Hecht, S.; Eisenreich, W.; Adam, P.; Amslinger, S.; Kis, K.; Bacher, A.; Arigoni, D.; Rohdich, F. Studies on the nonmevalonate pathway to terpenes: the role of the GcpE (IspG) protein. *Proc. Natl. Acad. Sci. U S A* **2001**, *98*, 14837-14842.

(72) Wolff, M.; Seemann, M.; Grosdemange-Billiard, C.; Trirsch, D.; Campos, N.; Rodriguez-Concepcion, M.; Boronat, A.; Rohmer, M. Isoprenoid biosynthesis via the methylerythritol phosphate pathway. (E)-4-hydroxy-3-methylbut-2-enyl diphosphate: chemical synthesis and formation from methylerythritol cyclodiphosphate by a cell-free system from Escherichia coli. *Tetrahedron Lett.* **2002**, *43*, 2555-2559.

(73) Kollas, A. K.; Duin, E. C.; Eberl, M.; Altincicek, B.; Hintz, M.; Reichenberg, A.; Henschker, D.; Henne, A.; Steinbrecher, I.; Ostrovsky, D. N.; Hedderich, R.; Beck, E.; Jomaa, H.; Wiesner, J. Functional characterization of GcpE, an essential enzyme of the non- mevalonate pathway of isoprenoid biosynthesis. *FEBS Lett.* **2002**, *532*, 432-436.

(74) Altincicek, B.; Kollas, A.; Eberl, M.; Wiesner, J.; Sanderbrand, S.; Hintz, M.; Beck, E.; Jomaa, H. LytB, a novel gene of the 2-C-methyl-D-erythritol 4-phosphate pathway of isoprenoid biosynthesis in Escherichia coli. *FEBS Lett.* **2001**, *499*, 37-40.

(75) Cunningham, F. X., Jr.; Lafond, T. P.; Gantt, E. Evidence of a role for LytB in the nonmevalonate pathway of isoprenoid biosynthesis. *J. Bacteriol.* **2000**, *182*, 5841-5848.

(76) Rohmer, M. The discovery of a mevalonate-independent pathway for isoprenoid biosynthesis in bacteria, algae and higher plants. *Nat. Prod. Rep.* **1999**, *16*, 565-574.

(77) Eisenreich, W.; Rohdich, F.; Bacher, A. Deoxyxyluose phosphate pathway to terpenoids. *Trends Plant Sci.* **2001**, *6*, 78-84.

(78) Rohmer, M. Isoprenoid biosynthesis via the mevalonate-dependent route. *Prog. Drug Res.* **1998**, *50*, 136-154.

(79) Putra, S. R.; Disch, A.; Bravo, J. M.; Rohmer, M. Distribution of mevalonate and glyceraldehyde 3-phosphate/pyruvate routes for isoprenoid biosynthesis in some gram-negative bacteria and mycobacteria. *FEMS. Microbiol. Lett.* **1998**, *164*, 169-175.

(80) Proteau, P. J. Biosynthesis of phytol in the cyanobacterium *Synechocystis sp.* UTEX 2470: utilization of the non-mevalonate pathway. *J. Nat. Prod.* **1998**, *61*, 841-843.

(81) Cane, D. E.; Rossi, T.; Tillman, A. M.; Pachlatko, J. P. Stereochemical studies of isoprenoid biosynthesis. biosynthesis of pentalenolactone from [U-$^{13}C_6$]glucose and [6-$^{2}H_2$]-glucose. *J. Am. Chem. Soc.* **1981**, *103*, 1838-1843.

(82) Seto, H.; Orihara, N.; Furihata, K. Studies on the biosynthsis of terpenoids produced by Actinomycetes. Part 4. Formation of BE-40644 by the mevelonate and nonmevalonate pathways. *Tetrahedron Lett.* **1998**, *39*, 9497-9500.

(83) Kuzuyama, T.; Takahashi, S.; Dairi, T.; Seto, H. Detection of the mevalonate pathway in streptomyces species using the HMG-CoA reductase gene. *J. Antibiot.* **2002**, *10*, 919-923.

(84) Orihara, N.; Kuzuyama, T.; Takahashi, S.; Furihata, K.; Seto, H. Studies on the biosynthesis of terpenoid compounds produced by actinomycetes. 3. Biosynthesis of the isoprenoid side chain of novobiocin via the non-mevalonate pathway in Streptomyces niveus. *J. Antibiot.* **1998**, *51*, 676-678.

(85) Li, S. M.; Henning, S.; Heide, L. Biosynthesis of the dimethylallyl moiety of novobiocin via a non-mevalonate pathway. *Tetrahedron Lett.* **1998**, *39*, 2717-2720.

(86) Schuricht, U.; Henning, L.; Findeisen, M.; Welzel, P.; Arigoni, D. The biosynthesis of moenocinol, the lipid part of the moenomycin antibiotics. *Tetrahedron Lett.* **2001**, *42*, 3835-3837.

(87) Hamano, Y.; Dairi, T.; Yamamoto, M.; Kuzuyama, T.; Itoh, N.; Seto, H. Growth-phase dependent expression of the mevalonate pathway in a terpenoid antibiotic-producing Streptomyces strain. *Biosci. Biotechnol. Biochem.* **2002**, 66, 808-819.

(88) Schwender, J.; Gemünden, C.; Lichtenthaler, H. K. Chlorophyta exclusively use the 1-deoxyxylulose 5-phosphate/2-C-methylerythritol 4-phosphate pathway for the biosynthesis of isoprenoids. *Planta* **2001**, *212*, 416-423.

(89) Lichtenthaler, H. K. The plants' 1-deoxyD-xylulose-5-phosphate pathway for biosynthesis of isoprenoids. *Fett/Lipid* **1998**, *100*, 128-138.

(90) Kleinig, H. The role of plastids in isoprenoid biosynthesis. *Annu. Rev. Plant Physiol. Plant Mol. Biol.* **1989**, *40*, 39-59.

(91) Boucher, Y.; Doolittle, W. F. The role of lateral gene transfer in the evolution of isoprenoid biosynthesis pathways. *Mol. Microbiol.* **2000**, *37*, 703-716.

(92) Piel, J.; Donath, J.; Bandemer, K.; Boland, W. Mevalonate-independent biosynthesis of terpenoid volatiles in plants: induced and constitutive emission of volatiles. *Angew. Chem. Int. Ed.* **1998**, *37*, 2478-2481.

(93) Itoh, D.; Karunagoda, R. P.; Fushie, T.; Katoh, K.; Nabeta, K. Nonequivalent labeling of the phytyl side chain of chlorophyll *a* in callus of the hornwort *Anthoceros punctatus*. *J. Nat. Prod.* **2000**, *63*, 1090-1093.

(94) Nabeta, K.; Kawae, T.; Saitoh, T.; Kikuchi, T. Syntheis of chlorophyll a and β-carotene from ^{2}H- and ^{13}C-labelled mevalonates and ^{13}C-labelled glycine in cultured cells of liverworts, *Heteroscyphus planus* and *Lophocoles heterophylla*. *J. Chem. Soc., Perkin Trans. 1* **1997**, 261-267.

(95) Lichtenthaler, H. K.; Zeidler, J.; Schwender, J.; Muller, C. The non-mevalonate isoprenoid biosynthesis of plants as a test system for new herbicides and drugs against pathogenic bacteria and the malaria parasite. *Z. Naturforsch. [C]* **2000**, *55*, 305-313.

(96) Dubey, V. S. Mevalonate-independent pathway of isoprenoids synthesis: A potential target in some human pathogens. *Curr. Sci.* **2002**, *83*, 685-688.

(97) Jomaa, H.; Wiesner, J.; Sanderbrand, S.; Altincicek, B.; Weidemeyer, C.; Hintz, M.; Turbachova, I.; Eberl, M.; Zeidler, J.; Lichtenthaler, H. K.; Soldati, D.; Beck, E. Inhibitors of the nonmevalonate pathway of isoprenoid biosynthesis as antimalarial drugs. *Science* **1999**, *285*, 1573-1576.

(98) Wiesner, J.; Henschker, D.; Hutchinson, D. B.; Beck, E.; Jomaa, H. In vitro and in vivo synergy of fosmidomycin, a novel antimalarial drug, with clindamycin. *Antimicrob. Agents Chemother.* **2002**, *46*, 2889-2894.

(99) Reichenberg; A. Wiesner, J.; Weidemeyer, C.; Dreiseidler, E.; Sanderbrand, S.; Altincicek, B.; Beck, E.; Schlitzer, M. Diaryl ester prodrugs of FR900098 with improved in vivo antimalarial activity. *Bioorg. Med. Chem. Lett.* **2001**, *11*, 833-835.

(100) Müller, C.; Schwender, J.; Disch, A.; Rohmer, M.; Lichtenthaler, F. W.; Lichtenthaler, H. K. Occurence of the 1-deoxy-D-xylulose 5-phosphate pathway of isopentenyl diphosphate biosynthesis in different algae groups. *Adv. Plant Lipid Res.* **1998**, 425-428.

(101) Disch, A.; Schwender, J.; Muller, C.; Lichtenthaler, H. K.; Rohmer, M. Distribution of the mevalonate and glyceraldehyde phosphate/pyruvate pathways for isoprenoid biosynthesis in unicellular algae and the cyanobacterium *Synechocystis PCC 6714*. *Biochem. J.* **1998**, *333*, 381-388.

CHAPTER TWO

Carotenoid Biosynthesis in *Euglena gracilis*

Introduction

The genus *Euglena* is a unicellular algal flagellate group which lies on the borderline between the plant and animal kingdom.[1,2] Most early biochemical studies reported for *Euglena* focused on its plantlike features such as photosynthesis. Enzymological studies, however, appear to reveal more of its animal-like features or its enzymatic characteristics independent of either plant or animal enzymes.[3] Owing to having both plant-like and animal-like features, *Euglena* species have been employed as model systems for various studies on structure and function in cell biology.[4] *Euglena* species are found in a very wide range of environments from fresh water to salt water. *E. deses* is common in mud banks exposed by tidal action, and *E. mutabilis* can be seen in pond water, salt water, and even mine sewage.[5]

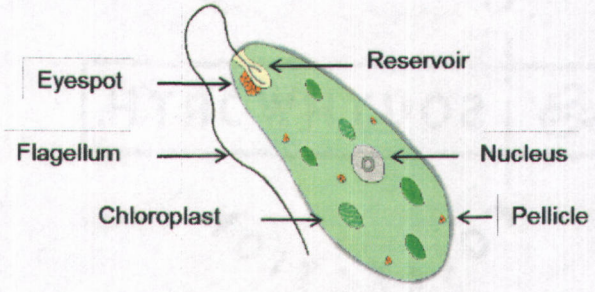

Fig.2.1. *Euglena* cell of the *E. gracilis* type, showing the main organelles.[6]

Structurally, *Euglena* species are characterized by distinct substructures such as chloroplasts, a flagellum, and an eyespot (Fig.2.1).[6] *Euglena* chloroplasts, which have great diversity in shape and number, contain chlorophylls *a* and *b*, carotenoids, and quinones and are used for species determination. The chloroplasts have a specialized function in photosynthesis and a genetic system independent of the

nucleus of the cell.[7] One emergent flagellum in *Euglena* species provides for locomotion to freely swim. The eyespot, also known as the stigma, is located on the surface of a reservoir, a chamber at the base of flagellum. The eyespot is composed of orange-red droplets, containing carotenoid pigments, flavins, lipids, and proteins which are individually surrounded by a membrane.[6] Some of the droplets appear to be separated from the main mass throughout the cytoplasm. The function of the eyespot is assumed to be a receptor for light perception which allows the organisms to move away from intense light (negative phototaxis) and from darkness to light (positive phototaxis).[8]

Among *Euglena* species, *E. gracilis* is the most well-defined species and mainly inhabits fresh water. For a long time, *E. gracilis* has been used as an accessible tool for biological investigations. There are several advantages for using *E. gracilis*: (1) it is able to be grown axenically, so its biological activity is not complicated by the presence of other organisms, (2) it grows on well-defined media containing inorganic or organic materials over a wide range of pH, which allows manipulation of the culture environment for various studies, (3) it can utilize various exogenous carbon sources for heterotrophic growth, (4) *E. gracilis* is able to interconvert between two forms, of which one is a photosynthetic, autotrophic and green form when grown in light, and the other is a non-photosynthetic, heterotrophic and etiolated form containing neither chloroplasts nor proplastids when grown in the dark.[9-11]

Aided by these features, several biosynthetic pathways and their enzymes have been characterized in *E. gracilis*.[3] One example is chlorophyll biosynthesis. Chlorophylls and heme, both tetrapyrrole derivatives, are derived from the committed precursor, 5-aminolevulinic acid (ALA) which is produced via two independent pathways, the C-5 pathway arising from glutamate and the Shemin pathway from the condensation of glycine and succinate.[3,12] Plants and most algae are able to utilize only the C-5 pathway, while photosynthetic bacteria, yeast, and animal mitochondria use only the Shemin pathway. Interestingly, *E. gracilis* was reported to have both ALA-forming pathways, producing plastid tetrapyrroles from glutamate and mitochondrial heme from glycine and succinate.[3]

There is a long history of studies on *E. gracilis* pigments. The identification and distribution of these metabolites have been explored in the normal green strain

as well as in the etiolated form. Carotenoid pigments are derived from phytoene, the first intermediate of carotenoid biosynthesis, formed by head-to-head condensation of two geranylgeranyl diphosphate (GGPP) molecules which are derived from four isoprene units, three isopentenyl diphosphates (IPP) and one dimethylallyl diphosphate (DMAPP).[13,14] Phytoene undergoes a series of desaturation and cyclization reactions to produce various carotenes, mainly β-carotene. Oxygen is introduced into the carotenes to form the xanthophylls, neoxanthin, diatoxanthin, and diadinoxanthin (Fig.2.2).

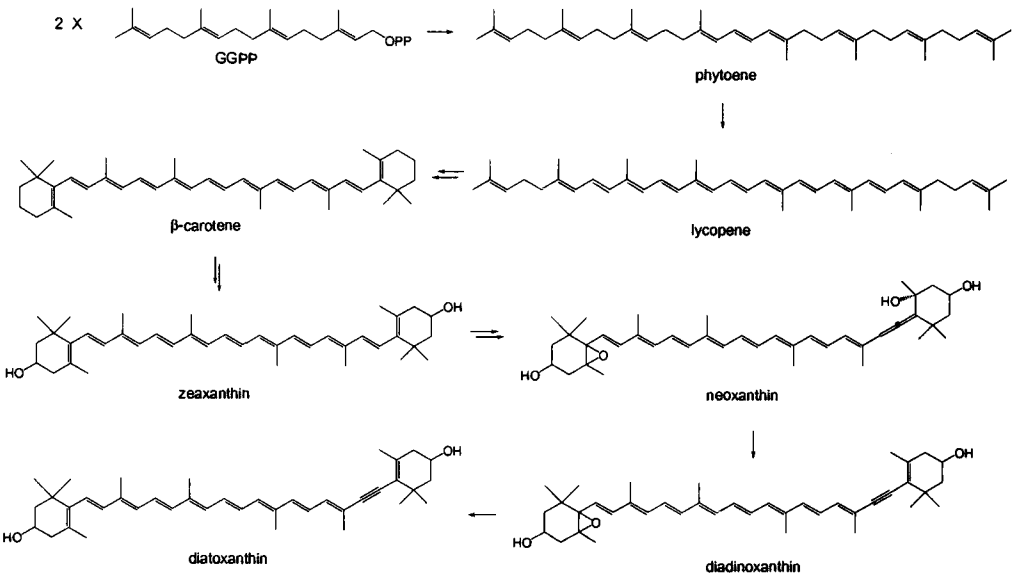

Fig.2.2. Sequence of the reactions in the biosynthesis of carotenoids.

Although all of the carotenoid pigments of *E. gracilis* have not been identified, more than ten compounds have been characterized, including *β*-carotene, diatoxanthin, diadinoxanthin, neoxanthin, and cryptoxanthin.[15] The major eyespot pigments were reported to be *β*-carotene, diatoxanthin, and diadinoxanthin, which make up 60 % of the eyespot pigments. In the case of diadinoxanthin, its identification was clarified in 1977, after initial characterization of this carotenoid as antheraxanthin.[15-18]

Initial studies on carotenoid biosynthesis in *E. gracilis* date from 1960,[19] shortly after the discovery of mevalonate (MVA) as a precursor in the MVA pathway

to isoprenoid compounds. Steele *et al.* initiated the study on the *E. gracilis* carotenoid biosynthesis.[19] They employed degradation studies of β-carotene isolated from incubation experiments with radiolabeled precursors such as [1-^{14}C]- or [2-^{14}C]-acetate, [2-^{14}C]-MVA, and [methyl-^{14}C]-3-hydroxy-3-methylglutaric acid (HMG) which are the precursors in the MVA pathway. Several related branched chain derivatives such as [4,4'-^{14}C]-β-dimethylacrylic acid, [4,4'-^{14}C]-β-dimethylacrylaldehyde, [4,4'-^{14}C]-dimethylallyl alcohol, [4,4'-^{14}C]-isovaleric acid, and [4,4'-^{14}C]-isoamyl alcohol were also examined. From these experiments, they determined that the methyl and carboxyl carbons of acetate were incorporated into around 30 % of the carbon skeleton of β-carotene, whereas other potential precursors were poorly incorporated. It was of interest that labeled MVA and HMG, the intermediates in the MVA pathway, were poorly incorporated into β-carotene. Consequently, they surmised that the poor incorporation of HMG might be attributed to utilization of the compound for growth, but not carotenogenesis, and labeled isovalerate, which was detected as acetate units, might be utilized as a source of carbon after preliminary degradation to smaller units. The poor incorporation of MVA as the committed precursor of isoprenoid biosynthesis was an unexpected result because a high degree of incorporation of the intact MVA was successfully reported in the carotenes of tomato fruit, carrot slices, and *Phycomyces blakesleeanus*.[20,21] They considered that the poor incorporation of MVA is attributed to the slow conversion of MVA into an active precursor of β-carotene.

In 1967, Goodwin *et al.* reexamined the incubation experiment with [2-^{14}C]-MVA into β-carotene, sterols, and quinones, and obtained similar results to Steele *et al.* including a very low incorporation of MVA into any of the isoprenoid compounds examined (0.022-0.060 %).[22] These results were interpreted to mean that MVA may not be able to penetrate the cell pellicle of *E. gracilis* to be utilized, rather than being an indication of a novel pathway of isoprenoid biosynthesis.[22] Cooper *et al.* suggested that radiolabeled pyruvate and succinate are efficient precursors to go through the chloroplasts for β-carotene biosynthesis.[23] Therefore, these preliminary studies drew the conclusion that carotenoid biosynthesis in *E. gracilis* occurs by the MVA pathway explaining the low incorporation of MVA and its related precursors into isoprenoids.

After discovery of the 2-*C*-methyl-D-erythritol-4-phosphate (MEP) pathway in the early 1990's, the isoprenoid biosynthetic pathway of *E. gracilis* attracted attention from scientists once again. The reason is that most photosynthetic organisms had been revealed to possess the MEP pathway in their chloroplasts. Despite the early work by Goodwin and others, *E. gracilis* would also be expected to use the MEP pathway for the formation of plastidic isoprenoids such as β-carotene and phytol. Evolutionarily, *E. gracilis* is proposed to have acquired its chloroplasts from a green alga through an endosymbiotic event,[24] and green algae had been shown to use the MEP pathway.[25]

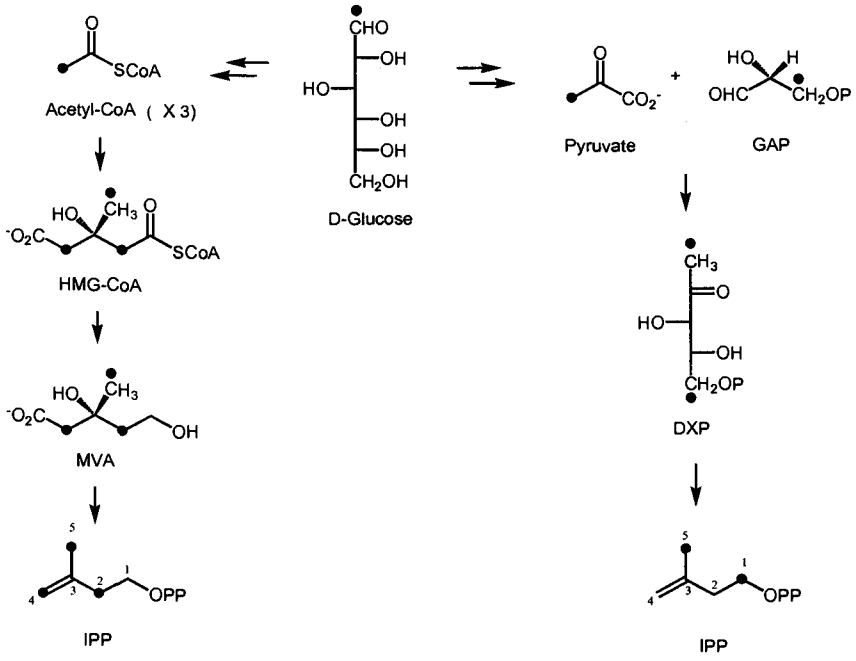

Fig.2.3. Labeling pattern for each pathway derived from [1-^{13}C]-glucose. Filled circles indicate ^{13}C labeled carbons.

In 1998, Rohmer, Lichtenthaler, *et al.* published a paper dealing with this subject.[26] They investigated the distribution of both pathways in unicellular algae, including *E. gracilis*. During this work, they differentiated the two pathways by examining incorporation patterns of isoprenoids derived from the [1-^{13}C]-glucose feeding experiment. Incorporation of [1-^{13}C]-glucose into IPP proceeds differently for each pathway (Fig.2.3). The [1-^{13}C]-glucose would be catabolized to [2-^{13}C]-acetate and the isotope labels would be subsequently introduced to IPP at C2, C4, and C5

via the MVA pathway, whereas [3-^{13}C]-glyceraldehyde-3-phosphate (GAP) and [3-^{13}C]-pyruvate derived from [1-^{13}C]-glucose would be utilized via the MEP pathway to provide [1-^{13}C]-IPP and [5-^{13}C]-IPP. In other words, even though C5 may be the inappropriate carbon to differentiate the pathways due to its enrichment via both pathways, C1 of IPP is the specific labeling site through the MEP pathway, and C2 and C4 of IPP are labeled via the MVA pathway. Therefore, the incubation experiment with [1-^{13}C]-glucose should offer a simple method to determine the pathway which each organism utilizes to produce isoprenoids .[26]

Based on this approach, isotopic abundances of each isoprene unit of isoprenoids from a range of organism were investigated. Isoprenoids examined in this study were classified as plastidic isoprenoids and cytosolic isoprenoids, according to their labeling patterns. The results from the experiment with [1-^{13}C]-glucose revealed that: (1) green algae and cyanobacteria utilize only the MEP pathway to synthesize isoprenoid compounds, (2) red algae and *Chrysophyta* are able to synthesize plastidic isoprenoids such as β-carotene and phytol via the MEP pathway and cytosolic sterols via the MVA pathway simultaneously, and (3) *E. gracilis* utilizes only the MVA pathway to produce phytol as well as cytosolic sterols (Table 2.1).

Table 2.1. Distribution of isoprenoid biosynthetic pathways in algae and cyanobacteria to various isoprenoid compounds based on published reports.

Organism	β-carotene	phytol	sterols
Cyanobacteria	MEP pathway	MEP pathway	-[a]
Chlorophyta	MEP pathway	MEP pathway	MEP pathway
Chrysophyta	MEP pathway	MEP pathway	MVA pathway
Rhodophyta	MEP pathway	MEP pathway	MVA pathway
E. gracilis	MVA pathway[b]	MVA pathway	MVA pathway

[a] Cyanobacteria do not produce sterols, but some can produce hopanoids, which are made via the MEP pathway.[27]
[b] Result based on work in 1960.[19]

Compared with other photosynthetic organisms, the MVA labeling pattern for plastidic isoprenoids of *Euglena* is a result entirely beyond expectations. Therefore, taking these results as well as previous ones, the authors drew the conclusion that among the photosynthetic organisms studied to date, this *Euglenophyte* is the only one for which no evidence for the MEP pathway could be found, even for the formation of plastidic isoprenoids.[26,28]

In this chapter, a reexamination of *E. gracilis* will be detailed, focusing on carotenoid biosynthesis. The reasons for conducting further studies on *Euglena* carotenoid biosynthesis are that carotenoid compounds were not examined in the previous studies by Disch *et al.* and Müller *et al.* and preliminary incubation experiments in our laboratory using [6-$^2H_2$]-glucose suggested that the MEP pathway may contribute at least a small amount to phytol and carotenoid biosynthesis. Glucose labeled at C6 will result in labeling of IPP in the same manner as glucose labeled at C1. In other words, C1 and C5 will have labels via the MEP pathway. Low levels of deuterium were observed at C1 of phytol and C3 and C28 of diadinoxanthin. These positions are derived from C1 of IPP. This evidence does not agree with the published results and warrants further investigation. Several incubation experiments with labeled glucose and acetate, as well as other potential precursors were carried out to trace the labeling patterns of the major carotenoid compounds in *E. gracilis: β*-carotene and diadinoxanthin (Fig.2.4).

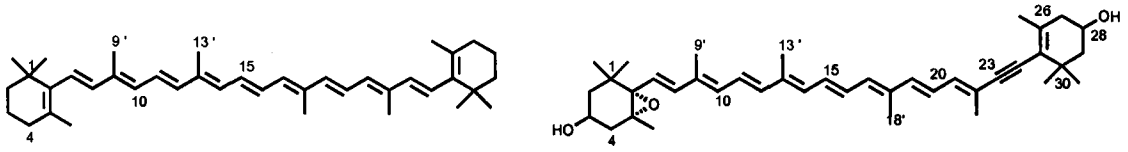

Fig.2.4. Structures of major carotenoids in *E. gracilis*.

Results and Discussion

MEP pathway in *E. gracilis*

In order to test the carotenoid biosynthetic pathway in *E. gracilis*, an incubation experiment using [1-^{13}C]-glucose was performed. As shown in Fig.2.3, this experiment gives us a preliminary idea about the presence of each pathway. If β-carotene and diadinoxanthin are produced via the MVA pathway, carbons corresponding to C2 and C4 of isoprene units will be labeled. If ^{13}C isotopes of [1-^{13}C]-glucose are seen at C1 of isoprene units, carotenoids are able to be synthesized via the MEP pathway.

In spite of the early conclusion in the 1960's that carotenoid biosynthesis occurs via the MVA pathway, the labeling patterns from the incubation experiment with [1-^{13}C]-glucose showed complicated features in both β-carotene and diadinoxanthin (Fig.2.5). Varying levels of incorporation were observed for all positions derived from IPP/DMAPP except C3, the carbon that wouldn't be labeled by either pathway. Considering the relative incorporation levels, the labeling pattern of carotenoids might be characterized as three parts: the first DMAPP unit, the two central IPP units, and the terminal IPP added to form GGPP. To differentiate these three parts, the intensities of carbons corresponding to C1 and C2 of each isoprene unit were compared, because C1 and C2 are the representative positions labeled from [1-^{13}C]-glucose via the MEP pathway and the MVA pathway, respectively. Signals of the backbone methyl carbons are excluded from the comparison due to their enhancement via both pathways. The incubation experiment using [1-^{13}C]-glucose was performed twice under the same conditions. In the case of the second experiment, the inverse gated proton decoupling technique[29] was applied to compare the peak intensity values for each carbon between labeled and unlabeled carotenoid compounds. Although this technique causes lower sensitivity because of the absence of the nuclear overhauser effect (NOE),[30] each signal strength is proportional to the number of carbons or incorporation level of the ^{13}C atoms.

In the case of β-carotene (Fig.2.5), similar incorporation levels at C1 (2.5) and C2 (2.4) were observed in the DMAPP-derived unit, which suggests that *E. gracilis* operates both pathways to produce DMAPP for carotenoid synthesis. In the two

central IPP-derived units, the incorporation level of C2 (2.1-2.3) appeared higher than C1 (1.5-1.6), which represents that the MVA pathway is preferably utilized to form these IPP-derived units. In contrast with the central IPP units, the MEP pathway appears to predominate for production of the terminal IPP, based on the observation that the incorporation at C1 (2.5) is 1.7 times higher than C2 (1.5).

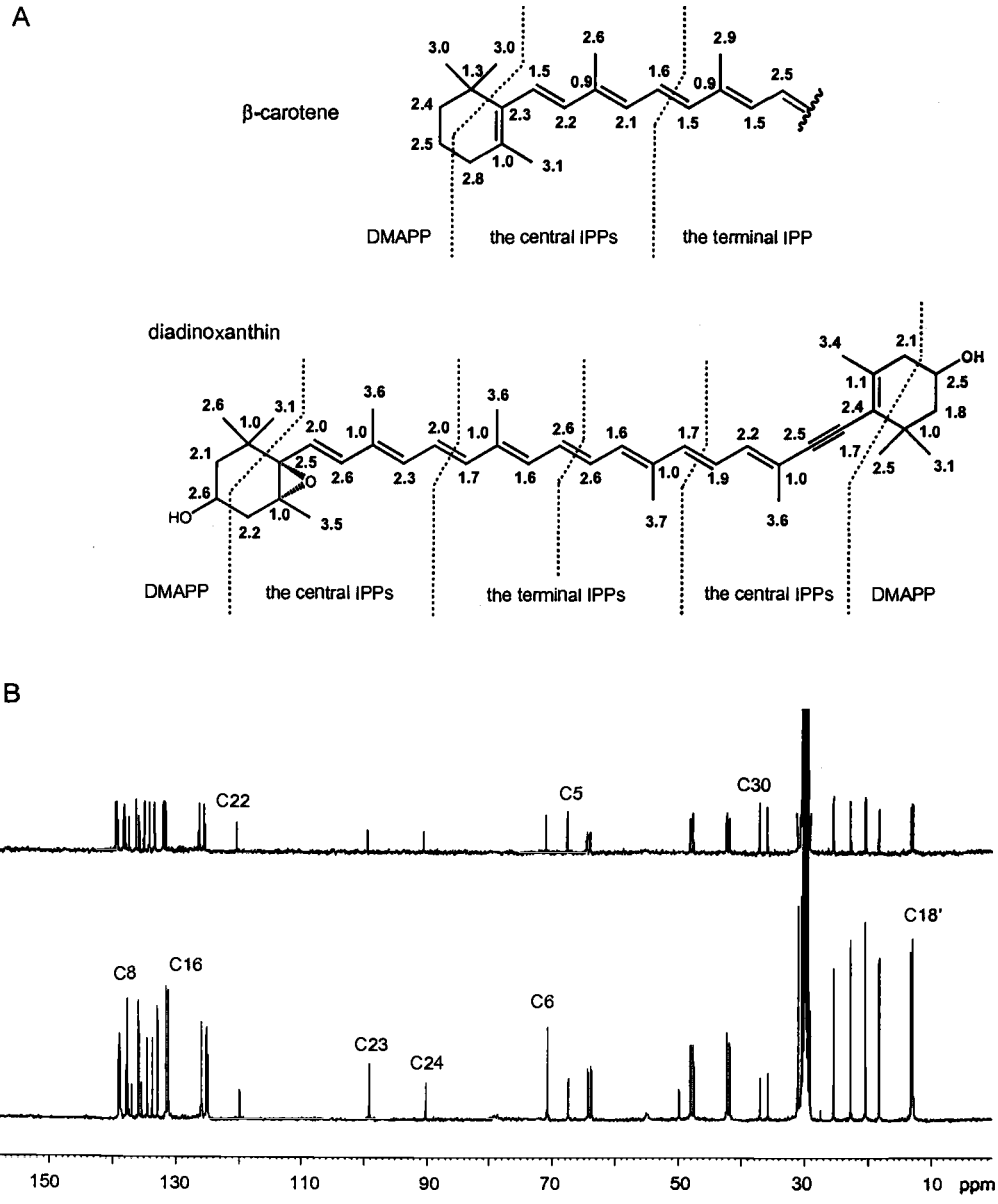

Fig.2.5. Incorporation levels (A) for β-carotene and diadinoxanthin from the [1-^{13}C]-glucose incubation experiment . ^{13}C-NMR Spectra (B) for unlabeled (upper) and [1-^{13}C]-glucose-labeled (lower) diadinoxanthin.

This labeling pattern also occurred in diadinoxanthin (Fig.2.5). The MEP pathway seems to be slightly preferred rather than the MVA pathway in the first DMAPP. In contrast, the MVA pathway has slight priority in the two central IPP units over the MEP pathway. In the terminal IPPs, the incorporation ratio of C1 (2.6) via the MEP pathway is 1.6 times higher than C2 (1.6) via the MVA pathway. These results were quite different with previous ones, which concluded that there was no existence of the MEP pathway for the production of isoprenoids in *E. gracilis*.[26,28] Although it is unclear exactly what the differential labeling of the isoprene units within the carotenoids means, there is now strong evidence that *E. gracilis* does in fact use the MEP pathway.

Although it is not comparable with the labeling pattern of *Euglena* carotenoid compounds, an unequivalent labeling pattern had been reported in β-carotene of liverworts, *Heteroscyphus planus* and *Lophocolea heterophylla*, from [2,2-$^{2}H_2$]-MVA, [2-^{13}C]-MVA, and [4,5-^{13}C]-MVA by Nabeta *et al.*[31] Through these incubation experiments, the labeled compounds were found to be efficiently incorporated into the FPP unit but not into the terminal IPP-derived unit of β-carotene. Based on these results, they suggested that β-carotene might be formed through condensation of cytosolic FPP synthesized via the MVA pathway and plastidic IPP made via the MEP pathway.

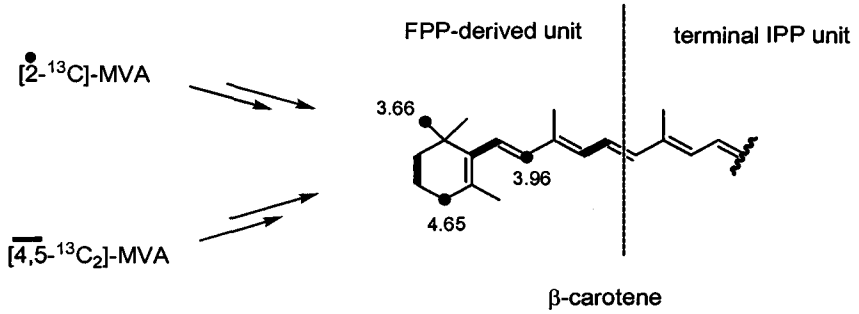

Fig.2.6. Labeling patterns for β-carotene of liverworts from the [2-^{13}C]-MVA (•) and from [4,5-$^{13}C_2$]-MVA (–) incubation experiments by Nabeta *et al.*[31] Numbers indicate ^{13}C enrichments in each carbon.

To confirm the preliminary result that *E. gracilis* is able to utilize the MEP pathway to produce carotenoids, further evidence was needed. An incubation

experiment using labeled DXP, a key intermediate of the MEP pathway, was regarded as a better way to elucidate this. Although DX itself is not a true intermediate of the MEP pathway, most organisms have enzymes which can catalyze phosphorylation of this sugar, and previous incubation experiments with labeled DX in other laboratories had demonstrated that labeled DX could be effectively assimilated and converted to DXP to elucidate the MEP pathway.[32-34] Based on this prior work, it seemed likely that *E. gracilis* could transform DX to DXP, so we decided to prepare the deuterated DX. In addition, the position labeled with deuterium in DX should be recognizable to readily discriminate the two pathways in the carotenoid NMR spectra. Although it is not known how DX is catabolized in various organisms, it was considered a possibility that DX labeled with deuterium at C1 might be broken down to labeled acetate which could be utilized via the MVA pathway,[35] leading to a complicated labeling pattern of carotenoid compounds. After due consideration, DX labeled at H5 with deuterium was prepared for the next incubation experiment, because H5 should be retained throughout the transformation of DX to IPP and the elongation reactions of the isoprene units. Consequently, [5-$^2H_2$]-DX will be converted to [1-$^2H_2$]-IPP and utilized for the formation of carotenoids. The synthetic scheme of [5-$^2H_2$]-DX was modified from known procedures[36,37] and is depicted in Figure 2.7.

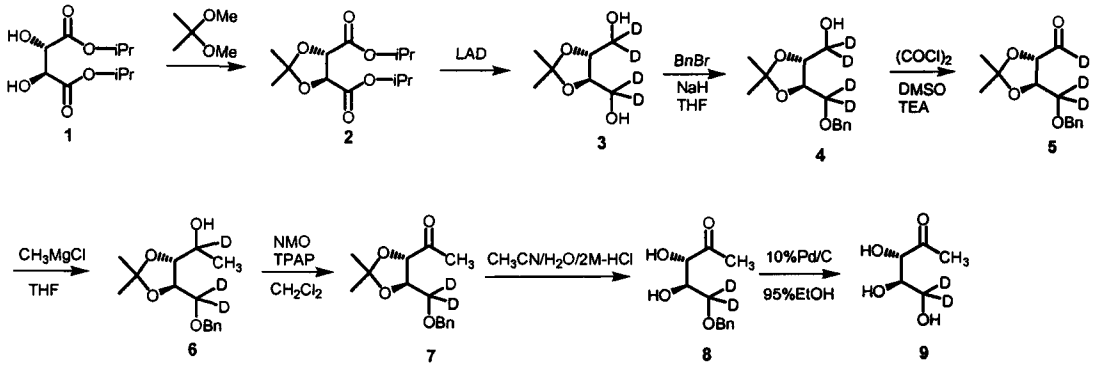

Fig.2.7. Synthesis of [5-$^2H_2$]-DX (**9**)

Diisopropyl-2,3-O-isopropylidene-D-tartrate (**1**) was employed as a starting material and was protected as a ketal. Deuterium was introduced into the ester carbons of the tartrate from $LiAlD_4$. After protecting one alcohol group with benzyl

bromide, Swern oxidation with dimethylsulfoxide (DMSO) and oxalyl chloride and methylation with a Grignard reagent followed. Further oxidation of the alcohol group was carried out with tetrapropylammonium perruthenate (TPAP), and a deprotection reaction of the ketal derivative was performed in a mixture of acetonitrile and dilute acid. The purified benzyl derivative (**8**) was deprotected with 10 % Pd/C in EtOH to provide the pure [5-$^2H_2$]-DX (**9**). The synthesized [5-$^2H_2$]-DX was dissolved in *dd*-H_2O and directly added to a solution of unlabeled glucose for the incubation experiment. For the incubation experiment using [5-$^2H_2$]-DX, *E. gracilis* was grown for 13 days instead of 7 days for a normal incubation period.

If the intact [5-$^2H_2$]-DX is incorporated into isoprenoid compounds via the MEP pathway, the isotopes would be observed in the sites corresponding to H1 of the IPP and DMAPP units. Based on the preliminary results with [1-^{13}C]-glucose, carotenoids would be expected to possess the isotopes at defined positions (Fig.2.8). If the labeled DX is catabolized to primary precursors, less specific labeling would be observed.

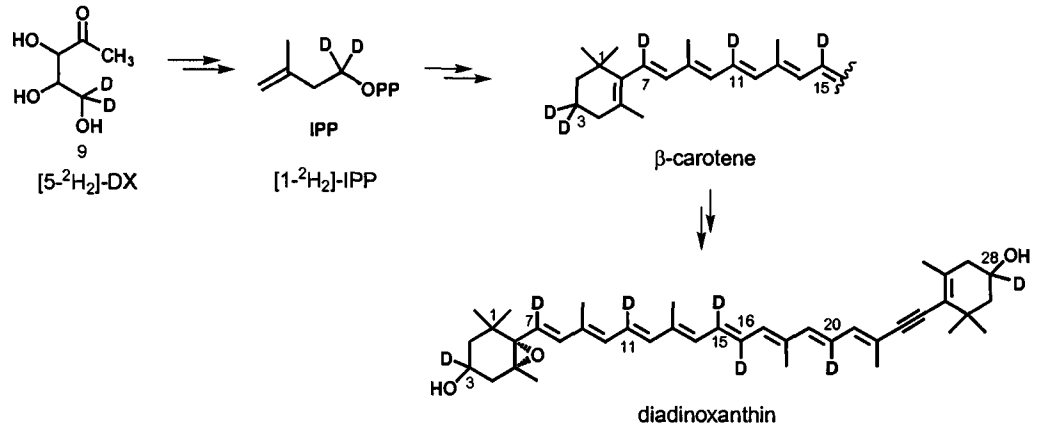

Fig.2.8. Predicted labeling patterns for carotenoids from [5-$^2H_2$]-DX via the MEP pathway.

In the ^{2}H-NMR spectrum of diadinoxanthin, peaks were found at 3.7, 3.8, 6.0, and 6.7 ppm (Fig.2.9). The peaks at 3.7 and 3.8 ppm correspond to the protons at H3 and H28 of diadinoxanthin. The peaks at 6.0 and 6.7 ppm represent olefinic protons at H7 and H11, H15, H16, and H20, respectively. All labeled positions are the sites corresponding to H5 of DX. There was no deuterium peak corresponding to

the methyl or methylene groups, which suggests that DX is not metabolized but directly incorporated into diadinoxanthin.

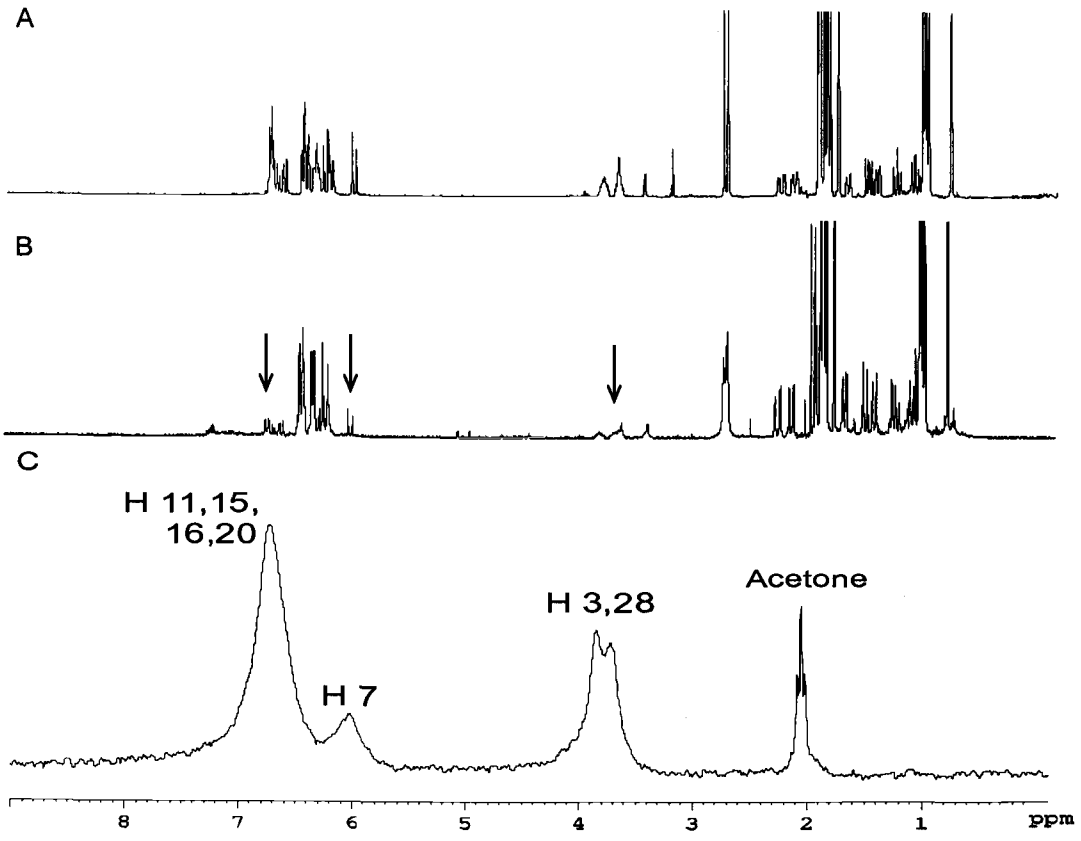

Fig.2.9. (A) ^{1}H-NMR spectrum for unlabeled diadinoxanthin and (B) ^{1}H-NMR and (C) ^{2}H-NMR spectra of diadinoxanthin from the [5-$^{2}H_2$]-DX incubation experiment. Arrows indicate the sites labeled with ^{2}H atoms.

The relative integration ratio of the three peaks at 3.8, 6.1, 6.7 ppm in the ^{2}H-NMR spectrum was 2.0/0.6/4.5, which varies slightly from the expected ratio (2.0/1.0/4.0). Such discrepancy may be attributed to several reasons including: (1) the low resolution of the ^{2}H-NMR spectrum itself, resulting in ambiguous integration and (2) the differential utilization of two pathways during the formation of each isoprene unit, as shown in the [1-^{13}C]-glucose incubation experiment. The percent incorporation levels of deuterium into diadinoxanthin were very high. Based on integration of the peaks in the ^{2}H-NMR spectrum and comparison to the natural abundance acetone peak, the percent incorporation of deuterium at the indicated positions was : H3, H28 = 94 %, H7 = 61 %, and H11, H15, H16, H20 = ~100 %.

These values clearly overestimate the percent incorporation because there are protons readily seen at these positions in the ^{1}H-NMR spectrum (Fig.2.9), but the ^{1}H-NMR spectrum does confirm that there is a major decrease in the proton signals at these sites. Integration of the corresponding peaks in the ^{1}H-NMR spectrum provides levels of deuterium incorporation at over 70 % (H3, H28 = 76 %, H7 = 74 %, and H11, H15, H16, H20 = 78 %). The high level of deuterium incorporation into diadinoxanthin is also supported by the mass spectrometric analysis. The dominant molecular ion peak for diadinoxanthin is at *m/z* = 589, which represents M+7. This could only occur if each isoprene unit in diadinoxanthin has derived from the labeled DX. It appears as though once *E. gracilis* has taken up DX from the medium and converted it to DXP, endogenous production of DXP ceases, and only labeled DX is utilized for carotenoid biosynthesis. Besides the ^{2}H-NMR spectrum, ^{1}H-NMR and MS spectra provided further information on the incorporation of the labeled DX into diadinoxanthin. In the case of the ^{1}H-NMR spectrum of diadinoxanthin, the signal intensity of each proton corresponding to the sites labeled with [5-$^2H_2$]-DX was decreased considerably in proportion to the incorporation of ^{2}H isotopes. In the FAB-MS spectrum, the largest ion peak was seen at *m/z* 589.5, which represents diadinoxanthin containing seven deuteriums (Table.II.2). This can only occur if the labeled DX is used for carotenoid synthesis with only minimal dilution by endogenous DXP. The presence of seven deuterium atoms indicates each isoprene unit has been labeled.

Like diadinoxanthin, the same result was obtained for β-carotene derived from the [5-$^2H_2$]-DX incubation experiment. Deuteriums of DX were introduced into H3, H7, and H11 and 15 arising from H1 of isoprene units with no other significant deuterium peaks (Fig.2.10). The spectrum clearly revealed the intact incorporation of [5-$^2H_2$]-DX without further catabolism. The integration ratio of each peak was calculated as 2.1 : 1.0 : 2.0. Compared with the theoretical ratio of 2.0 : 1.0 : 2.0, the incorporation of [5-$^2H_2$]-DX into β-carotene seems to be more compatible than for diadinoxanthin. The percent incorporation levels of deuterium into β-carotene relative to the natural abundance deuterium in the chloroform peak were: H3 = 40 %, H7 = 39 %, and H11 and H15 = 38 %. These values actually underestimated the incorporation because the values reflect the percentage of molecules in which both C3 and C28 positions retain the maximum two deuterium atoms each. The percent incorporation would be higher if considering labeling at only one of the two positions. Proton integrations

corresponding to H3, H7, and H11 and 15 also are considerably decreased, as found in diadinoxanthin, again indicating a high level of deuterium incorporation. In the FAB-MS spectrum, *m/z* 546.4 was detected as the largest ion peak which results from the molecular ion of natural *β*-carotene plus ten deuteriums, the maximum number of deuteriums possibly retained from the labeled DX (Table 2.2).

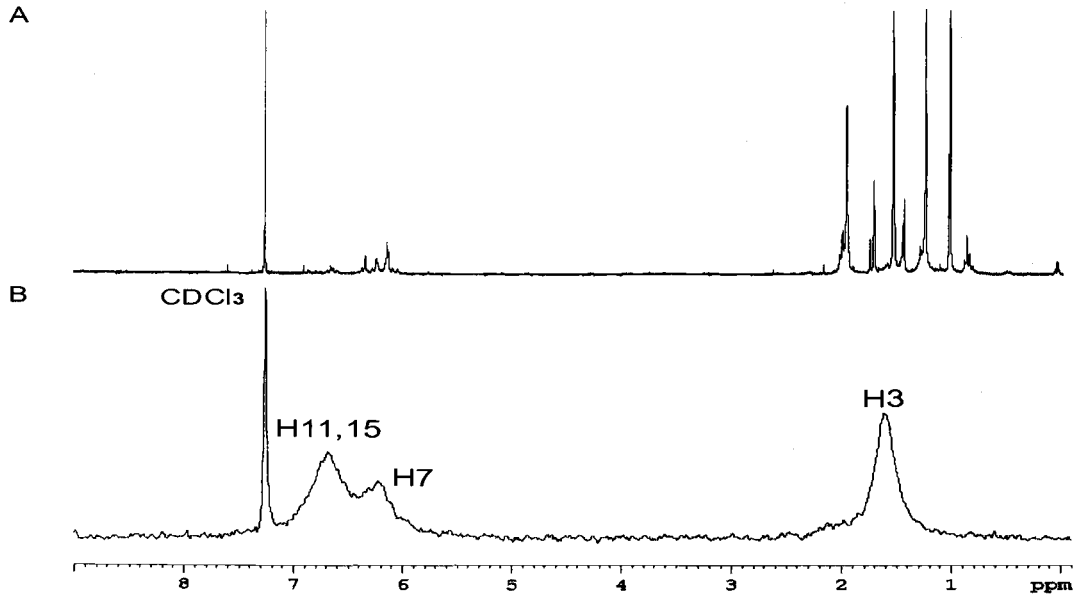

Fig.2.10. ^{1}H-NMR spectrum (A) and ^{2}H-NMR spectrum (B) for *β*-carotene from the [5-$^{2}H_2$]-DX incubation experiment.

Interestingly, the incubation experiment with [5-$^{2}H_2$]-DX revealed an unexpected finding, that is, the identification of the carotenoid precursor, phytoene, in the wild-type photosynthetic *Euglena*. Phytoene is known as the first precursor in carotenoid biosynthesis, which is modified through desaturations, cyclizations, and oxidations to provide various carotenoid compounds.[13,38] In spite of such a fact, the presence of phytoene in photosynthetic flagellates has been difficult to confirm based on the failure of its detection *in vivo*.[39] At one time, an alternate pathway of carotenoid biosynthesis, which bypasses the phytoene step, had been proposed.[40] In 1974, the identification of phytoene was reported with several non-photosynthetic mutants of *E. gracilis* var. *bacillaris* which indirectly suggests a role in carotenoid biosynthesis.[41] Phytoene, however, was not detected in photosynthetic *E. gracilis* var. *bacillaris* or *E. gracilis* strain *Z* in further studies.[42] Therefore, Gross *et al.* drew the

conclusion that phytoene should be formed in carotenoid biosynthesis considering the identification of phytoene in nonphotosynthetic, dark grown *Euglena* species, even though it has not been empirically detected in the actively photosynthetic *Euglena* species, and a failure to identify it was presumed to indicate that the rate limiting step in carotenoid biosynthesis is the formation of phytoene which would be transformed too fast to be accumulated to detectable levels.[42]

From the incubation experiment with [5-$^2H_2$]-DX, phytoene was discovered during the isolation of β-carotene (Fig.2.11). Following the general procedure, β-carotene is purified by silica flash column chromatography (silica gel) and a subsequent silica prep-TLC step. After several trials, however, β-carotene was still mixed with a significant impurity which was seen at the same R_F value as β-carotene on the TLC plate. Changing to a reversed phase C_{18} TLC plate led to the separation of β-carotene from the mixture, and the impurity turned out to be phytoene. Because phytoene was not isolated under normal culture conditions and is not commercially available, its NMR assignment was based on data in a paper published by Granger *et al.* in 1973.[43]

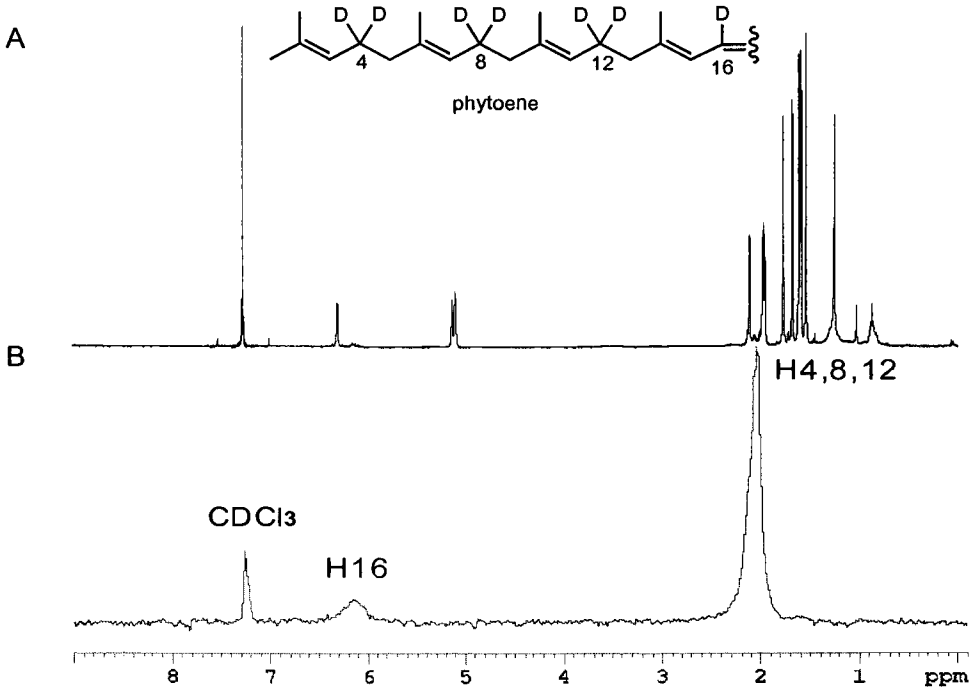

Fig.2.11. Structure and ^{1}H-NMR spectrum (A) and ^{2}H-NMR spectrum (B) for phytoene from the [5-$^2H_2$]-DX incubation experiment.

The ^{2}H-NMR spectrum of phytoene showed two peaks at 2.0 and 6.2 ppm, corresponding to twelve deuteriums in methylene groups and two deuteriums in olefinic groups, respectively. The percent incorporation levels of deuterium into phytoene relative to the natural abundance deuterium in the chloroform peak were: methylenes = 53 %, olefins = 42 %. In the ^{1}H-NMR spectrum, the proton integration of deuterated positions also decreased remarkably, and in the FAB-MS spectrum, a molecular ion peak of the labeled phytoene appeared at *m/z* 558.5 as M+14 which is the maximum number of deuterium atoms possible from direct incorporation of DX (Table 2.2).

Table 2.2. Mass spectral data for carotenoids from incubation of *E. gracilis* with [5-$^{2}H_2$]-DX. The regions shown includes the molecular ion and isotopomers for each carotenoid.

Diadinoxanthin		β-Carotene		Phytoene	
m/z	Relative intensity (%)	*m/z*	Relative intensity (%)	*m/z*	Relative intensity (%)
582.4[a]	1.0	536.3[a]	1.0	544.5[a]	1.0
583.4	1.5	537.3	1.4	545.5	1.4
584.4	3.3	538.4	1.9	546.5	1.8
585.5	5.9	539.3	2.4	547.5	0.8
586.5	9.9	540.4	2.9	548.5	0.4
587.5	17.4	541.4	3.7	549.4	0.3
588.5	27.3	542.4	6.2	553.5	0.8
589.5[b]	31.5	543.4	8.1	554.5	0.2
590.5	15.4	544.4	11.3	555.5	1.3
591.5	5.0	545.4	14.7	556.5	2.3
		546.4[b]	17.8	557.5	1.8
		547.4	7.5	558.5[b]	3.1
		548.4	2.6	559.5	1.7
				560.5	0.7

[a] MW of unlabeled carotenoid
[b] Carotenoid with maximum retention of deuterium from [5-$^{2}H_2$]-DX

Such a direct identification of phytoene is considered to be a result worth mentioning for its identification in photosynthetic, not mutant nor nonphotosynthetic, *Euglena* species, as well as for confirmation of the role of the MEP pathway for the formation of all carotenoid compounds derived from phytoene. Accumulation of phytoene *in vivo* under these conditions is likely attributed to a deuterium isotope effect on the desaturation steps of carotenoid biosynthesis.

In view of the results so far achieved from the incubation experiments using [1-^{13}C]-glucose and [5-$^{2}H_2$]-DX, it has been established that *E. gracilis* undoubtedly possesses the MEP pathway and appears to utilize both the MVA and the MEP pathways to produce the carotenoid compounds, β-carotene and diadinoxanthin under standard incubation conditions. However, when supplied with the specific MEP pathway precursor DX, *Euglena* predominantly uses the MEP pathway for carotenoid biosynthesis.

Various precursors in carotenoid biosynthesis in *E. gracilis*

Besides the exciting finding that *E. gracilis* is able to operate the MEP pathway to produce carotenoid compounds, a variety of other carbon sources were found to be utilized for carotenoid biosynthesis. These results were obtained during the investigation of phytol biosynthesis in *E. gracilis* (see Chapter Three). In fact, several potential precursors from the leucine metabolic pathway had been examined for the formation of β-carotene of *E. gracilis*[19] because the contribution of these precursors to carotenoid biosynthesis was revealed in *Phycomyces blakesleeanus*.[21] The previous results revealed low incorporation of the labeled compounds, and isovalerate was reported to be metabolized to smaller compound(s) before its incorporation into β-carotene.[19] In order to investigate leucine or its metabolites as possible precursors, [2-^{13}C]-leucine, the *N*-acetylcysteamine (NAC) derivative of [U-$^{13}C_4$]-acetoacetate, and [1,2,3,4-$^{13}C_4$]-dimethylacrylic acid were examined. The compounds structurally related to the leucine metabolic pathway, such as [1-^{13}C]-butyric acid, 3-[$^{2}H_3$]-methyl-3-butenoic acid and its NAC derivative, were also used for the incubation experiments (Fig.2.12).

The metabolic pathway for the conversion of leucine into HMG-CoA and IPP is known as an additional route for isoprenoid biosynthesis in plants.[44] HMG-CoA has

been generally regarded to be readily cleaved to acetyl-CoA and acetoacetyl-CoA to be reutilized through the standard MVA pathway.[13] In 1999, the contribution of leucine to isoprenoid biosynthesis was studied with several trypanosomatid species, which are primitive eukaryotic protozoa.[45] Through this study and additional incubation experiments, some trypanosomatid species turned out to directly utilize the main carbon backbone of leucine for sterol synthesis with little breakdown of HMG-CoA.[46]

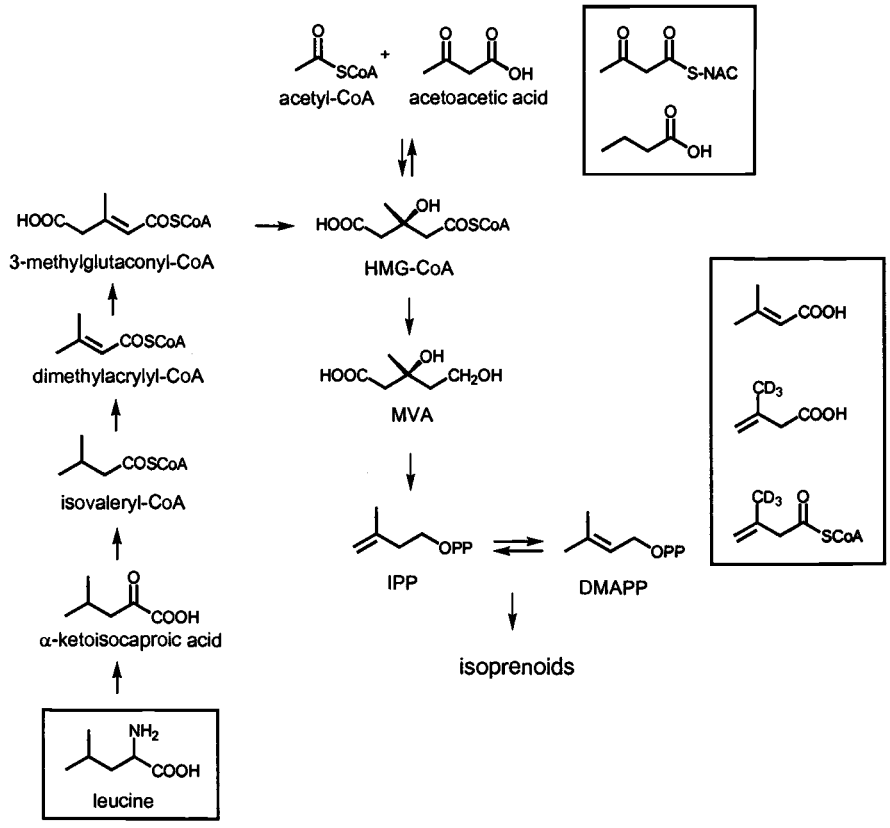

Fig.2.12. Metabolic pathways to isoprenoids from acetate and leucine. Compounds in boxes were used for the incubation experiments.

Based on these findings, an incubation experiment with [2-^{13}C]-leucine was performed. If the intact leucine is incorporated into carotenoids in *E. gracilis* as it is for sterols in trypanosomatids, ^{13}C isotopes from [2-^{13}C]-leucine should be distinctly found at only C1 of the isoprene units in carotenoids. If not in the intact form, labeled acetate would be incorporated into carotenoids at more sites.

The ^{13}C-NMR spectra of carotenoids showed the ^{13}C isotope enrichment at C1 and C3 of the isoprene unit which arises from the catabolic pathway of [2-^{13}C]-leucine to produce [1-^{13}C]-acetate (Fig.2.13). Although the incorporation of label from leucine into carotenoids was clearly found, the incorporation levels in the carotenoids were low, in the range of 1.5-2.2-fold enhancements for the labeled carbons of β-carotene. Such a low incorporation level for carotenoids might be attributed to the various fates of leucine within the cells. Leucine might be also recycled as $^{13}CO_2$, which could explain the weak enrichment at methyl carbons of acetate. From this experiment, the possibility that leucine may be the intact precursor of carotenoid biosynthesis was ruled out, but leucine was found to be another carbon source for the formation of carotenoid compounds in *E. gracilis*. When leucine is incorporated into carotenoids, degradation to acetate appears to be the main route for utilization.

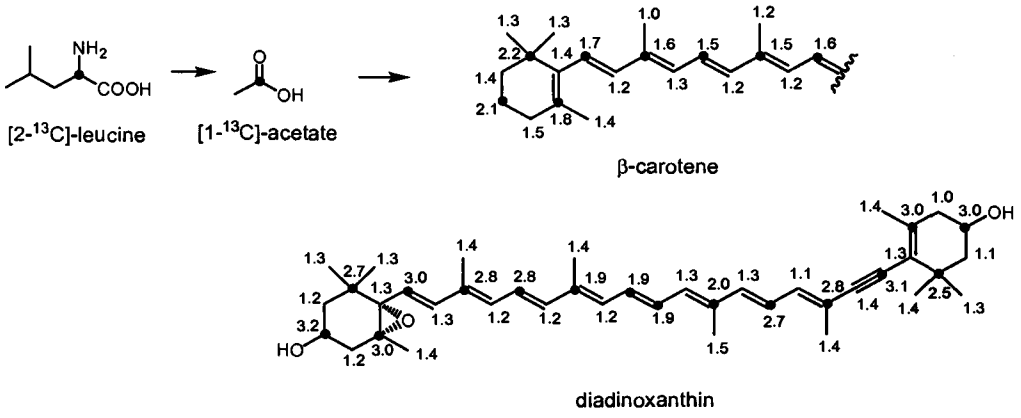

Fig.2.13. Incorporation levels for carotenoid compounds from the incubation experiment with [2-^{13}C]-leucine. Filled circles indicate enhanced ^{13}C isotopes derived from [2-^{13}C]-leucine.

An incubation experiment using the *N*-acetylcysteamine (NAC) derivative of [U-$^{13}C_4$]-acetoacetate gave rise to an interesting result. The NAC derivative of [U-$^{13}C_4$]-acetoacetate was synthesized from ethyl [U-$^{13}C_4$]acetoacetate and assigned by doublets for C1 and C4 and doublets of doublets for C2 and C3 due to two adjacent ^{13}C atoms (Fig.2.14).[47]

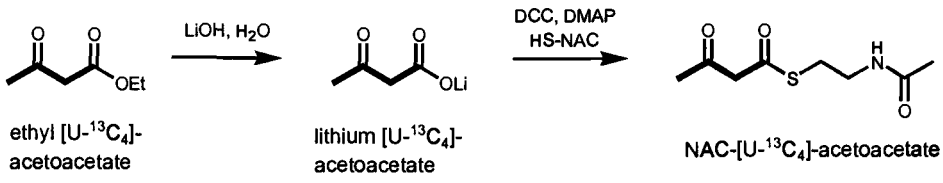

Fig.2.14. Synthesis of NAC-[1,2,3,4-$^{13}C_4$]-acetoacetate. Bold lines indicate sequential ^{13}C enriched positions.

Acetoacetyl-CoA is an intermediate in isoprenoid biosynthesis via the MVA pathway, which is produced by the condensation of two acetyl-CoA molecules. It also can be readily cleaved to form two acetyl-CoA molecules by a thiolase. Even if the NAC derivative of [U-$^{13}C_4$]-acetoacetate is a precursor in carotenoid biosynthesis, it may only be incorporated as the metabolized form, acetate, after the β-oxidation reaction, which would lead to the same labeling pattern as with [1,2-$^{13}C_2$]-acetate. Additionally, when the incubation experiment is performed with an acetoacetate derivative, β-oxidation inhibitors are often added in the medium to prevent acetoacetate from being catabolized to acetate by the β-oxidation reaction to improve the chances of intact incorporation of acetoacetate.[47] Although attempts were made to grow *E. gracilis* in the presence of pentynoic acid as a β-oxidation inhibitor, only poor growth was observed. Because of this result, the NAC derivative of [U-$^{13}C_4$]-acetoacetate was used without the β-oxidation inhibitor.

After the experiment (1.7 % incorporation for ^{13}C signals of diadinoxanthin), the analysis of carotenoids indicated not only the incorporation of doubly-labeled acetate, which would arise from catabolism of acetoacetate, but also the intact incorporation of NAC-[U-$^{13}C_4$]-acetoacetate which is transformed to acetoacetyl-CoA and condensed with acetate to produce HMG-CoA through the MVA pathway to lead to doublets of doublets in the carbons corresponding to C2 and C3 of the isoprene unit and doublets in C1 and C5 (Fig.2.15). In the partial spectrum of labeled diadinoxanthin, C1 is coupled with C1' and C2 (coupling constants J = 35 and 35 Hz), and C6 is correlated with C5 and C7 by 31 and 57 Hz coupling constants. Doublets were also seen for C1-C2 (J = 36 Hz) and C5-C6 (J = 31 Hz) of diadinoxanthin, which results from the incorporation of [1,2-$^{13}C_2$]-acetate obtained from cleavage of NAC-[U-

$^{13}C_4$]-acetoacetate. Through the incubation experiment with NAC-[U-$^{13}C_4$]-acetoacetate, it was found that acetoacetate is able to be utilized as the intact form for carotenoid compounds, as well as being metabolized to acetate.

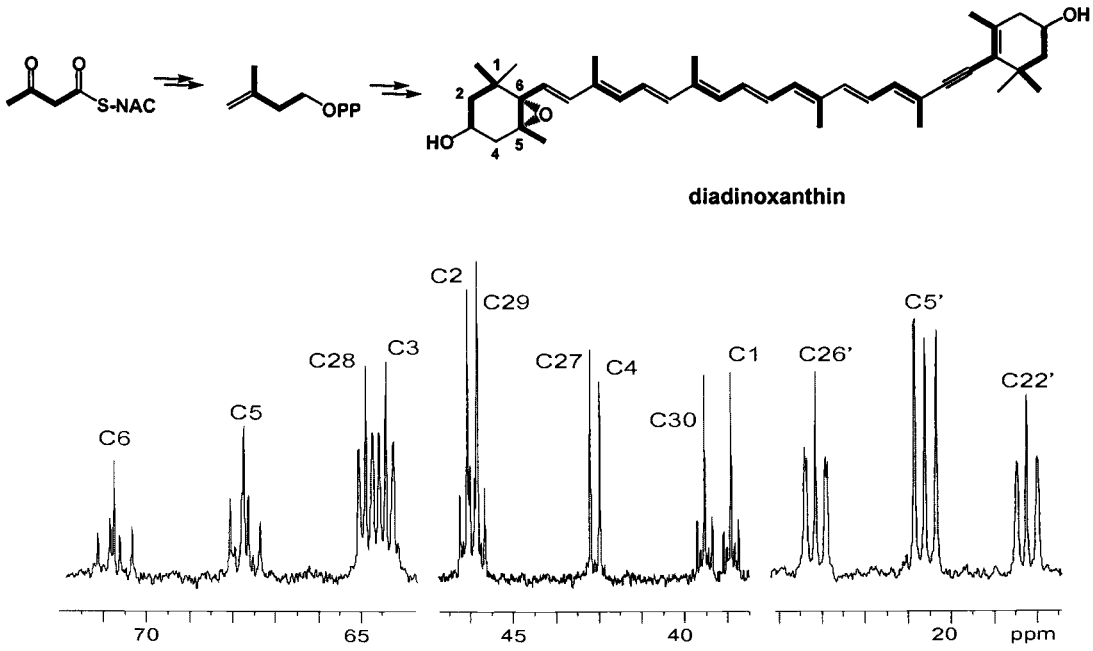

Fig.2.15. Incorporation pattern and the ^{13}C-NMR spectrum for diadinoxanthin from the incubation experiment with NAC-[1,2,3,4-$^{13}C_4$]-acetoacetate. Bold lines indicate sequential ^{13}C enriched positions.

The intact incorporation of another C_4 skeleton was found for carotenoids from the incubation experiment using [1-^{13}C]-butyric acid. Through the labeling pattern, carotenoids clearly displayed enrichment of the ^{13}C isotopes at the positions corresponding to only C1 of the isoprene unit. The enhancements observed in carotenoids, especially in diadinoxanthin were quite high (7.8-26.3; Fig.2.16). This labeling pattern suggests that [1-^{13}C]-butyric acid undergoes sequential dehydrogenation, hydroxylation, and oxidation reactions to provide [1-^{13}C]-acetoacetate, which is transformed to acetoacetyl-CoA and directly incorporated into carotenoids via the MVA pathway with minimal degradation.

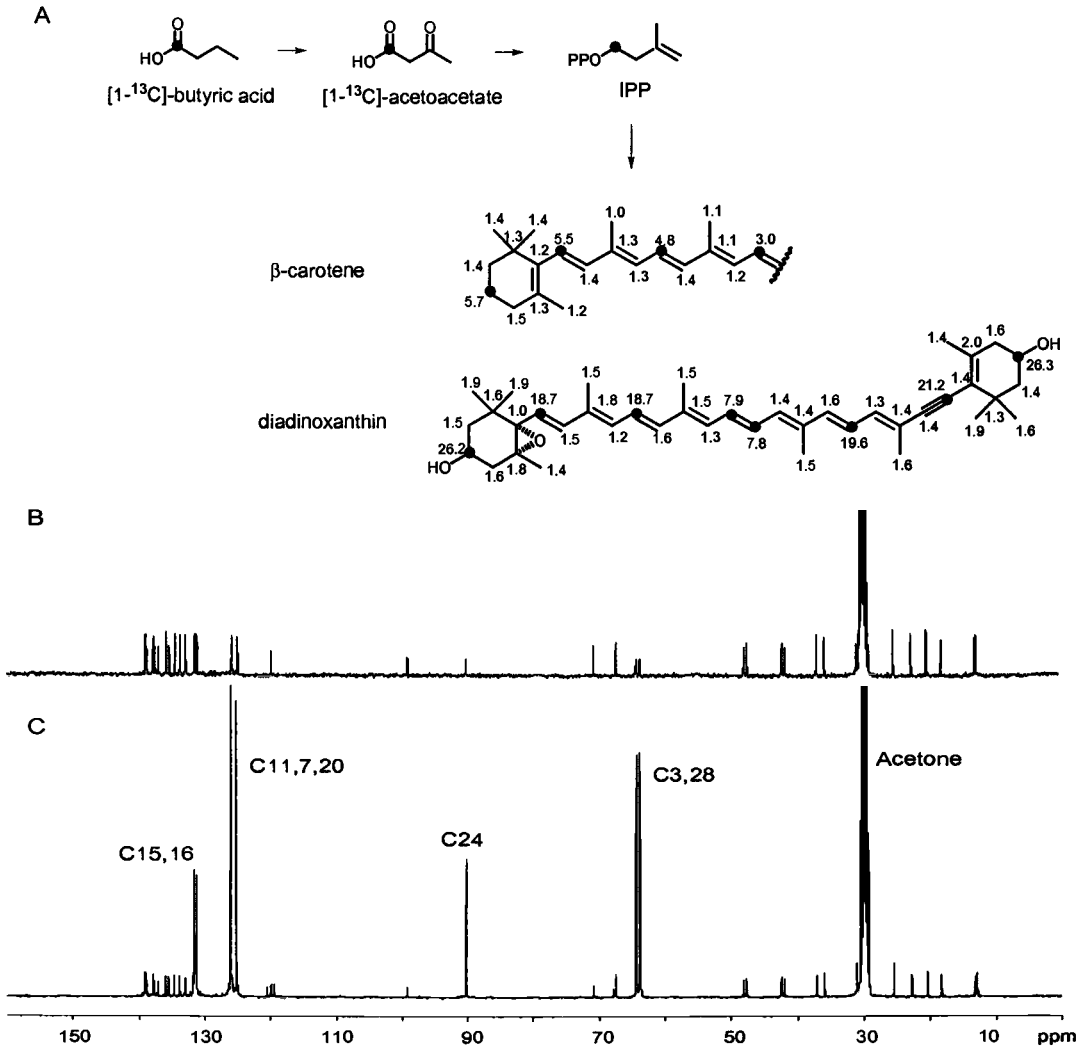

Fig.2.16. Incorporation levels for carotenoids (A) from the incubation experiment with [1-^{13}C]-butyric acid. ^{13}C-NMR Spectra of unlabeled (B) and labeled (C) diadinoxanthin. Filled circles indicate enhanced ^{13}C isotopes.

Putting together the results from the incubation experiments with [2-^{13}C]-leucine and [1-^{13}C]-butyric acid, several interesting features regarding the incorporation levels into β-carotene and diadinoxanthin were observed: (1) Enrichment of ^{13}C isotopes in the [1-^{13}C]-butyric acid incubation experiment were much higher than in the [2-^{13}C]-leucine incubation experiment, which means that the intact butyric acid is utilized extensively for the formation of carotenoids, whereas leucine is more readily used for other essential metabolites, (2) Comparing the

incorporation levels for each carotenoid, the labeled precursors were predominantly incorporated into diadinoxanthin, rather than β-carotene. This might be explained by differing pool size for β-carotene and diadinoxanthin. Consequently, there may be greater dilution of the label in β-carotene and higher incorporation of ^{13}C isotopes in the diadinoxanthin structure in *E. gracilis.*

Investigating other possible precursors, incubation experiments with C_5 compounds structurally similar to the isoprene unit were performed, such as [1,2,3,4-$^{13}C_4$]-dimethylacrylic acid, 3-[$^2H_3$]-methyl-3-butenoic acid, and NAC-3-[$^2H_3$]-methyl-3-butenoate. If these labeled compounds are incorporated into carotenoids without breakdown, doublets and doublets of doublets derived from [1,2,3,4-$^{13}C_4$]-dimethylacrylic acid and deuteriums derived from 3-[$^2H_3$]-methyl-3-butenoic acid and NAC-3-[$^2H_3$]-methyl-3-butenoate would be detected in the ^{13}C-NMR spectra and in the ^2H-NMR spectra.

[1,2,3,4-$^{13}C_4$]-Dimethylacrylic acid was prepared from ethyl [U-$^{13}C_4$]-acetoacetate using diethyl phosphorochloridate and lithium dimethylcuprate and then base hydrolysis (Fig.2.17).[48,49] The deuterated compound, 3-[$^2H_3$]-methyl-3-butenoic acid was synthesized from diketene with cobalt(II) iodide and a deuterated Grignard reagent, and its NAC derivative was prepared, following the same method as for NAC-[1,2,3,4-$^{13}C_4$]-acetoacetate (Fig.2.16).[47,50]

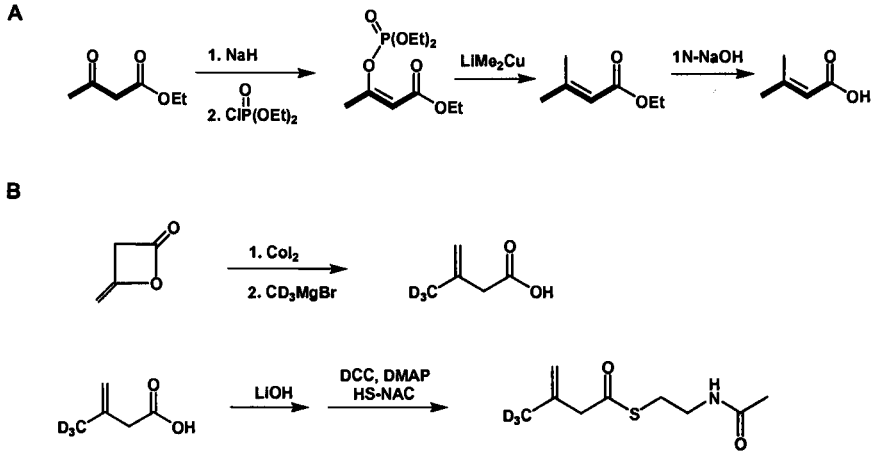

Fig.2.17. Syntheses of (A) [1,2,3,4-$^{13}C_4$]-dimethylacrylic acid and (B) 3-[$^2H_3$]-methyl-3-butenoic acid and its NAC derivative. Bold lines indicate sequential ^{13}C enriched positions. The D stands for deuterium.

In contrast with the intact incorporation of NAC-[U-$^{13}C_4$]-acetoacetate and [1-^{13}C]-butyric acid into carotenoids, the ^{13}C-NMR spectra of carotenoids from the incubation experiment with [1,2,3,4-$^{13}C_4$]-dimethylacrylic acid (0.8 % incorporation for ^{13}C signals of diadinoxanthin) showed a labeling pattern consistent with the [U-$^{13}C_6$]-glucose incubation experiment, with no doublets of doublets for any carbon, which represents that dimethylacrylic acid is catabolized into acetate and reutilized, presumably after transformation to HMG-CoA (Fig.2.18).

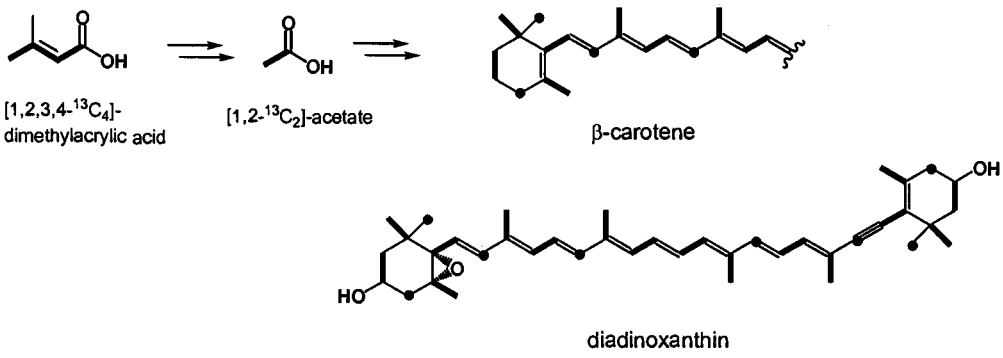

Fig.2.18. Labeling patterns for β-carotene and diadinoxanthin from the [1,2,3,4-$^{13}C_4$]-dimethylacrylic acid incubation experiment. Bold lines indicate sequential ^{13}C enriched positions, and filled circles indicate enhanced ^{13}C singlets.

In the incubation experiment with 3-[$^2H_3$]-methyl-3-butenoic acid, there was no significant peak in the ^2H-NMR spectra of carotenoids. Subsequently, the activated form of 3-[$^2H_3$]-methyl-3-butenoic acid, NAC-3-[$^2H_3$]-methyl-3-butenoic acid, was also employed to potentially improve its bioavailability in *E. gracilis*, but neither this compound nor degradation products were incorporated into carotenoids. These results indicate that 3-methyl-3-butenoate, a double bond isomer of dimethylacrylic acid, was not a precursor for isoprenoid biosynthesis, whereas dimethylacrylic acid can be utilized after being metabolized by *E. gracilis.*

Based on the above incubation experiments with C_4 and C_5 compounds similar to the IPP structure, several carbon sources for carotenoid synthesis were found, such as leucine, NAC-acetoacetate, butyric acid, and dimethylacrylic acid. These precursors could be utilized either intact (NAC-acetoacetate, butyric acid) or after catabolism, presumably to acetate (leucine, dimethylacrylic acid).

Experimental

Instruments

All ^{1}H, ^{2}H, and ^{13}C nuclear magnetic resonance (NMR) spectra were recorded on a Bruker AC 300 spectrometer operating at 300 MHz for ^{1}H and 75 for ^{13}C, and on a Bruker AM 400 spectrometer operating at 400.13 MHz for ^{1}H, 100.13 MHz for ^{13}C, and 61.42 MHz for ^{2}H. Chemical shifts of NMR spectra are shown as δ, and references are based on deuterated NMR solvents as an internal standard ($CHCl_3$ at 7.26 ppm for ^{1}H-NMR and $^{13}CDCl_3$ at 77.0 ppm for the center line of the triplet in ^{13}C-NMR, acetone at 2.08 ppm for ^{1}H-NMR and acetone-d_6 at 30.7 ppm for the center line of the septet in ^{13}C-NMR, CH_3OH at 3.4 ppm for ^{1}H-NMR and CD_3OD at 50.2 ppm for the center line of the septet in ^{13}C-NMR). The inverse-gated decoupled technique was applied for determining ^{13}C isotopic enhancement levels. Incorporation levels for ^{13}C signals of isoprenoids in the incubation experiments using labeled compounds were calculated on the basis of the intensities of the target peak relative to the intensity of an unenriched peak. This ratio was compared with the ratio for the corresponding peaks from the natural abundance ^{13}C-NMR spectrum for unlabeled isoprenoids to determine the relative incorporation level. Absolute ^{13}C enrichments were determined by integration of ^{13}C satellite peaks in the ^{1}H-NMR spectrum. Levels of incorporation from ^{2}H-NMR spectra were calculated on the basis of the integration of the target peak relative to the natural abundance of the deuterium signal of $CHCl_3$ (0.5 mL, 0.016 %) and acetone (0.5 mL, 0.016 %) each. Phosphoric acid (85 % in H_2O) was used as an external standard (δ_p 0.0 ppm) for ^{31}P NMR spectra operating at 121.4 MHz of a Bruker AC 300 spectrometer. Low and high-resolution chemical ionization mass spectra (CIMS) and fast atom bombardment mass spectra (FABMS) were recorded on a Kratos MS50TC spectrometer. Cultures were grown in a Hoffman illuminated incubator. Harvesting of *Euglena* cells was done with a Beckman J2-HS centrifuge and lyophilization of the cells utilized a Labconco freeze dry system.

Biosynthetic experiments

An axenic culture of *E. gracilis* strain *Z* (UTEX 753, identical to SAG 1224-25) was obtained from UTEX, The Culture Collection of Algae at the University of Texas at Austin.

For maintenance of the organism, *E. gracilis* was cultivated in modified media containing D-glucose (1.0 g/L), $(NH_4)_2HPO_4$ (1.0 g/L), KH_2PO_4 (1.0 g/L), $MgSO_4 \cdot 7H_2O$ (0.2 g/L), $CaCl_2 \cdot 2H_2O$ (0.02 g/L), sodium citrate·$2H_2O$ (0.5g/L), thiamine·HCl (10 μg/L), vitamin B_{12} (0.5 μg /L) and trace metals.[51] Trace metals were prepared with $FeCl_3 \cdot 6H_2O$ (3.2 mg/L), $MnCl_2 \cdot 4H_2O$ (1.8 mg/L), $CoCl_2 \cdot 6H_2O$ (1.1 mg/L), $ZnSO_4 \cdot 7H_2O$ (0.4 mg/L), $Na_2MoO_4 \cdot 2H_2O$ (0.3 mg/L), $CuSO_4 \cdot 5H_2O$ (0.02 mg/L). Seed cultures were inoculated into medium (200 mL) and were grown at 30 °C for 7-10 days under constant illumination with 40 W cool-white fluorescent lights (200-210 ftc). For mass cultivation, the seed cultures were inoculated into medium (5-6 L), aerated and grown for 7-13 days under the same condition as the seed cultures. For incubation experiments with labeled compounds, the labeled compounds were mixed with unlabeled D-glucose (1 g/L) at a ratio of 1:60 to 1:10 (w/w).

Inorganic salts for the culture media were purchased from Mallinckrodt, and D-glucose, vitamin B_{12}, and thiamine·HCl were from Sigma-Aldrich. Labeled compounds ([1-^{13}C]-glucose, [U-$^{13}C_4$]-acetoacetate, [2-^{13}C]-leucine, and [1-^{13}C]-butyric acid) were purchased from Cambridge Isotope Laboratories, Inc. and Sigma-Aldrich. For the syntheses of [5-$^{2}H_2$]-deoxy-D-xylulose, [1,2,3,4-$^{13}C_4$]-acetoacetyl-*N*-acetylcysteamine, [1,2,3,4-$^{13}C_4$]- dimethylacrylic acid, 3-[methyl-$^{2}H_3$]-3-butenoic acid, and 3-[methyl-$^{2}H_3$]-3-butenoyl-*N*-acetylcysteamine, $LiAlD_4$, ethyl-[1,2,3,4-$^{13}C_4$]-acetoacetate, and CD_3MgI were purchased from Cambridge Isotope Laboratories and Sigma-Aldrich and employed as isotope sources. For syntheses, commercial grade reagents and starting materials from Sigma-Aldrich were used without further purification, and most organic solvents were dried before use as recommended.[52] Synthetic reactions were carried out in oven-dried glassware under a positive pressure of argon. The β-carotene standard was purchased from Sigma-Aldrich. Water was deionized using a Milli Q Millipore system for all experiments. Silica gel (Merck, grade 60, 220-400 mesh) was used for flash column chromatography.[53]

Merck glass-backed TLC plates (silica gel 60 F254 and RP-C_{18}) were employed for thin layer chromatography (TLC) and preparative TLC (prep-TLC).

Isolation of carotenoids

After cultivation, cells were harvested by centrifugation at 7000 rpm (JA-10 rotor, 8671 *g*) for 10 min and lyophilized to obtain 0.3-0.5 g of dry weight per liter. The lyophilized cells were extracted three times (30 min each) with a mixture of $CHCl_3$ and MeOH (2:1) at room temperature to provide a crude extract, which was applied to a silica gel flash chromatography column. The column was developed with mixtures of 15-50 % EtOAc in hexanes to separate four fractions which were determined by color of pigments. The fractions 1 (orange color) and 2 (yellow color) contain the non-polar compounds (R_f = 0.8-0.9 and 0.7, silica gel TLC plate, 5 % EtOAc in hexanes). Fraction 3 is the chlorophyll-containing fraction (R_f = 0.5-0.6, silica TLC plate, 10 % EtOAc in hexanes). Fraction 4 (orange-red) contains the polar compounds (R_f = 0.2-0.3, silica gel TLC plate, 30 % EtOAc in hexanes). After the organic solvent was evaporated, each fraction was processed to separate the isoprenoids: β-carotene, phytoene, or diadinoxanthin.

Fraction 1 was applied on silica prep-TLC plates, which were developed in a mixture of cyclohexane, hexanes, and toluene (4:4:1). An orange band (R_f = 0.4) was carefully scraped from TLC plates and extracted with $CHCl_3$ to provide 1 mg/L (avg. yield) of β-carotene. When the [5-$^2H_2$]-DX incubation experiment was carried out, β-carotene needed to be separated from phytoene by using prep RP-C_{18} TLC with a mixture of petroleum ether, acetonitrile, and MeOH (20:35:45). Diadinoxanthin (2 mg/L, avg. yield) was purified from the fraction 4 by using a Sephadex LH-20 column (2.5 × 28 cm) with MeOH as eluent. β-Carotene, phytoene, and diadinoxanthin obtained from the *E. gracilis* were analyzed by mass spectrometry and NMR spectroscopy. ^{13}C- and ^1H-NMR assignments for β-carotene[54] and ^1H-NMR assignments for phytoene[43] and diadinoxanthin[55] were previously published. ^{13}C-NMR signals for diadinoxanthin were assigned as follows based on HSQC (Heteronuclear Single Quantum Coherence) and HMBC;

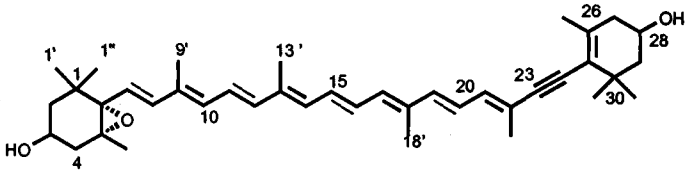

carbon#	ppm	carbon#	ppm	carbon#	ppm	carbon#	ppm
1	35.88	11	126.04	21	135.96	1'	25.48
2	48.14	12	139.16	22	119.92	1"	30.02
3	63.83	13	137.60	23	99.21	5'	20.44
4	41.97	14	134.64	24	90.25	9'	13.14
5	67.47	15	131.67	25	124.93	13'	12.93
6	70.78	16	131.26	26	138.85	18'	12.85
7	126.04	17	133.82	27	42.39	22'	18.26
8	137.87	18	137.15	28	64.36	26'	22.76
9	135.49	19	138.97	29	47.66	30'	29.16
10	132.96	20	125.20	30	37.11	30"	31.11

Synthesis of [5-$^2H_2$]-Deoxy-D-xylulose[36,37]

Diisopropyl-2,3-O-isopropylidene-D-tartrate (**2**)

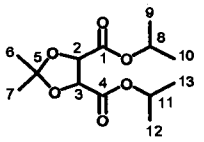

2

Diisopropyl-D-tartrate (**1**, 5.53 g, 23.6 mmol) in 40 mL of dry toluene was treated with 2,2-dimethoxypropane (4.35 mL, 35.4 mmol) and *p*-toluene sulfonic acid monohydrate (0.04 g, 0.21 mmol). The solution was refluxed overnight using a Dean-Starke trap in an oil bath at 120 °C. The reaction mixture was concentrated *in vacuo*, dissolved with EtOAc, washed with saturated $NaHCO_3$, brine and *dd*-H_2O, dried over anhydrous $MgSO_4$, and concentrated again. Flash column chromatography (silica gel, 20 % EtOAc in hexanes) afforded the oily product (5.40 g, 83.4 % yield): ^1H NMR (300 MHz, $CDCl_3$) δ 5.1 (m, 2 H, H-8,11), 4.65 (s, 2H, H-2,3), 1.45 (s, 6H, H-6,7), 1.25 (d, J = 6.3 Hz, 12H, H-9,10,12,13); ^{13}C NMR (75MHz, $CDCl_3$) δ, 169.4 (C-1,4), 113.8 (C-5), 77.5 (C-2,3), 69.8 (C-8,11), 26.5 (C-5), 21.8 (C-9,10,12,13). HRMS (CI) calcd. for $C_{13}H_{23}O_6$ (M^++1) 275.14946, found 275.14982.

[1-$^2H_2$-4-$^2H_2$]-2,3-O-isopropylidene-D-tartrate (**3**)

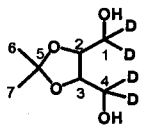

3

The ketal **2** (5.37 g, 19.6 mmol) in 40 mL of dry THF was added, over a 40 min period, to a vigorously stirred suspension of

$LiAlD_4$ (1.8 g, 43.0 mmol) in 30 mL of dry THF at 0 °C under Ar gas, stirred at 0 °C for 2 h, and quenched with 10 mL of *dd*-H_2O and 50 mL of 3 N NaOH. After diethylether was added, the ethereal layer of the reaction mixture was filtered over Celite. After removing the solvent, flash column chromatography (silica gel, 80 % EtOAc in hexanes) of crude **3** gave the oily product (2.80 g, 86.1% yield): ^{1}H NMR (300 MHz, $CDCl_3$) δ 3.95 (s, 2H, H-2,3), 1.4 (s, 6H, H-6,7); ^{13}C NMR (75MHz, $CDCl_3$) δ 109.4 (C-5), 78.2 (C-2,3), 27.1 (C-6,7). HRMS (CI) calcd. for $C_7H_{11}D_4O_4$ (M^++1) 167.12214, found 167.12194.

[1-$^2H_2$-4-$^2H_2$]-2,3-O-isopropylidene-4-O-benzyl-D-tartrate (**4**)

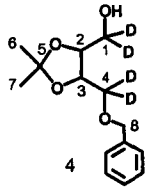

To a solution of NaH (60 % in mineral oil, 0.73 g, 18.0 mmol) in 50 mL of dry THF at 0 °C was added **3** (2.74 g, 16.5 mmol) in 15 mL of dry THF over a 10 min period. The slurry was warmed to room temperature and stirred for 1 h. After *n*-Bu_4NI (10 mg, catalytic amount) was added, 2.16 mL of benzyl bromide (3.10 g, 18.1 mmol) was added over a 40 min period. The reaction mixture was stirred for 1 h and then 1 M HCl solution was added until the precipitate was dissolved. After 200 mL each of *dd*-H_2O and EtOAc were added, the organic layer was washed with saturated $NaHCO_3$ solution, brine, and *dd*-H_2O. The organic layers were dried over anhydrous $MgSO_4$, concentrated, and the crude product was by purified in flash column chromatography (silica gel, 20 % EtOAc in hexanes) to afford **4** (3.50 g, 82.7 % yield): ^{1}H NMR (300 MHz, $CDCl_3$) δ 7.2-7.5 (m, 5H), 4.6 (s, 2H, H-8), 4.1 (d, *J* = 8.3 Hz, 1 H, H-3), 3.9 (d, *J* = 8.3 Hz, 1 H, H-2), 1.4 (s, 6 H, H-6,7); ^{13}C NMR (75MHz, $CDCl_3$) δ 137.5, 128.4, 127.7, 127.6 , 109.2 (C-5), 79.4 (C-2), 76.3 (C-3), 73.5 (C-8), 26.9 (C-7), 26.8 (C-6). HRMS (CI) calcd. for $C_{14}H_{17}D_4O_4$ (M^++1) 257.16909, found 257.16738.

[1-^{2}H-4-$^2H_2$]-2,3-O-isopropylidene-4-O-benzyl-D-threose (**5**)

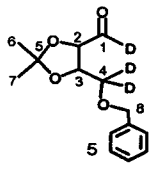

To a solution of oxalyl chloride (2.24 g, 17.6 mmol) in 30 mL of dry CH_2Cl_2 at -78 °C was added DMSO (2.49 mL, 35.2 mmol). After the solution was stirred for 5 min, a solution of [1-$^2H_2$-4-$^2H_2$]-2,3-O-isopropylidene-4-O-benzyl-D-tartrate (**4**, 3.47 g, 13.5 mmol) in 20 mL of dry CH_2Cl_2 was added and stirred at -78 °C for 1 h. The reaction was warmed to room

temperature and 6 mL of TEA was added dropwise. The reaction mixture was stirred at room temperature for 1.5 h before *dd*-H_2O was added. The reaction mixture was extracted with diethylether and the organic layers were washed with *dd*-H_2O and brine. The organic layers were dried with anhydrous $MgSO_4$, concentrated, and used for the next reaction without further purification. HRMS (CI) calcd. for $C_{14}H_{15}D_3O_4$ (M^+) 253.13934, found 253.13955.

[2-^{2}H-5-$^2H_2$]-3,4-*O*-isopropylidene-5-*O*-benzyl-1-deoxy-D-xylitol (**6**)

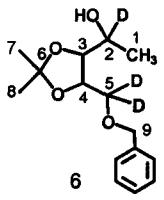

6

To a solution of 1,4,4-$^2H_3$-2,3-*O*-isopropylidene-4-*O*-benzyl butanal (**5**, 3.43 g, 13.5 mmol) in 50 mL of dry THF at -78 °C was added dropwise 13.5 mL of methyl magnesium chloride solution (3 M in diethylether, 40.6 mmol) in diethylether. After the reaction mixture was stirred at -78 °C for 2 h, the mixture was warmed to room temperature and stirred overnight. The reaction was quenched with 20 mL of saturated NH_4Cl solution and extracted with diethylether. The extract was dried over anhydrous $MgSO_4$, filtered, and concentrated. The residue was purified by flash column chromatography (silica-gel, 10 % EtOAc in hexane) to afford 2.37 g (65 % yield for two steps) of [2-^{2}H-5-$^2H_2$]-3,4-*O*-isopropylidene-5-*O*-benzyl-1-deoxy-D-xylulose as a mixture of diastereomers: ^{1}H NMR (300 MHz, $CDCl_3$) δ 7.2-7.4 (m, 5H), 4.6 (s, 2H, H-9), 4.1 (d, *J* = 7.8 Hz, 1H, H-4), 3.7(d, *J* = 7.8 Hz, 1H, H-3), 1.4 (s, 6H, H-7,8), 1.2 (s, 3H, H-1); ^{13}C NMR (75MHz, $CDCl_3$) δ 137.3, 128.5, 127.8, 109.0 (C-6), 81.6 (C-4), 77.3 (C-3), 73.7 (C-9), 26.9 (C-8), 26.8 (C-7), 19.0 (C-1). HRMS (CI) calcd. for $C_{15}H_{20}D_3O_4$ (M^++1) 270.17846, found 270.17846.

[5-$^2H_2$]-3,4-*O*-isopropylidene-5-*O*-benzyl-1-deoxy-D-xylulose (**7**)

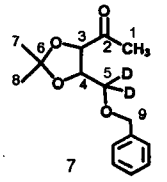

7

To a solution of [2-^{2}H-5-$^2H_3$]-3,4-*O*-isopropylidene-5-*O*-benzyl-1-deoxy-D-xylitol (**6**, 2.34 g, 8.69 mmol) in 20 mL of dry CH_2Cl_2 was added 1 g of finely ground molecular sieves (4 Å), NMO (1.43 g, 12.2 mmol), and TPAP (70 mg, 0.2 mmol). The reaction mixture was stirred at room temperature overnight, filtered through Celite and Florisil, concentrated, and purified by flash column chromatography (silica gel, 50 % EtOAc in hexanes) to give **7** (2.18 g, 94.4 % yield): ^{1}H NMR (300 MHz, $CDCl_3$) δ 7.2-7.4 (m, 5H), 4.6 (s, 2H, H-9), 4.2(s, 2H, H-3,4), 2.3 (s, 3H, H-1), 1.5 (s, 3H, H-7), 1.4 (s, 3H,

H-8); ^{13}C NMR (75MHz, $CDCl_3$) δ 208.2 (C-2), 137.8, 128.3, 127.6, 110.9, 81.8 (C-3), 77.1 (C-4), 73.4 (C-9), 26.8 (C-1), 26.3 (C-8), 26.2 (C-7). HRMS (CI) calcd. for $C_{15}H_{18}D_2O_4$ (M^+) 266.14871, found 266.14904.

[5-$^2H_2$]-5-*O*-benzyl-1-deoxy-D-xylulose (**8**)

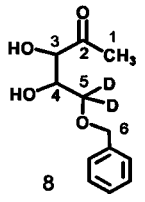
8

The isopropylidene group was removed by acid hydrolysis of [5-$^2H_2$]-3,4-*O*-isopropylidene-5-*O*-benzyl-1-deoxy-D-xylulose (**7**, 2.15 g, 8.07 mmol) with 120 mL of CH_3CN-H_2O-2 M HCl (90:6:3). After the reaction mixture was stirred at room temperature for 36 h, the mixture was concentrated, dissolved in CH_2Cl_2, washed with saturated Na_2CO_3 and brine, filtered over anhydrous Na_2SO_4, and concentrated. The residue was purified by flash column chromatography (silica gel, 40 % EtOAc in hexanes) to give [5-$^2H_2$]-5-*O*-benzyl-1-deoxy-D-xylulose (1.76 g, 96.4 % yield): ^1H NMR (300 MHz, $CDCl_3$) δ 7.2-7.5 (m, 5H), 4.58 (s, 2H, H-6), 4.3 (d, *J* = 4.4 Hz, 1H, H-4), 3.7 (d, *J* = 4.5 Hz, 1H, H-3), 2.25 (s, 3H, H-1); ^{13}C NMR (75MHz, $CDCl_3$) δ 208.1 (C-2), 137.6, 127.9, 127.8, 128.5, 77.1 (C-3), 73.5 (C-6), 70.3 (C-4), 25.5 (C-1). HRMS (CI) calcd. for $C_{12}H_{15}D_2O_4$ (M^++1) 227.12524, found 227.12551.

[5-$^2H_2$]-1-deoxy-D-xylulose (**9**)[37]

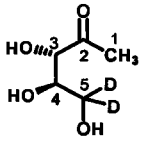
9

Hydrogenolysis of [5-$^2H_2$]-5-*O*-benzyl-1-deoxy-D-xylulose (**8**, 1.72 g, 7.60 mmol) in 100 mL of 95 % (v/v) EtOH under a positive pressure of hydrogen (1atm) at room temperature in the presence of 10 % Pd/C gave [5-$^2H_2$]-1-deoxy-*D*-xylulose (**9**, 1.03 g, 99.1 % yield): ^1H NMR (300 MHz, $CDCl_3$) δ 3.41-4.26 (m, 2H, H-3,4), 1.29, 1.34, 2.15 (3 s, 3H, H-1, in a ratio of 4:1:1, total of 3H); ^{13}C NMR (75MHz, $CDCl_3$) δ 212.4 (C-2), 78.6 (C-3), 73.6 (C-4), 26.7 (C-1). HRMS (CI) calcd. for $C_5H_9D_2O_4$ (M^++1) 137.07829, found 137.07821.

Synthesis of NAC [1,2,3,4-$^{13}C_4$]-acetoacetate[47]

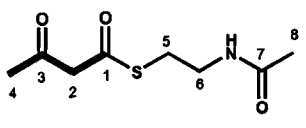

To a solution of ethyl [U-$^{13}C_4$]-acetoacetate (1.01 g, 7.53 mmol) in 5 mL of *dd*-H_2O was added 1.9 mL of 4 M LiOH. The reaction mixture was stirred in a water bath at 40 °C for 5 h. After the mixture was concentrated in a rotary evaporator, the yellow residue

was dissolved in a minimum amount of *dd*-H_2O and acidified with a 10% H_2SO_4 solution in an ice bath. The acidified solution was saturated with NaCl, before extraction with diethylether. The extract was dried over anhydrous Na_2SO_4. After filtration and concentration *in vacuo*, the colorless oil (0.55 g) was dissolved in 40 mL of dry CH_2Cl_2 in an ice bath and combined with 6 g of finely ground molecular sieves (4 Å). After stirring for 15 min, a solution of *N*-acetylcysteamine (0.65 g, 5.40 mmol) in 10 mL of dry CH_2Cl_2 and a mixture of 1,3-dicyclohexyl carbodiimide (1.59 g, 5.40 mmol) and 4-dimethylaminopyridine (24 mg, 0.20 mmol) in 10 mL of dry CH_2Cl_2 were simultaneously added into the reaction, and the reaction mixture was stirred at room temperature overnight. After the reaction mixture was filtered over Celite and concentrated, the crude product was purified by flash column chromatography (silica gel, 5 % MeOH in $CHCl_3$), followed by column chromatography (RP-C_8, 5 % CH_3CN in H_2O) to provide pure product (1.02 g, 18.4 % yield): ^1H NMR (300 MHz, $CDCl_3$), for keto form δ 6.2 (br s, NH), 3.7 (dt, *J* = 131.0, 6.2 Hz, 2H, H-2), 3.4(q, *J* = 6.1 Hz, 2H, H-6), 3.0 (t, *J* = 6.1 Hz, 2H, H-5), 2.2 (ddd, *J* = 128.3, 6.1, 1.3 Hz, 3H, H-4), 2.0 (s, 3H, H-8); for enol form δ 5.4 (dm, *J* = 167.4, 2.89 Hz, 1H, H-2), 6.2 (br s, NH), 3.4(q, *J* = 6.1 Hz, 2H, H-6), 3.0 (t, *J* = 6.1 Hz, 2H, H-5), 2.0 (s, 3H, H-8), 1.9 (ddd, *J* = 128.3, 6.2, 4.0 Hz, 3H, H-4); ^{13}C NMR (75 MHz, $CDCl_3$), for keto form δ 199.9 (dd, *J* = 42.4, 36.9 Hz, C-3), 192.2 (d, *J* = 45.8 Hz, C-1), 170.5 (C-7), 58.0 (ddd, *J* = 46.0, 36.6, 14.1 Hz, C-2), 39.0 (C-6), 30.4 (dd, *J* = 42.5, 14.1 Hz, C-4), 29.2 (C-5), 23.1 (C-8); for enol form δ 194.2(dd, *J* = 62.8, 4.5 Hz, C-1), 174.0 (dd, *J* = 69.7, 48.3 Hz, C-3), 170.5 (C-7), 23.1 (C-8), 39.8 (C-6), 99.7 (ddd, *J* = 69.5, 62.9, 6.5 Hz, C-2), 27.7 (C-5), 21.0 (dt, *J* = 48.3, 5.5 Hz, C-4); HRMS (CI) calcd for $^{13}C_4C_4H_{13}NO_3S$ 207.0750, found 207.0746.

Synthesis of [1,2,3,4-$^{13}C_4$]-dimethylacrylic acid[48,49]

3-(Diethoxyphosphoryloxy)-[1,2,3,4-$^{13}C_4$]-butyric acid ethyl ester

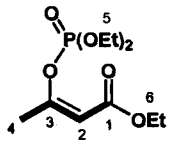

A solution of ethyl [1,2,3,4-$^{13}C_4$]-acetoacetate (0.55 g, 4.10 mmol) in 5 mL of dry diethylether was added to a grey suspension of NaH (60 % in mineral oil, 0.18 g, 4.51 mmol) in 10 mL of dry diethylether in a water bath at 10 °C. After 20 min, diethylchlorophosphate (0.78 g, 4.51 mmol) was introduced and stirring was continued at room temperature for 4 h. After the suspension was mixed with solid NH_4Cl for 20 min, it was filtered through

Celite, concentrated, and purified by flash column chromatography (silica gel, 40 % EtOAc in hexanes) to give a pure product (1.11 g, 90.2 % yield): ^{1}H NMR (300 MHz, $CDCl_3$) δ 5.3 (ddd, *J* = 163.0, 6.7, 3.4 Hz, 1H, H-2), 4.2 (q, *J* = 7.1 Hz, 4H, H-5-CH_2), 4.1 (qd, *J* = 7.1, 3.1 Hz, 2H, H-6-CH_2), 2.1 (dt, *J* = 129.5, 5.6 Hz, 3H, H-4), 1.3 (t, *J* = 7.1 Hz, 6H, H-5-CH_3), 1.2 (t, *J* = 7.1 Hz, 3H, H-5-CH_3); ^{13}C NMR (75 MHz, $CDCl_3$) δ 163.6 (dd, *J* = 78.4, 4.4 Hz, C-1), 158.0 (ddd, *J* = 84.7, 48.6, 6.5 Hz, C-3), 105.3 (ddt, *J* = 85.8, 78.4, 7.8 Hz, C-2,), 64.8 (C-5-CH_2), 59.7 (C-6-CH_3), 21.5 (dt, *J* = 48.7, 6.2 Hz, C4), 16.0 (C-5-CH_3), 14.2 (C-6-CH_3), 10.9 (C-5-CH_3), 10.5 (C-6-CH_3): ^{31}P (121.4 MHz) δ -7.5 ; HRMS (CI) calcd for $^{13}C_4C_6H_{19}O_6P$ 270.1054, found 270.1056.

[1,2,3,4-$^{13}C_4$]-Dimethylacrylic acid ethyl ester

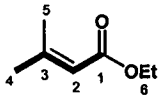

To a suspension of CuI (1.41 g, 7.40 mmol) in 20 mL of dry diethylether was added dropwise 9.3 mL of 1.6 M CH_3Li (0.325 g, 14.8 mmol) in diethylether at –30 °C, and the mixture was cooled to –78 °C. To the mixture was added 3-(diethoxyphosphoryloxy)-[1,2,3,4-$^{13}C_4$]-butyric acid ethyl ester and stirred at –78 °C for 4 h. The reaction mixture was transferred into a separatory funnel with 30 mL of saturated NH_4Cl solution and extracted with diethylether. The extract was washed with a mixture of 10 % NH_4Cl in brine and then brine, dried over anhydrous $MgSO_4$, filtered, and concentrated to give a yellow solution containing a small amount of diethylether to avoid the loss of product owing to excess evaporation. The crude product was used for the next step without purification: ^{1}H NMR (400 MHz, $CDCl_3$) δ 5.7 (dm, *J* = 159.7 Hz, 1H, H-2), 4.1 (qd, 2H, H-6-CH_2, *J* = 7.1, 3.0 Hz), 2.1 (m, 2H, H-5), 1.9 (dt, *J* = 126.7, 6.2 Hz, 3H, H-4), 1.3 (t, *J* = 7.1 Hz, 3H, H-6-CH_3); ^{13}C NMR (100 MHz, $CDCl_3$) δ 166.8 (dd, *J* = 75.7, 6.1 Hz, C-1), 156.4 (dd, *J* = 71.9, 40.7 Hz, C-3), 116.1 (ddd, *J* = 75.9, 72.1, 3.8 Hz, C-2), 59.4 (C-6-CH_2), 27.5 (ddd, *J* = 40.7, 7.38, 3.9 Hz, C-4), 20.1 (d, *J* = 40.0 Hz, C-5), 14.3 (C-6-CH_3); HRMS (CI) calcd for $^{13}C_4C_3H_{12}O_2$ 132.0972, found 132.1177.

[1,2,3,4-$^{13}C_4$]-Dimethylacrylic acid

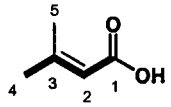

A solution of [1,2,3,4-$^{13}C_4$]-dimethylacrylic acid ethyl ester in 3 mL of 95 % ethanol was treated with 5 mL of 1 N NaOH solution at room temperature for 2 h. After adding 5 mL of *dd*-H_2O and saturating with NaCl, the

mixture was washed with CH_2Cl_2 and acidified with 1 mL of 3 N HCl solution in an ice bath. The aqueous phase was extracted with diethylether, and the solvent was evaporated to give white needles (0.385, 75.7 % yield): ^{1}H NMR (300 MHz, $CDCl_3$) δ 1.9 (dtd, $3H_4$, J = 126.9, 6.1, 1.9 Hz), 2.1 (m, $3H_5$), 5.7 (dm, $1H_2$, J = 160.3 Hz); ^{13}C NMR (75 MHz, $CDCl_3$) δ 20.5 (d, C_5, J = 39.7 Hz), 27.5 (ddd, C_4, J = 40.4, 7.3, 4.1 Hz), 115.6 (td, C_2, J = 72.5, 3.8 Hz), 159.5 (dd, C_3, J = 71.7, 40.4 Hz), 171.8 (dd, C_1, J = 73.3, 6.3 Hz); HRMS (CI) calcd for $^{13}C_4CH_8O_2$ 104.0659, found 104.0652.

Syntheses of 3-[$^2H_3$]-Methyl-3-butenoic acid and its NAC derivative [47,50]

3-[$^2H_3$]-Methyl-3-butenoic acid

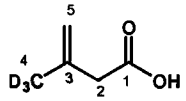

Diketene (0.84 g, 9.99 mmol) was added to CoI_2 (0.36 g, 1.09 mmol) in 15 mL of dry diethylether at -78 °C and then CD_3MgI (1.86 g, 11.0 mmol) was added dropwise. After the reaction mixture was stirred for 5 h, it was quenched with 6 N HCl solution at -78 °C and extracted with diethylether. The ethereal extract was extracted with 3N-NaOH. After the aqueous layer was acidified with 6 N HCl solution, the product was extracted with diethylether, and the ethereal extract was washed with brine, dried over anhydrous $MgSO_4$, and concentrated to provide a yellow oil (1.00 g, 97 % yield): ^{1}H NMR (400 MHz, $CDCl_3$) δ 5.0 (s, 1H, H-5), 4.9 (s, 1H, H-5), 3.1 (s, 2H, H-2); ^{13}C NMR (100 MHz, $CDCl_3$) δ 177.9 (C-1), 137.8 (C-3), 115.3 (C-5), 43.1 (C-2); HRMS (FAB) calcd for $C_5H_5{}^2H_3O_2$ 103.0713, found 103.0713.

NAC 3-[$^2H_3$]-methyl-3-butenoate

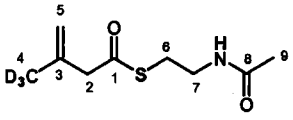

Dry 3-C^2H_3-but-3-enoic acid (0.80 g, 7.76 mmol) was dissolved in 60 mL of dry CH_2Cl_2 and combined with 7 g of finely ground molecular sieves (4 Å) in an ice bath. After stirring for 15 min, a solution of *N*-acetylcysteamine (1.02 g, 8.53 mmol) in 10 mL of dry CH_2Cl_2 and a mixture of 1,3-dicyclohexyl carbodiimide (2.50 g, 8.53 mmol) and 4-dimethylaminopyridine (38 mg, 0.31 mmol) in 10 mL of dry CH_2Cl_2 were added simultaneously to the reaction mixture at 0 °C. The reaction was warmed to room temperature and stirred overnight. After filtration and concentration *in vacuo*, the crude product was purified by flash column chromatography (silica gel, 2 % MeOH in

$CHCl_3$) to give the product (1.08 g, 68.4 % yield): ^1H NMR (300 MHz, $CDCl_3$) δ 6.2 (br s, NH), 5.0 (d, *J* = 1.6 Hz, 1H, H-5), 4.9 (dt, *J* = 1.5, 1.2 Hz, 1H, H-5), 3.4 (td, *J* = 6.3, 6.0 Hz, 2H, H-7), 3.2 (d, *J* = 1.1 Hz, 2H, H-2), 3.0 (t, *J* = 6.4 Hz, 2H, H-6), 2.0 (s, 3H, H-9); ^{13}C NMR (75 MHz, $CDCl_3$) δ 197.5 (C-1), 170.4 (C-8), 138.0 (C-3), 116.0 (C-5), 52.6 (C-2), 39.5 (C-7), 28.5 (C-6), 23.0 (C-9); HRMS (CI) calcd for $C_9H_{13}{}^2H_3NO_2S$ 205.1090, found 205.1090.

References

(1) Johnson, L. P. In *The Biology of Euglena*; Buetow, D. E., Ed.; Academic Press: New York, 1968; Vol. 1, pp. 1-25.

(2) Gojdics, M. *The genus Euglena*; University of Wisconsin Press, Madison, 1953.

(3) Kitaoka, S.; Nakano, Y.; Miyatake, K.; Yokota, A. In *The Biology of Euglena*; Buetow, D. E., Ed.; Academic Press: New York, 1989; Vol. 4, pp. 1-137.

(4) Wolken, J. J. *Euglena; an experimental organism for biochemical and biophysical studies*; 2nd ed.; Appleton-Century-Crofts, New York, 1967.

(5) Lackey, J. B. In *The Biology of Euglena*; Buetow, D. E., Ed.; Academic Press: New York, 1968; Vol. 1, pp. 27-44.

(6) Leedale, G. F. In *The Biology of Euglena*; Buetow, D. E., Ed.; Academic Press: New York, 1968; Vol. 3, pp. 1-27.

(7) Edelman, M.; Kahana, Z. E. In *The Biology of Euglena*; Buetow, D. E., Ed.; Academic Press: New York, 1989; Vol. 4, pp. 335-351.

(8) Cox, E. R. *Phytoflagellates*; Elsevier, New York, 1980.

(9) Anding, C.; Brandt, R. D.; Ourisson, G. Sterol biosynthesis in *Euglena gracilis Z.* Sterol precursors in light- grown and dark-grown *Euglena gracilis Z. Eur. J. Biochem.* **1971**, *24*, 259-263.

(10) Brandt, R. D.; Pryce, R. J.; Anding, C.; Ourisson, G. Sterol biosynthesis in *Euglena gracilis Z.* Comparative study of free and bound sterols in light and dark grown *Euglena gracilis Z. Eur. J. Biochem.* **1970**, *17*, 344-349.

(11) Goodwin, T. W.; Gross, J. A. Carotenoid distribution in bleached substrains of *Euglena gracilis. J. Protozool.* **1958**, *5*, 292-295.

(12) Richards, W. R. In *Pigment-Protein Complexes in Plastids: Synthesis and Assembly*; Sundqvist, C., Ryberg, M., Eds.; Academic Press: San Diego, 1993, pp. 91-178.

(13) Britton, G. In *Carotenoids*; Britton, G., Liaaen-Jensen, S., Pfander, H., Eds.; Birkhäuser: Basel, 1998; Vol. 3, pp. 13-147.

(14) Kleinig, H. The role of plastids in isoprenoid biosynthesis. *Annu. Rev. Plant Physiol. Plant Mol. Biol.* **1989**, *40*, 39-59.

(15) Heelis, D. V.; Kernick, W.; Phillips, G. O.; Davies, K. Separation and identification of the carotenoid pigments of stigmata isolated from light-grown cells of *Euglena gracilis* strain *Z. Arch. Microbiol.* **1979**, *121*, 207-211.

(16) Krinsky, N. I.; Goldsmith, T. H. The carotenoids of the flagellated alga, Euglena gracilis. *Arch. Biochem. Biophys.* **1960**, *91*, 271-279.

(17) Goodwin, T. W.; Jamikorn, M. Carotenoid synthesis in two varieties of Euglena gracilis. *J. Protozool.* **1954**, *1*, 216-219.

(18) Nitsche, H. Heteroxanthin in *Euglena gracilis. Arch. Mikrobiol.* **1973**, *90*, 151-155.

(19) Steele, W.; Gurin, S. Biosynthesis of β-carotene in *Euglena gracilis. J. Biol. Chem.* **1960**, *235*, 2778-2785.

(20) Braithwaite, G. D.; Goodwin, T. W. Studies in carotenogenesis. 27. Incorporation of [2-^{14}C] acetate, DL-[2-^{14}C] mevalonate and ^{14}C-labelled carbon dioxide into carrotroot preparations. *Biochem. J.* **1960**, *76*, 194-197.

(21) Chichester, C. O.; Yokoyama, H.; Nakayama, T. O.; Lukton, A.; Mackinney, G. Leucine metabolism and carotene biosynthesis. *J. Biol. Chem.* **1959**, *234*, 598-602.

(22) Threlfall, D. R.; Goodwin, T. W. Nature, intracellular distribution and formation of terpenoid quinones in *Euglena gracilis. Biochem. J.* **1967**, *103*, 573-588.

(23) Cooper, C. Z.; Benedict, C. R. *Plant Physiol.* **1967**, *42*, S44-S45.

(24) Douglas, S. E.; Turner, S. Molecular evidence for the origin of plastids from a cyanobacterium-like ancestor. *J. Mol. Evol.* **1991**, *33*, 267-273.

(25) Lichtenthaler, H. K. The plants' 1-deoxyD-xylulose-5-phosphate pathway for biosynthesis of isoprenoids. *Fett/Lipid* **1998**, *100*, 128-138.

(26) Disch, A.; Schwender, J.; Muller, C.; Lichtenthaler, H. K.; Rohmer, M. Distribution of the mevalonate and glyceraldehyde phosphate/pyruvate pathways for isoprenoid biosynthesis in unicellular algae and the cyanobacterium *Synechocystis PCC 6714. Biochem. J.* **1998**, *333*, 381-388.

(27) Flesch, G.; Rohmer, M. Prokaryotic hopanoids: the biosynthesis of the bacteriohopane skeleton. Formation of isoprenic units from two distinct acetate pools and a novel type of carbon/carbon linkage between a triterpene and D-ribose. *Eur. J. Biochem.* **1988**, *175*, 405-411.

(28) Müller, C.; Schwender, J.; Disch, A.; Rohmer, M.; Lichtenthaler, F. W.; Lichtenthaler, H. K. Occurence of the 1-deoxy-D-xylulose 5-phosphate pathway of isopentenyl diphosphate biosynthesis in different algae groups. *Adv. Plant Lipid Res.* **1998**, 425-428.

(29) *One-dimentional and two-dimentional NMR spectra by modern pulse techniques*; Nakanishi, K., Ed.; University Science Books: Mill Valley, 1990.

(30) Noggle, J. H.; Schirmer, R. E. *The Nuclear Overhauser Effect-Chemical Application*; Academic Press, New York, 1971.

(31) Nabeta, K.; Kawae, T.; Saitoh, T.; Kikuchi, T. Syntheis of chlorophyll a and β-carotene from ^{2}H- and ^{13}C-labelled mevalonates and ^{13}C-labelled glycine in cultured cells of liverworts, *Heteroscyphus planus* and *Lophocoles heterophylla*. *J. Chem. Soc., Perkin Trans. 1* **1997**, 261-267.

(32) Broers, S. T. J. Ph. D. Dissertation, Eidgenössische Technische Hochschule, Zürich, 1994.

(33) Schwender, J.; Zeidler, J.; Groner, R.; Muller, C.; Focke, M.; Braun, S.; Lichtenthaler, F. W.; Lichtenthaler, H. K. Incorporation of 1-deoxy-D-xylulose into isoprene and phytol by higher plants and algae. *FEBS Lett.* **1997**, *414*, 129-134.

(34) Schwarz, M. K. Ph.D. Dissertation, Eidgenössische Technische Hochschule, Zürich, 1994.

(35) Thiel, R.; Adam, K. P. Incorporation of [1-13C]-deoxy-D-xylulose into isoprenoids of the liverwort Conocephalum conicum. *Phytochem.* **2002**, *59*, 269-274.

(36) Taylor, S. V., Vu, L. D., and Begley, T. P. Chemical and enzymatic synthesis of 1-deoxy-D-xylulose-5-phosphate. *J. Org. Chem.* **1998**, *63*, 2375-2377.

(37) Kennedy, I. A.; Hemscheidt, T.; Britten, J. F.; Spenser, I. D. 1-Deoxy- D-xylulose. *Can. J. Chem.* **1995**, *73*, 1329-1333.

(38) Armstrong, G. In *Comprehensive Natural Product Chemistry*; Cane, D. E., Ed.; Elsevier: New York, 1999; Vol. 2, pp. 321-352.

(39) Dolphin, W. Photoinduced carotenogenesis in chlorotic *E. gracilis*. *Plant Physiol.* **1970**, *46*, 685-691.

(40) Briton, G. In *Aspects of Terpenoid Chemistry and Biochemistry*; Goodwin, T. W., Ed.; Academic Press: New York, 1971, pp. 255-289.

(41) Gross, J. A.; Stroz, R. J. Evidence for phytoene in Euglena mutants. *Plant Sci. Lett.* **1974**, *3*, 67-73.

(42) Gross, J. A.; Stroz, R. J.; Britton, G. Carotenoid hydrocarbons of *Euglena gracilis* and derived mutants. *Plant Physiol.* **1975**, *55*, 175-177.

(43) Granger, P.; Maudinas, B.; Herber, R.; Villoutreix, J. Proton and carbon-13 NMR spectra of cis- and trans- phytoene isomers. *J. Magn. Res.* **1973**, *10*, 43-50.

(44) Nes, W. D.; Bach, T. J. Evidence for a mevalonate shunt in a tracheophyte. *Proc. R. Soc. Lond. B* **1985**, *225*, 425-444.

(45) Ginger, M. L.; Chance, M. L.; Goad, L. J. Elucidation of carbon sources used for the biosynthesis of fatty acids and sterols in the trypanosomatid Leishmanis mexicana. *Biochem. J.* **1999**, *342*, 397-405.

(46) Ginger, M. L.; Prescott, M. C.; Reymonds, D. G.; Chance, M. L.; Goad, L. J. Utilization of leucine and acetate as carbon souces for sterol and fatty acid biosynthesis by old and new world *Leishmanis* species, *Endotrypanum monterogeii* and *Trypanosoma cruzi*. *Eur. J. Biochem.* **2000**, *267*, 2555-2566.

(47) Liu, Y.; Li, Z.; Vederas, J. C. Biosynthetic incorporation of advenced precursors into dehydrocurvularin, a polyketide phytotoxin from *Alternaria cinerariae*. *Tetrahedron* **1998**, *54*, 15937-15958.

(48) Sum, F.-W.; Weiler, L. Stereoselective synthesis of β-substituted α,β-unsaturated esters by dialkylcuprate coupling to the enol phosphate of β-keto esters. *Can. J. Chem.* **1979**, *57*, 1431-1441.

(49) Winter, R. E. K.; Jian, Z. A Convenient preparation of 3-[$^2H_3$]-methyl-3-buten-1-ol. *J. Labelled Compd. Radiopharm.* **1992**, *31*, 787-791.

(50) Fujisawa, T.; Sato, T.; Gotoh, Y. Reaction of diketene with grignard reagents in the presence of cobalt catalyst. A convenient method for the synthesis of 3-methylenealkanoic acids leading to terpenoids. *Bull. Chem. Soc. Jpn.* **1982**, *55*, 3555-3559.

(51) Battersby, A. R.; Hodgson, G. L.; Hunt, E.; McDonald, E.; Saunders, J. Biosynthesis of porphyrins and related macrocycles. Part VI. Nature of the rearrangement process leading to the natural type III porphyrins. *J. Chem. Soc., Perkin Trans. 1* **1976**, *3*, 273-282.

(52) Perrin, D. D.; Armarego, W. L. F. *Purification of Laboratory Chemicals*; 3rd ed.; Pergamon Press, New York, 1988.

(53) Still, W. C.; Kahn, M.; Mitra, A. Rapid chromatographic technique for preparative separations with moderate resolution. *J. Org. Chem.* **1978**, *43*, 2923-2925.

(54) Packer, L. *Carotenoids*; Academic Press, San Diego, 1992.

(55) Tsushima, M.; Mune, E.; Maoka, T.; Matsuno, T. Isolation of stereoisomeric epoxy carotenoids and new acetylenic carotenoid from the common freshwater goby *Rhinogobius brunneus*. *J. Nat. Prod.* **2000**, *63*, 960-964.

CHAPTER THREE

Phytol Biosynthesis in *Euglena gracilis*

Introduction

Phytol, a diterpenoid alcohol, is generally known as the compound derived from hydrolysis of chlorophylls (Chl), *a* and *b*. The formation of phytol, or the phytyl sidechain of Chl, has been of interest to scientists who have studied chlorophyll biosynthesis. The last step of chlorophyll biosynthesis is a prenylation reaction which has been regarded to occur by transfer of geranylgeranyl diphosphate (GGPP), the general precursor of diterpenoids, or phytyl diphosphate (PDP) to chlorophyllides (Chlide), *a* and *b* catalyzed by chlorophyll synthase (EC 2.5.1.62) (Fig.3.1). The consecutive reductions of geranylgeranyl chlorophyll (Chl_{GG}) provide phytyl chlorophyll (= chlorophyll; Chl_P) through the reduced intermediates, dihydrogeranylgeranyl chlorophyll (Chl_{DHGG}) and tetrahydrogeranylgeranyl chlorophyll (Chl_{THGG}). PDP produced by the reduction of GGPP can alternatively be directly condensed with Chlides.[1,2]

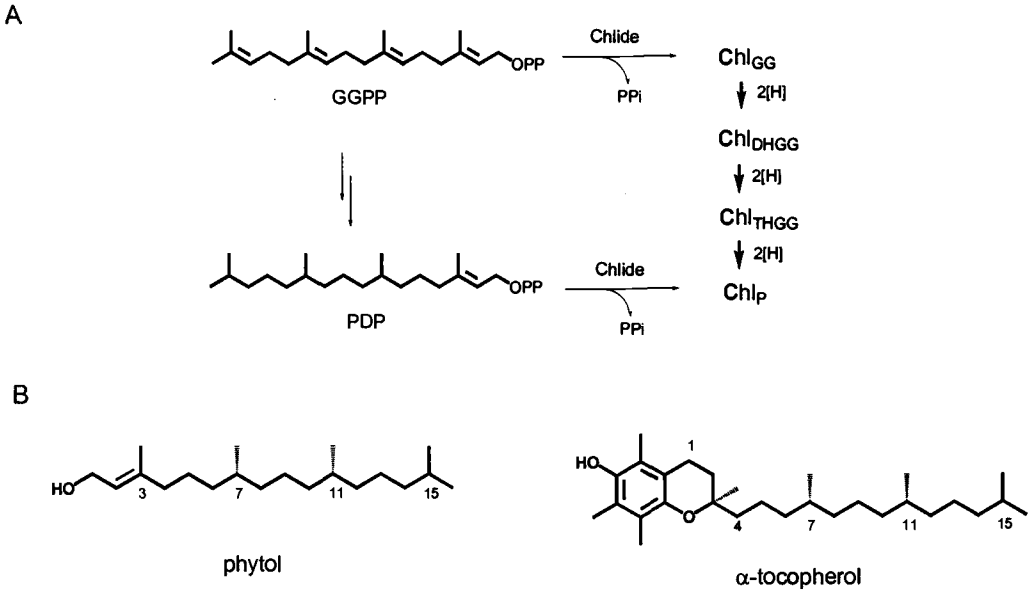

Fig.3.1 Formation of chlorophylls from GGPP and PDP (A). The structures of phytol and α-tocopherol (B).

Even though the mechanism of prenylation and the conversion of Chl_{GG} to Chl_p or GGPP to PDP is not clearly clarified yet, phytol biosynthesis has now been shown to mainly occur by the 2-*C*-methyl-D-erythritol-4-phosphate (MEP) pathway.[3,4] According to findings to date, green algae and cyanobacteria utilize only the MEP pathway to synthesize isoprenoid compounds, including phytol, while red algae and higher plants are able to synthesize plastidic isoprenoids such as β-carotene and phytol via the MEP pathway and cytosolic sterols via the MVA pathway simultaneously. *Euglena gracilis*, however, was reported to utilize only the MVA pathway to produce phytol as well as cytosolic sterols.[5,6]

The investigation of phytol biosynthesis in *E. gracilis* was initiated in 1977, in a manner similar to the early studies on carotenoid biosynthesis. A key difference was the use of a stable isotope precursor. Based on the finding that carotenoid biosynthesis in *E. gracilis* occurs by the MVA pathway,[7] Battersby *et al.* performed incubation experiments with [1-^{13}C]-acetate and [2-^{14}C]-MVA to see the labeling pattern in phytol.[8] The results showed clear enhancement of carbons corresponding to C1 and C3 of IPP from the experiment with [1-^{13}C]-acetate, which was consistent with the MVA pathway. The direct incorporation of [2-^{14}C]-MVA, however, was very low (0.07 %) (Fig.3.2). Battersby *et al.* drew the conclusion that *E. gracilis* mainly utilizes acetate for isoprenoid biosynthesis based on the labeling pattern which was consistent with the MVA pathway, and the impermeability of cell barriers to MVA resulted in the poor incorporation of MVA into isoprenoids.

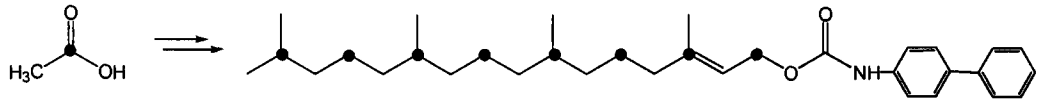

[1-^{13}C]-acetate

phytyl biphenyl-4-ylcarbamate

Fig.3.2. Incorporation pattern for phytol from the incubation experiment with [1-^{13}C]-acetate by Battersby *et al.* Phytyl biphenyl-4-ylcarbamate was prepared from the pure phytol. Filled circles indicate ^{13}C labeled carbons.

Once the MEP pathway was discovered in the early 1990's, *E. gracilis* was considered for a reinvestigation of the formation of phytol. Like red algae and higher plants, *E. gracilis* is proposed to have acquired its chloroplasts through an

endosymbiotic event, most likely from a green alga.[9] Most photosynthetic eukaryotes including green algae had been shown to use the MEP pathway. Red algae and higher plants had been revealed to possess the MEP pathway in their chloroplasts, whereas green algae use the MEP pathway for all isoprenoids. Therefore, *E. gracilis* would also be expected to use the MEP pathway for phytol biosynthesis, despite the early work by Battersby and others.

In 1998, Rohmer, Lichtenthaler *et al.* investigated the distribution of both pathways in *E. gracilis* by examining incorporation patterns of isoprenoids derived from [1-^{13}C]-glucose.[5] For *E. gracilis*, the ^{13}C isotopic abundances of phytol and ergosterol indicated a labeling pattern arising from the MVA pathway, showing high isotopic enrichments of more than four-fold in C2 (4.6-4.8) and C4 (4.7-5.0) positions derived from the MVA pathway and low abundances in the C1 positions (1.3-1.7) arising from the MEP pathway (Fig.3.3).[5] The methyl positions were also heavily labeled which would be expected from both pathways.

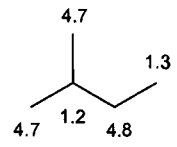

Isoprene units of phytol

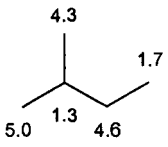

Isoprene units of ergosterol

Fig.3.3. Isotopic abundances in isoprene units of phytol and ergosterol from *E. gracilis* after incubation experiment with [1-^{13}C]-glucose by Rohmer *et al.*[5] Isotopic abundances are indicated as mean values for all carbon atoms.

An experiment supporting this result was carried out by performing GC-MS analysis of phytol and ergosterol when [1-$^{2}H_1$]-deoxy-D-xylulose (DX) and [2-^{13}C]-MVA were used as precursors.[6] The percent incorporations of [1-$^{2}H_1$]-DX and [2-^{13}C]-MVA into phytol were 3-5 % and 2-4 % and into ergosterol were 3-6 % and 20-32 %, respectively. Although the weak incorporations of labeled DX into phytol and ergosterol were observed, these might be attributed to indirect incorporation of deuterium from smaller intermediate(s) due to the breakdown of DX. In addition, the low incorporation of labeled MVA into phytol might result from impermeability of cell barriers to MVA, as was previously suggested. These results led to the declaration

that *E. gracilis* is the only photosynthetic organism for which no evidence for the MEP pathway could be found, even for the formation of chloroplast isoprenoids.[5,6]

Similar results were obtained in our preliminary experiments using [1-^{13}C]-glucose and [5-$^{2}H_2$]-DX. The relative incorporation of label into phytol from the incubation experiment with [1-^{13}C]-glucose indicated the labeling pattern consistent with the MVA pathway, as was observed by Rohmer *et al.* Carbons corresponding to C2, C4, and C5 of the isoprene unit were enriched 3.3-4.3-fold with ^{13}C isotopes from labeled glucose. For C1 of IPP discretely incorporated via the MEP pathway, there was essentially no enrichment (Fig.3.4).

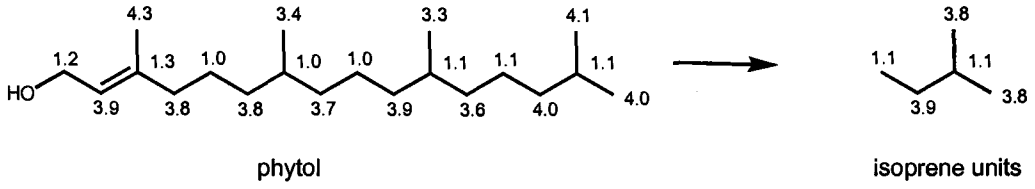

Fig.3.4. Relative incorporation levels for phytol from the [1-^{13}C]-glucose incubation experiment. The ratios for the isoprene unit are the average values from the corresponding carbons of each isoprene unit.

From the [5-$^{2}H_2$]-DX incubation experiment, the overall deuterium incorporation percentage into phytol was very low. The labeling pattern of phytol revealed no intact incorporation of [5-$^{2}H_2$]-DX into phytol (Fig.3.5). In the ^{2}H-NMR spectrum of phytol, there was little deuterium signal at 4.1 ppm corresponding to H1 of the isoprene unit which is the critical position labeled from [5-$^{2}H_2$]-DX via the MEP pathway. Deuteriums were introduced to H2, the methylene groups, and methyl groups. It appears as though DX is metabolized to acetate prior to utilization for phytol biosynthesis. The percent incorporation levels of deuterium into phytol relative to the natural abundance deuterium in the chloroform peak were: methylenes = 1 %, methyls = 2 %, H3' = 0.5 %.

Therefore, the overall results such as the labeling pattern from the [1-^{13}C]-glucose incubation experiment and the ^{2}H-NMR spectrum from the [5-$^{2}H_2$]-DX incubation experiment suggest that: (1) DX is not directly utilized for phytol biosynthesis in *E. gracilis*, (2) label from DX is incorporated into phytol only after degradation, presumably to [2-$^{2}H_2$]-acetate, and (3) all current data support the

formation of phytol via the MVA pathway. Additionally, ergosterol, a representative cytosolic isoprenoid, was isolated from the [5-$^2H_2$]-DX incubation experiment. The ^{2}H-NMR spectrum of ergosterol showed a possible weak direct incorporation of labeled DX (Fig.3.6). The percent incorporation levels of deuterium into ergosterol relative to the natural abundance deuterium in the chloroform peak were: methylenes = 7 %, olefins = 6 %. However, there was no peak at ~0.8 ppm for the methyls of ergosterol derived from catabolism of [5-$^2H_2$]-DX, compared with the phytol spectrum. This result suggests that ergosterol might not be produced from the metabolized DX but from the intact form with much lesser contribution than carotenoids.

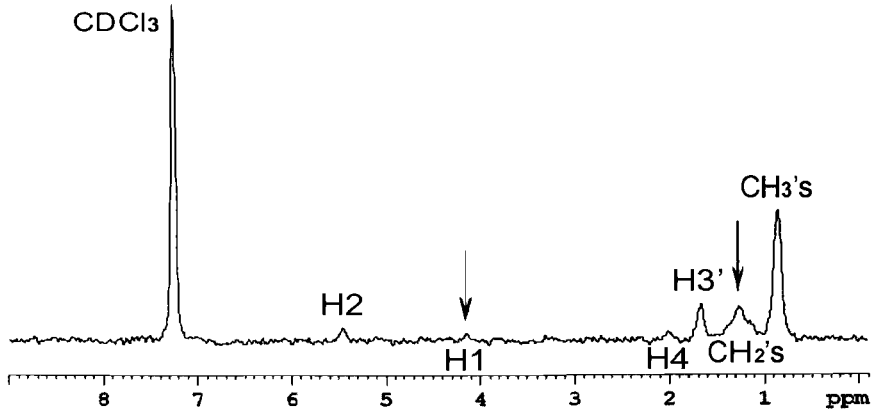

Fig.3.5. ^{2}H-NMR spectrum for phytol from the [5-$^2H_2$]-DX incubation experiment. Arrows indicate sites of expected labeling via the MEP pathway.

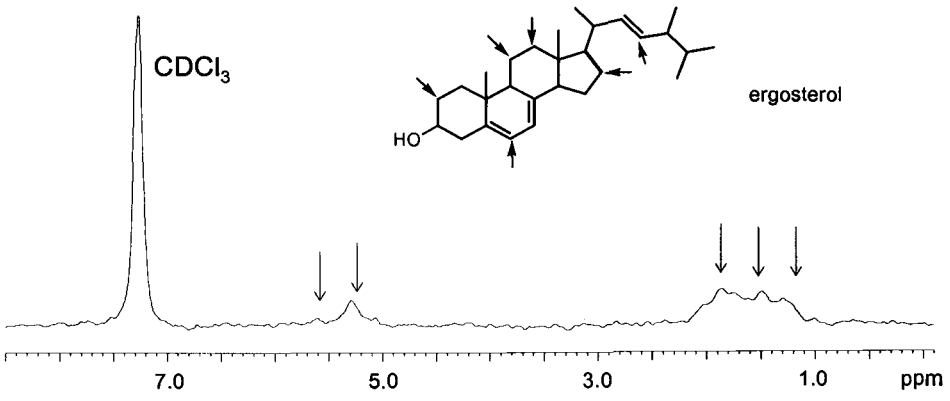

Fig.3.6. ^{2}H-NMR spectrum for ergosterol from [5-$^2H_2$]-DX incubation experiment. Arrows indicate sites of expected labeling via the MEP pathway.

However, an interesting result was observed when [U-$^{13}C_6$]-glucose was used in an incubation experiment in order to possibly see a low level involvement of the MEP pathway for phytol formation. Because, in the case of *Streptomyces aeriouvifer* which is reported to simultaneously operate the MEP pathway for the formation of the primary metabolite, menaquinone-9, and the MVA pathway for the production of the secondary metabolite, naphterpin, a small contribution of the MEP pathway was observed for the formation of naphterpin by detecting the long-range couplings from C1 and C2 to C4 of the isoprene unit.[10] The labeling pattern of phytol arising from the incubation experiment with [U-$^{13}C_6$]-glucose could be predicted on the basis of each pathway. In the MVA pathway, [U-$^{13}C_6$]-glucose would be catabolized by glycolysis into [1,2-$^{13}C_2$]-acetate, which is assembled into MVA and then phytol. In view of the labeling pattern of phytol, three acetate units constitute C1-C2, C3-C5, and C4 of the isoprene unit, which appear as doublets in the C1-C2 and C3-C5 pairs due to the intact ^{13}C-^{13}C bonds and an enhanced singlet for C4 arising from the loss of the carboxyl carbon in the last decarboxylation step to form IPP (Fig.3.7).

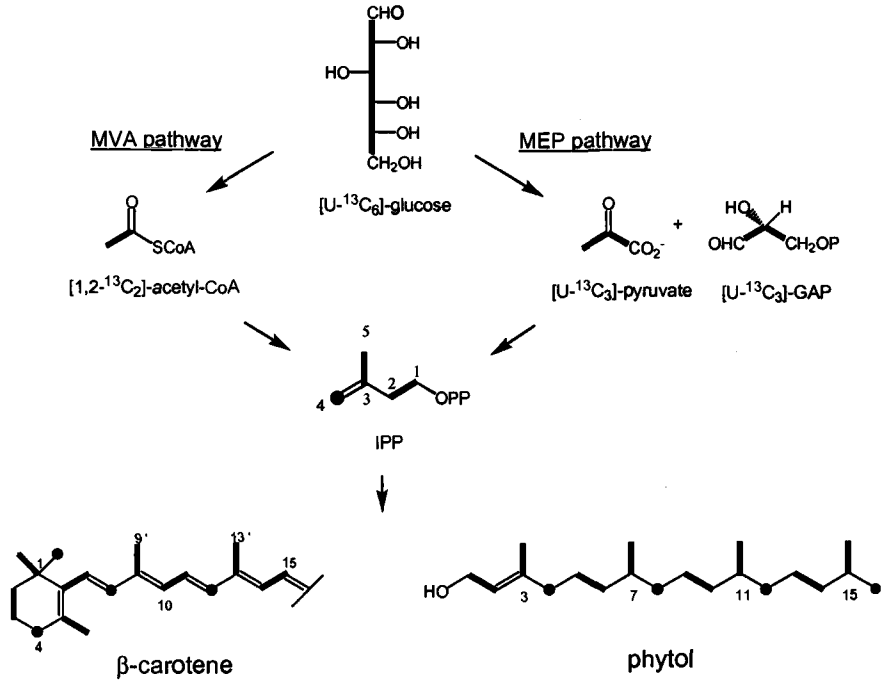

Fig.3.7. Predicted labeling patterns for β-carotene and phytol from [U-$^{13}C_6$]-glucose incubation experiment via both pathways. Bold bonds and filled circles show doublets due to coupled ^{13}C isotopes and enriched singlets in the ^{13}C-NMR spectra, respectively.

In the case of the incubation experiment with [U-$^{13}C_6$]-glucose unlike the [1-^{13}C]-glucose incubation experiment, the MEP pathway provides the same general labeling pattern as the MVA pathway, because [U-$^{13}C_6$]-glucose can be converted to [U-$^{13}C_3$]-GAP and [U-$^{13}C_3$]-pyruvate composing C1-C2-C4 and C3-C5 of the isoprene unit via the MEP pathway, respectively (Fig.3.7). Consequently, carbons of C1-C2 and C3-C5 from [U-$^{13}C_3$]-GAP and [U-$^{13}C_3$]-pyruvate appear mainly as doublets. The C4 fragmented from [U-$^{13}C_3$]-GAP during the transformation of DXP to MEP is shown as a broadened singlet under a normal ^{13}C-NMR conditions. The broadening is due to the long range coupling relationships between C4-C2 ($^2J_{C\text{-}C}$= 3.8 Hz) and C4-C1 ($^3J_{C\text{-}C}$= 2.3 Hz) of 2-*C*-methyl-D-erythritol which can be seen with sufficient resolution of the ^{13}C spectrum or with specialized NMR techniques such as the modified HMBC (Heteronuclear Multiple Bond Connectivity) and TANGO (Testing for Adjacent Nuclei with a Gyration Operator)-HMBC techniques effectively employed to elucidate the MEP pathway.[10,11] Therefore, regardless of which isoprenoid pathway operates, the incubation experiments with [U-$^{13}C_6$]-glucose should lead to the same general coupling pattern in all isoprenoids.

In contrast with the predictions, however, the labeling pattern of phytol from the incubation experiment with [U-$^{13}C_6$]-glucose was an utterly different and unique pattern. [U-$^{13}C_6$]-Glucose (10 % of total glucose) appeared to be efficiently assimilated into phytol, and its overall incorporation level was 9.5 % by integrating the ^{13}C enrichment at H1 of phytol. Figure 3.8 clearly depicts the observed coupling pattern of each carbon in phytol showing doublets and singlets at the different positions in contrast to the expected coupling pattern. Instead of C4, C8, C12, and C16 singlets, the branching methyl carbons (C3', C7', C11', and C15') were observed as intense singlets. The carbons of C3-C4, C7-C8, C11-C12, and C15-C16 all appeared as doublets as C1-C2, C5-C6, C9-C10, and C13-C14, reflecting an intact $^{13}C_2$ origin.

This inconsistent labeling pattern makes it appear that a transposition simply occurs between C4 and C5 in the isoprene unit. A transposition between C4 and C5 was reported by Nabeta *et al.* in 1998.[12] They observed the transposition in the phytol structure isolated from the liverwort, *Heteroscyphus planus,* but did not explain it, presumably because it was a minor contribution. Unlike the liverwort, the

transposition was essentially complete and was the predominant feature in the formation of *Euglena* phytol.

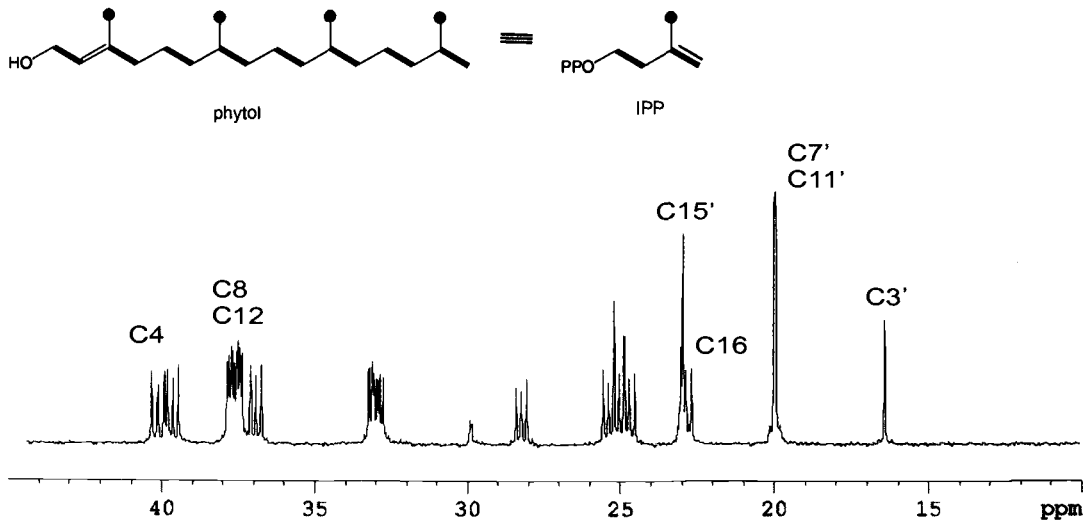

Fig.3.8. Observed labeling pattern and ^{13}C-NMR spectrum for phytol from the [U-$^{13}C_6$]-glucose incubation experiment.

How could the transposition occur in phytol biosynthesis? One possible way considered for the transposition was the reversible isomerization of IPP to DMAPP catalyzed by IPP isomerase. This reaction involves the protonation of IPP to form a tertiary carbocation which is deprotonated at C2 to form DMAPP.[13] In this structure, the bond of C2-C3 could rotate, leading to the exchange of C4 to C5. When [U-$^{13}C_6$]-glucose is utilized for isoprenoid biosynthesis, IPP could be isomerized to DMAPP molecules which show different labeling patterns. One DMAPP may retain the same labeling pattern as the IPP origin. The other appears as doublets at C1-C2 and C3-C4 and singlet at C4 which can, in turn, be isomerized to IPP showing the labeling pattern inconsistent with the IPP origin. If differentially labeled isoprene units are incorporated into phytol, the ^{13}C-NMR spectrum should be scrambled with doublets at both C3-C5 and C3-C4 and enhanced singlets at C4 and C5 (Fig.3.9). But the observed ^{13}C-NMR spectra of phytol and carotenoids displayed each unique labeling pattern with no sign of a mixed labeling pattern. The labeling pattern of phytol was characterized as doublets between C1-C2 and C3-C4 and a singlet at C5 in the

isoprene unit, whereas carotenoids appeared as the labeling pattern, showing doublets at C1-C2 and C3-C5 and a singlet at C4. These patterns suggest that there is no equilibration of the DMAPP methyl groups mediated by IPP:DMAPP isomerase.

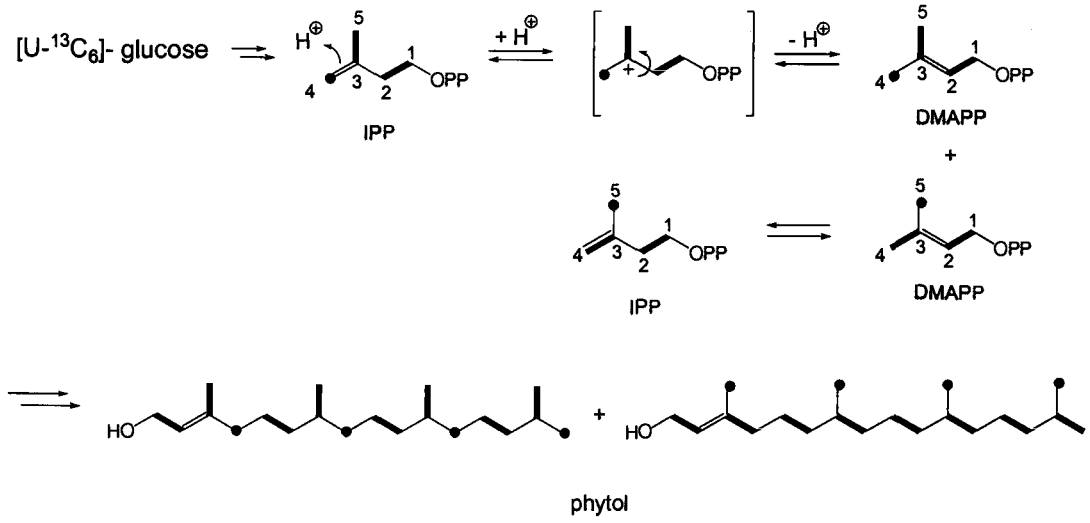

Fig.3.9. Predicted labeling pattern for phytol affected by IPP isomerase.

Because such an unusual labeling pattern of phytol was completely unexpected, a subsequent incubation experiment with [1,2-$^{13}C_2$]-acetate was conducted to confirm this finding. The labeling pattern of phytol from this experiment was qualitatively the same as the [U-$^{13}C_6$]-glucose incubation experiment, showing doublets for C1-C2 and C3-C4 and an intense singlet for C5 of the isoprene unit. These preliminary results suggest that an alternate biosynthetic pathway operates to form phytol, independent of both the MVA and the MEP pathways. The initial constraints for phytol biosynthesis are that three acetate or acetate-like units would be assembled into the isoprene units of phytol, accompanied by loss of a carboxyl carbon from one acetate unit to produce the C_5 skeleton. This conclusion is based on the equivalent high incorporation levels at C2, C4, and C5 of the isoprene unit from the experiments with [1-^{13}C]-glucose and the labeling pattern obtained from the incubation experiment with [1,2-$^{13}C_2$]-acetate. Based on these findings, further experiments were done to investigate the possible precursors that would be assembled into phytol, resulting in the observed unique labeling pattern.

In Chapter Three, results about the incubation experiments using labeled compounds will be described to elucidate possible precursors for phytol biosynthesis. The possible formation of phytol via the polyketide pathway will be discussed.

Results and Discussion

Investigation of possible precursors for phytol biosynthesis

On the basis of the preliminary finding that only the methyl carbon from the acetate is introduced into the branching methyls of phytol, a methylation reaction to the C_4 linear structure were regarded as a possible route to form the isoprene unit. For the methylation reaction, *S*-adenosylmethionine (SAM), a methyl group donor in biosynthesis of numerous methylated metabolites, was the first to be considered. In order to test the contribution of SAM in phytol biosynthesis, [methyl-^{13}C]-methione, as a precursor of SAM was used for an incubation experiment. If the branching methyl groups of phytol could be derived from SAM, the enhanced ^{13}C isotope peaks would be detected in C3', 7', 11', and 15'. The ^{13}C-NMR spectrum of phytol, however, displayed almost even intensities for all carbons, which reveals that the branching methyl carbons of phytol are not generated via typical biological methylations, but apparently from the methyl carbon of acetate via a decarboxylation reaction.

After lack of incorporation of label from [methyl-^{13}C]-methione, other potential intermediates for the formation of the isoprene unit that would explain the inconsistent labeling pattern of phytol were considered. Figure 3.10 displays the metabolic routes from acetate and leucine to IPP through HMG-CoA, and the boxed compounds are the potential precursors employed in further incubation experiments to elucidate phytol biosynthesis. The metabolic pathway for the conversion of leucine into HMG-CoA is known as an additional route to provide precursors for isoprenoid biosynthesis in some organisms.[14-16] HMG-CoA formed from leucine had been considered to be readily cleaved to acetyl-CoA and acetoacetyl-CoA before reutilization.[17] In 1999, however, the contribution of leucine to isoprenoid biosynthesis was found to be different for some trypanosomatid species which are primitive eukaryotic protozoa.[18] Through this study, some trypanosomatid species were found to directly utilize leucine for synthesis of sterols with little breakdown of the HMG-CoA formed from leucine.[19]

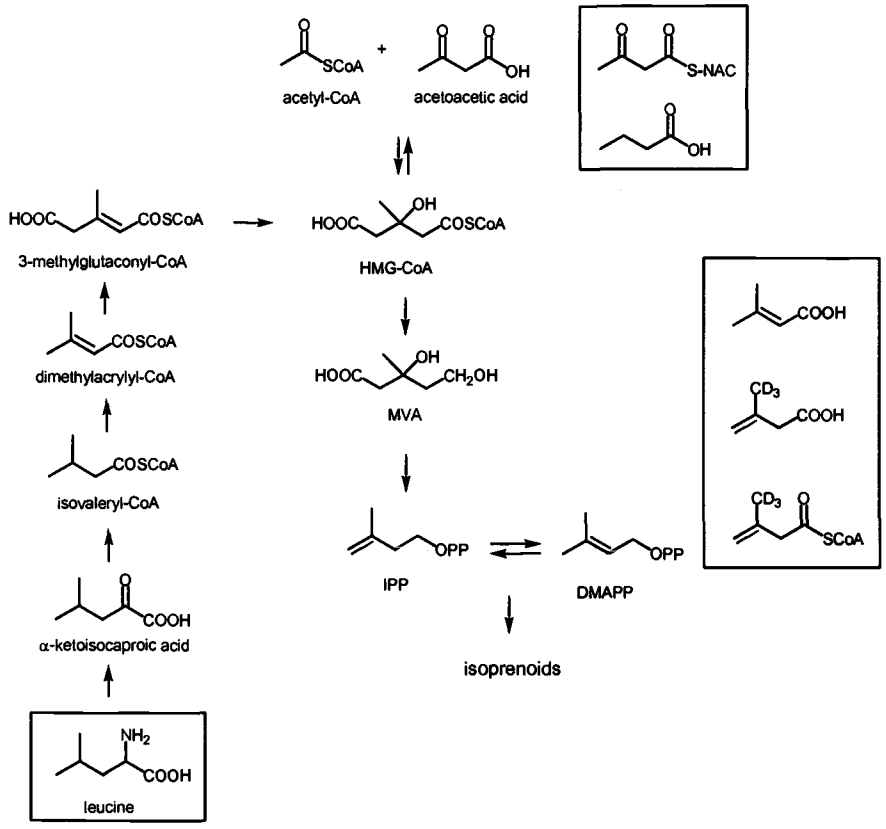

Fig.3.10. Metabolic pathways to isoprenoids from acetate and leucine. Compounds in boxes were used for the incubation experiments.

In view of phylogeny, trypanosomatids are flagellated eukaryotes which are regarded to have the same ancestor as photosynthetic euglenoid flagellates,[20,21] including *E. gracilis*, which acquired chloroplasts during a relatively late step in the evolutionary process. If so, similar metabolic pathways could be shared between trypanosomatids and photosynthetic euglenoid flagellates. Based on this relationship, incubation experiments with labeled leucine and other compounds were considered to be reasonable for elucidation of phytol biosynthesis.

In order to investigate leucine as a precursor, an incubation experiment with [2-^{13}C]-leucine was performed. If the intact leucine is incorporated into phytol in *E. gracilis* as though it is into sterols in trypanosomatids, ^{13}C isotopes from [2-^{13}C]-leucine should be distinctly detected in only the positions corresponding to C1 of the

isoprene units in phytol. If leucine is catabolized to acetate, the ^{13}C label will end up at C1 of acetate, and C1 and C3 positions of the isoprene units will be labeled.

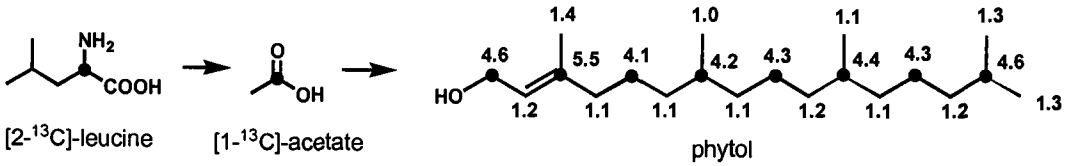

Fig.3.11. Enrichments in phytol from the incubation experiment with [2-^{13}C]-leucine. Filled circles indicate enhanced ^{13}C isotopes derived from [2-^{13}C]-leucine after catabolism to [1-^{13}C]-acetate.

The ^{13}C-NMR spectrum of phytol from this incubation experiment showed ^{13}C isotope enrichment at the C1 and C3 positions of the isoprene units, which arise from the catabolism of [2-^{13}C]-leucine to [1-^{13}C]-acetate (Fig.3.11). The enrichments displayed a range of 4.1-5.5 for carbons corresponding to C1 and C3 of the isoprene unit, while the carbons derived from methyl carbon of acetate showed essentially no enrichment (1.0-1.4). From this experiment, the possibility that leucine may be an intact precursor for phytol biosynthesis was ruled out, but leucine was observed to be a good general carbon source for the formation of phytol in *E. gracilis*.

Through the previous experiments to investigate carotenoid biosynthesis, the *N*-acetylcysteamine (NAC) derivative of [U-$^{13}C_4$]-acetoacetate was incorporated intact to a small extent into carotenoid compounds. From the same incubation experiment, the fate of the labeled compound as a precursor was also examined in phytol biosynthesis. If the C_4 skeleton of the NAC derivative goes into phytol without breakdown as shown in carotenoid biosynthesis, evidence would be provided that acetoacetate might be condensed with an acetate-like C_2 unit, in a manner different than in the MVA pathway.

For the initial incubation with NAC-[U-$^{13}C_4$]-acetoacetate, pentynoic acid was employed as a β-oxidation inhibitor to avoid β-oxidation of the labeled compound.[22] Unfortunately, the inhibitor turned out to hamper the growth of *E. gracilis*. Because of the poor growth with pentynoic acid, a second experiment was carried out without the β-oxidation inhibitor. After the experiment (1.6 % ^{13}C enrichment integrated at H1 of phytol), the spectrum of phytol did not show doublets of doublets for any carbons, and

the labeling pattern was consistent with the [U-$^{13}C_6$]-glucose and [1,2-$^{13}C_2$]-acetate incubation experiments showing doublets at C1-C2 and C3-C4 of the isoprene unit and singlets at the branching methyl carbons (Fig.3.12). This result suggests that, unlike for carotenoid biosynthesis, the catabolized form of NAC-[U-$^{13}C_4$]-acetoacetate is utilized for phytol biosynthesis rather than the intact form.

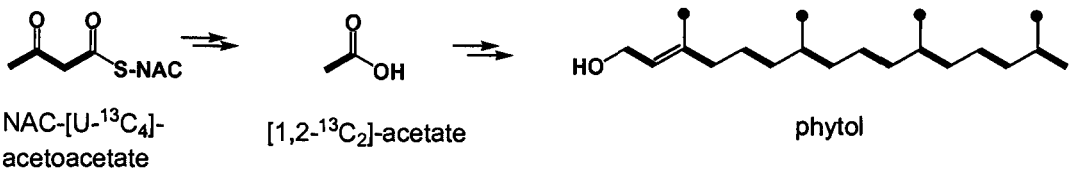

Fig.3.12. Labeling pattern for phytol from the NAC-[1,2,3,4-$^{13}C_4$]-acetoacetate incubation experiment. Bold lines indicate sequential ^{13}C enriched positions.

Such preference for acetate in phytol biosynthesis also occurred in the incubation experiment with [1-^{13}C]-butyric acid. In case of carotenoid biosynthesis, butyric acid is an intact precursor showing major enhancement only at carbons corresponding to C1 of the isoprene unit. In contrast, phytol was labeled at C1 and C3 of the isoprene unit consistent with catabolism to [1-^{13}C]-acetate (Fig.3.13). The [1-^{13}C]-butyric acid is apparently transformed to [1-^{13}C]-acetate through the β-oxidation reaction which involves dehydrogenation, hydration, oxidation, and thiolation reactions.

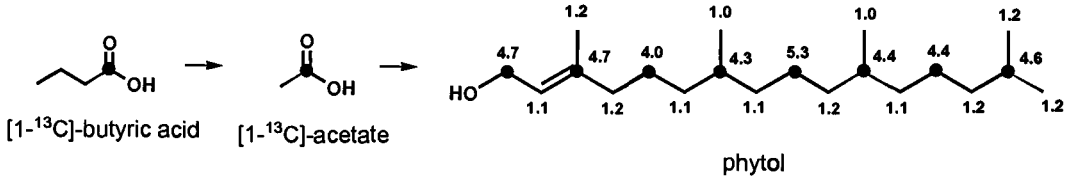

Fig.3.13. Incorporation levels for phytol from the incubation experiment with [1-^{13}C]-butyric acid. Filled circles indicate enhanced ^{13}C isotopes.

Because these C_4 precursors did not specifically label phytol, further incubation experiments with C_5 compounds structurally similar to the isoprene unit, such as dimethylacrylic acid, 3-methyl-3-butenoic acid, and NAC-3-methyl-3-

butenoate, were conducted to elucidate phytol biosynthesis. If [1,2,3,4-$^{13}C_4$]-dimethylacrylic acid is incorporated into phytol without degradation, doublets for C1 and C4 and doublets of doublets for C2 and C3 from dimethylacrylic acid should be detected in the ^{13}C-NMR spectrum for the individual isoprene units. The labeling pattern of phytol (3.0 % ^{13}C enrichment integrated at H1 of phtol), however, was again consistent with the incubation experiment using [U-$^{13}C_6$]-glucose or [1,2-$^{13}C_2$]-acetate, which had no sign of doublets of doublets in any carbon but did have doublets at carbons corresponding to C1-C2 and C3-C4 of the isoprene unit and singlets in the branching methyl carbons (Fig.3.14).

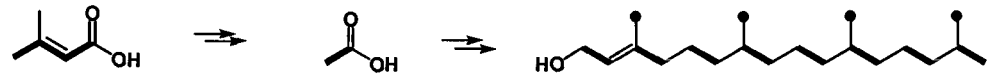

[1,2,3,4-$^{13}C_4$]-dimethylacrylic acid

[1,2-$^{13}C_2$]-acetate

phytol

Fig.3.14. Labeling pattern for phytol from the [1,2,3,4-$^{13}C_4$]-dimethylacrylic acid incubation experiment. Bold lines indicate sequential ^{13}C isotopes and filled circles indicate enriched carbons with ^{13}C isotopes.

In the incubation experiment with 3-[$^2H_3$]-methyl-3-butenoic acid, there was no significant peak in the ^{2}H-NMR spectrum of phytol. Subsequently, the activated form of 3-[$^2H_3$]-methyl-3-butenoic acid, NAC-3-[$^2H_3$]-methyl-3-butenoic acid, was also employed to potentially improve its bioavailability in *E. gracilis*, but neither this compound nor its breakdown compound(s) was incorporated into phytol at all. This result indicates that 3-methyl-3-butenoate, a double bond isomer of dimethylacrylic acid, was not a precursor in phytol biosynthesis, while dimethylacrylic acid at least can be utilized after catabolism by *E. gracilis*.

Based on the above incubation experiments with C_4 and C_5 compounds similar to the IPP structure, two main features were realized: (1) several general carbon sources for phytol are utilized, such as leucine, NAC-acetoacetate, butyric acid, and dimethylacrylic acid, but all after catabolism, presumably to acetate, and (2) phytol biosynthesis can be clearly distinguished from carotenoid biosynthesis in *E. gracilis*, which is different from in other photosynthetic organisms.

Formation of phytol via polyketide biosynthesis?

After the failure of attempts to elucidate phytol biosynthesis using reasonable isoprenoid pathway precursors, a different pathway for phytol biosynthesis was considered, such as the polyketide (PK) biosynthetic pathway, instead of the isoprenoid pathway. The incubation experiments clearly indicate that all of the carbons in phytol ultimately arise from acetate. Based on the structure, a modified type I PK synthase (PKS) would be expected. Phytol can be viewed as having an aliphatic C_{16} polyketide backbone which is modified with four methyl groups at C_1 derived carbons. The PK backbone is composed of a starter unit and extender units. For phytol, acetate would be the starter unit, while malonate would be the extender unit. The endogenous malonate unit is regarded to be produced through carboxylation of acetate catalyzed by an acetate carboxylase which is a member of a CO_2-fixing mutienzyme complex in *Euglena* species and requires ATP, CO_2, and Mg^{2+} for the activity.[23,24] The addition of four methyl groups originated from acetate units seems to successively occur at alternating chain extension steps to provide the branching methyl groups in the phytol structure.

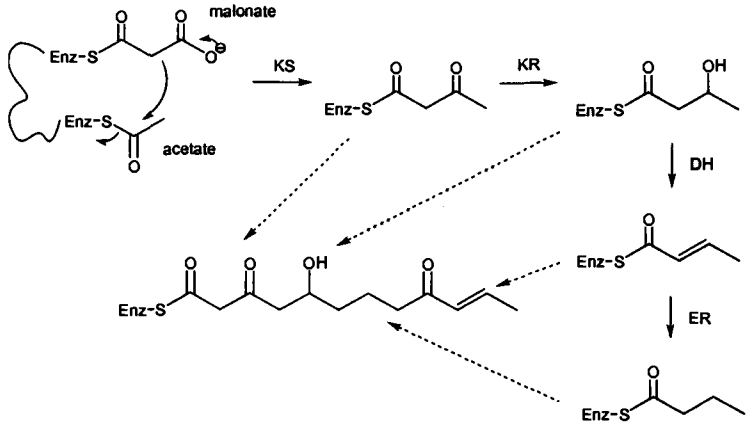

Fig.3.15. Polyketide synthetic cycle. Each dotted arrow represents the possible C_2 units that can be incorporated into the PK structure.

The general aliphatic PK backbone is established through repetitive condensation reactions of C_2 units derived from acetyl-CoA and malonyl-CoA. In the

PK biosynthetic cycle (Fig.3.15), the first step is loading the starter acetate unit onto an acyl carrier protein (ACP). As the acetate unit is attached to a β-ketoacyl synthase (KS) domain, an extender malonate is bound to the ACP. The acetate unit is condensed with the malonate unit by a concomitant decarboxylation reaction. The first C_2 unit of the condensed C_4 unit undergoes modifications such as a reduction by a ketoreductase (KR), dehydration by a dehydratase (DH), and a final reduction again by an enoyl reductase (ER). Either modified C_2 units or the unmodified acetyl moiety can be individually joined into the PK backbone, which leads to the structural diversity of PK compounds.

In order to investigate whether phytol biosynthesis occurs by the PK pathway, incubation experiments using [1-^{13}C-2-$^{2}H_3$]-acetate, [2-^{13}C-2-$^{2}H_3$]-acetate, and [2-^{13}C]-malonic acid were considered, because they are general precursors in the PK pathway and are commonly employed to clarify details of PK biosynthesis.[25,26] If malonate is incorporated only into the proposed extender units, then strong support for a PK pathway will have been obtained. The correlation between ^{2}H and ^{13}C from [2-^{13}C-2-$^{2}H_3$]- or [1-^{13}C-2-$^{2}H_3$]-acetates can be used to determine the number of attached deuterium atoms by measuring the α- or β-shifts of corresponding carbons in the ^{13}C-NMR spectrum. For example, the signal of carbon directly bound to one deuterium is observed as an upfield shift by 300 ~ 500 ppb from the natural ^{13}C signal (the α-shift). The shifted peak appears as a 1:1:1 triplet with low intensity due to ^{2}H-^{13}C spin couplings, which gives a rise to interference from monitoring α-shifted signals in the ^{13}C-NMR spectrum. To overcome the low intensities of the α-shifted peaks caused by coupling, compounds from the [2-^{13}C-2-$^{2}H_3$]-acetate incubation experiment are generally subjected to a ^{1}H- and ^{2}H-decoupled ^{13}C-NMR technique which results in a single shifted peak instead of split peaks. In contrast, the β-shift arises from a carbon which bears one deuterium atoms two-bonds away. The ^{13}C signal would be shifted 20 ~ 100 ppb upfield from the natural ^{13}C signal due to a single deuterium. The signal shift of carbons for both α- and β-shifts increases in proportion to the number of attached deuterium atoms.

A preliminary result that phytol might be produced via PK biosynthesis was obtained by carrying out the incubation experiment using [2-^{13}C]-malonic acid. If the malonate is utilized as the extender unit via PK biosynthesis, enhanced ^{13}C signals

would be designated in C2, C4, C6, C8, C10, C12, and C14, but not in C16 derived from the starter acetate unit, nor in the branching methyl carbons of phytol. The incorporation levels in phytol from the incubation experiment using [2-^{13}C]-malonic acid was 4.3% by integrating the ^{13}C enrichment at H2 of phytol. The carbons, C2, C4, C6, C8, C10, C12, and C14 corresponding to C2 of [2-^{13}C]-malonic acid, were highly labeled with ^{13}C isotopes in a range of 3.3 - 4.3, while enhancements of other carbons were 1.0 ~ 1.6. Although [2-^{13}C]-malonic acid can be decarboxylated to [2-^{13}C]-acetate to provide some labeling of the starter acetate and branching methyl groups, the enrichment levels for these carbons (max. 1.6) is much lower that for the alternating backbone carbons (Fig.3.16). This result implies that the aliphatic C_2 units of phytol except for the terminal C_2 unit (C15 and C16) are mainly produced from malonate as the extender unit via PK biosynthesis. The branching methyl carbons appear to come from acetate units rather than malonate. This experiment was repeated and the same results were observed.

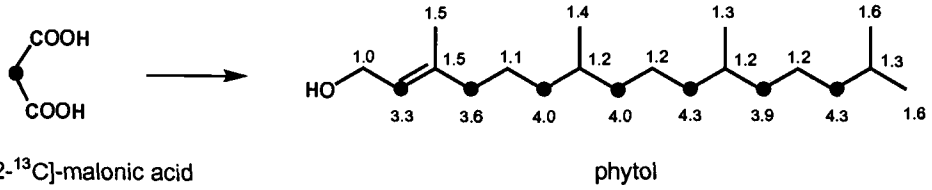

[2-^{13}C]-malonic acid phytol

Fig.3.16. ^{13}C Enrichments for phytol from the [2-^{13}C]-malonic acid incubation experiment.

To gather more evidence to confirm this finding, further experiment using [2-^{13}C-2-$^{2}H_3$]-acetate or [1-^{13}C-2-$^{2}H_3$]-acetate were considered, which would discriminate the PK-type pathway from the MVA-type pathway. The fate of deuterium atoms in the acetates differs for two pathways. The ^{13}C isotopes in the acetates are used as reporter isotopes to observe deuterium shifts by the ^{13}C-NMR analysis. If [1-^{13}C-2-$^{2}H_3$]-acetate is incorporated by the MVA-type pathway, two deuteriums would be retained at C4 of the isoprene unit, while only one deuterium would remain at C_2 due to loss of a deuterium either in the isomerization to DMAPP or during elongation to GGPP. Consequently, C2, C6, C10, and C14 of phytol would retain one deuterium, which results in single β-shifted peaks at C1, C5, C9, and C13 due to correlation with

one deuterium two-bonds away. Carbons C3, C7, and C11 would appear to be doubly β-shifted peaks due to two deuteriums attached to C4, C8, and C12. The DMAPP-derived carbon, C16, would hold three deuteriums (Fig.3.17).

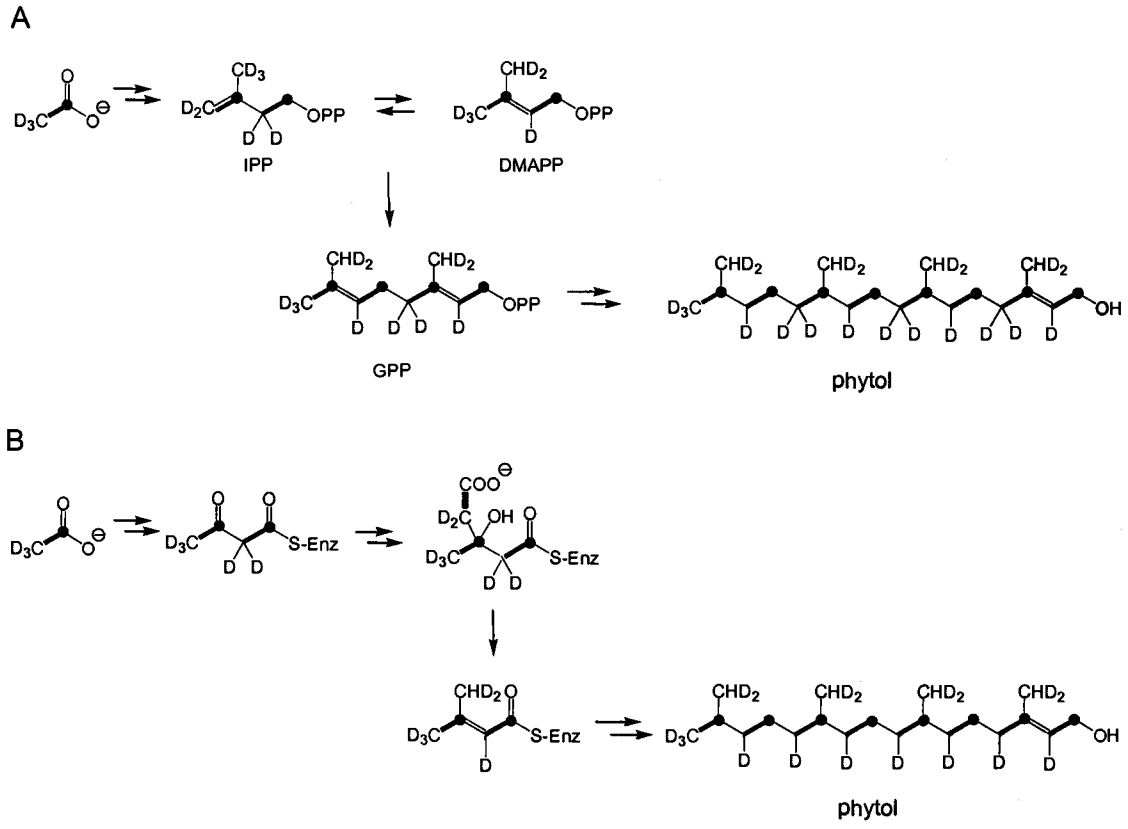

Fig.3.17. Predicted labeling patterns of the MVA -type (A) and the PK-type (B) pathways. Bold lines and filled circles indicate the intact acetate and labeled carbons.

In contrast, if [1-^{13}C-2-$^{2}H_3$]-acetate is utilized for the formation of phytol via the PK-type pathway, three deuteriums should be retained on C16 of phytol due to the intact incorporation of the starter acetate unit, whereas methylene carbons (C2, C4, C6, C8, C10, C12, and C14) would be bound to one deuterium which arises from the loss of one deuterium during the dehydration reaction catalyzed by the dehydratase. The branching methyl groups originated from the methyl carbon of the acetate unit should possess two deuteriums after the loss of one deuterium during the addition step. Consequently, the ^{13}C-NMR spectrum of phytol obtained from this experiment would show one triply shifted peak at C15 and single β-shifted peaks at C1, C3, C5,

C7, C9, C11, and C13 (Fig.3.17). Therefore, the number of deuterium retained at C4, C8, and C12 should help to determine which pathway is utilized for phytol biosynthesis.

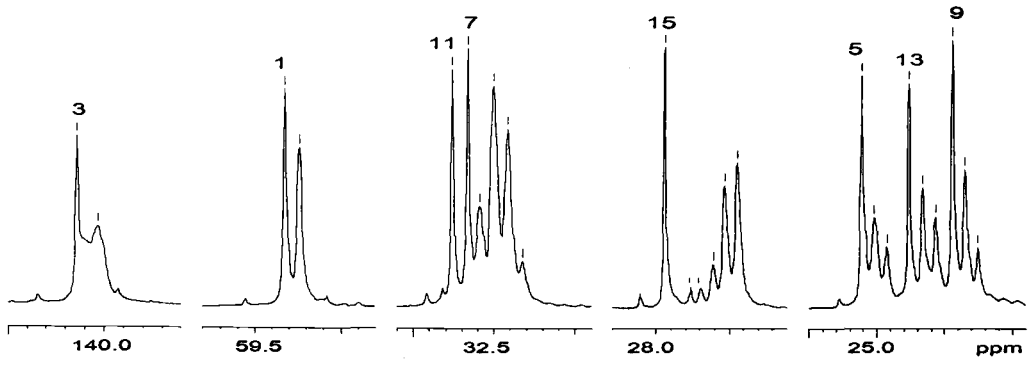

Fig.3.18. Partial spectra for phytol from the incubation experiment using [1-^{13}C-2-$^{2}H_3$]-acetate (supplemented with unlabeled glucose). Bars indicate the β-isotope shifted peaks.

However, the ^{13}C-NMR spectrum of phytol from the [1-^{13}C-2-$^{2}H_3$]-acetate incubation experiment showed more complicated patterns than were expected (Fig.3.18), except for C1. The ^{13}C signal of C1 appeared as a singly β-shifted peak –85 ppb upfield, which reflects the correlation between C1 and one deuterium atom bound to C2 (Table 3.1). Methylene carbons C6, C10, and C14 retained either one or two deuterium atoms based on both singly (–92 ~ –101 ppb) and doubly β-shifted peaks (–181 ~ –198 ppb), which implies the correlation between each carbon and two deuteriums instead of one deuterium which is supposed to be retained theoretically by both pathways. Methine carbons C7 and C11 revealed multiple isotope shifted peaks, probably with some overlap. Based on the magnitude of the shifts, peaks representing from one to four neighboring deuterium atoms appeared to be present. Another methine C15 derived from the starter acetate unit had 5 or 6 shifted peaks, which conflicts with the expected three deuteriums. The furthermost peak from the natural C15 signal was detected –501 ppb upfield, which represents up to 5 or 6 adjacent deuterium atoms. Unlike the other methyl-bearing carbons, C3 seemed to have only one β-shifted peak –107 ppb upfield, even though the shifted peak of C3 was observed with low resolution.

Table 3.1. Differences of the ^{13}C chemical shifts between natural and β-shifted signals from the [1-^{13}C-2-$^{2}H_3$]-acetate incubation experiment (supplemented with unlabeled glucose).

carbon #	β-shifted peaks (ppb)				
1	–85				
3	–107				
5	–96	–181			
7	–76	–158	–246	–335	
9	–92	–185			
11	–97	–173	–255	–335	
13	–101	–198			
15	–179	–248	–332	–413	–502

In the ^{2}H-NMR spectrum of phytol, the peaks were distinctly seen at H2, H4, H3', the methylene groups, and the other methyl groups of which the integration ratios were 1.0 : 0.8 : 2.8 : 5.1 : 11.7 (Fig.3.19). Although the ratios did not exactly fit with the expected 1 : 2 : 2 : 7 : 9 for the MVA-type pathway nor the 1 : 1 : 2 : 5 : 9 for the PK-type pathway, they seem to be more compatible with the ratios from the PK-type pathway. The percent incorporation levels of deuterium into phytol relative to the natural abundance deuterium in the chloroform peak were: H2 = 3 %, H4 = 2 %, H3' = 9 %, methylenes = 15 %, and methyls = 36 %. Comparing the ratios of H2, H4, and the methylene groups, the ratios 1.0 : 0.8 : 5.1 fit better the 1 : 1 : 5 ratio from the PK-type pathway rather than at the 1 : 2 : 7 ratio from the MVA-type pathway. The ratio (4.2) between the other methyls and H3' lies close to the 4.5 ratio for both pathways, so no firm conclusions can be made based on these values. However, according to the integration ratios, deuteriums attached to the branching methyls seem to be retained at a higher level than those in the linear backbone. This feature might be attributed to the different precursors, that is, the branching methyls originate from acetate unit, whereas the carbons of the linear backbone come from malonate. The

potential for exchange of deuterium atoms with solvent is much greater at C2 of malonyl-CoA than at C2 of acetyl-CoA.

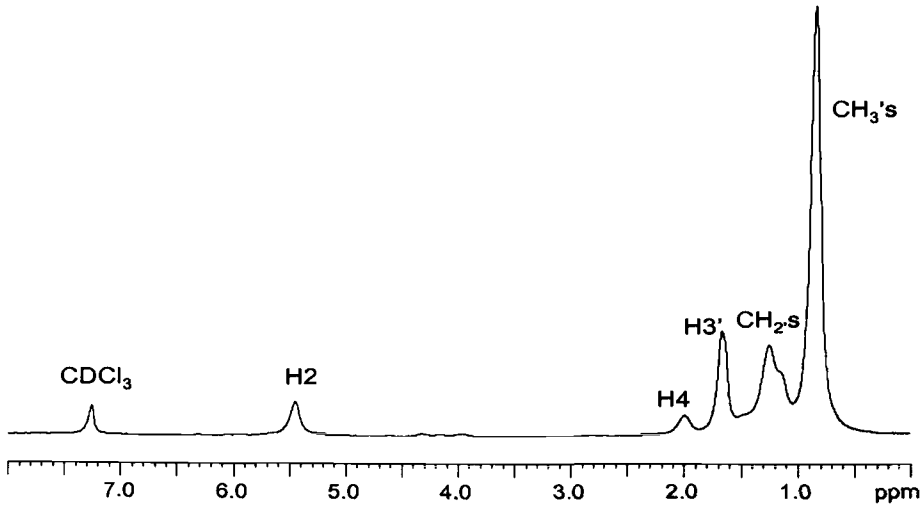

Fig.3.19. ^{2}H-NMR spectrum for phytol from the [1-^{13}C-2-$^{2}H_3$]-acetate incubation experiment.

Although the ^{2}H-NMR spectrum is suggestive of a PK-type pathway to phytol, the analysis of the ^{13}C-NMR spectrum of phytol from the [1-^{13}C-2-$^{2}H_3$]-acetate experiment did not explicitly determine the pathway for phytol biosynthesis on account of the unexpected several β-shifted peaks. These unexpected β-shifts apparently arise from deuterium atoms on neighboring carbons in a situation that should not occur if the labeled acetate is diluted by endogenous pools of acetate. Our results, however, elucidated a significant correlation between neighboring labeled acetates, which might represent that the exogenous labeled acetates are readily utilized to produce phytol, rather than being diluted with endogenous acetates, either from the unlabeled glucose in the medium or by photosynthesis through several steps. Consequently, to decrease the assimilation of exogenous labeled acetates into adjacent C_2 units of phytol, *E. gracilis* was grown using a culture medium (6L) containing [1-^{13}C-2-$^{2}H_3$]-acetate (0.5 g) with unlabeled acetate (6 g) instead of unlabeled glucose (6 g). One disadvantage of this experiment was that *E. gracilis* grows more slowly in the acetate-containing medium, which led to a longer incubation time to approach the stationary growth phase.

Although there were still small peaks due to the β-shifts correlated with deuterium in the adjacent acetate unit, the ^{13}C-NMR spectrum of phytol from the incubation experiment using [1-^{13}C-2-$^{2}H_3$]-acetate and unlabeled acetate mainly showed the retention of deuterium for the intact acetate units (Fig.3.20). Carbons C1, C5, C9, and C13 distinctly appeared as singly β-shifted peaks by –83, –94, –95, and –102 ppb, respectively (Table 3.2), which are similar values to the previous experiment using [1-^{13}C-2-$^{2}H_3$]-acetate and unlabeled glucose. These carbons should be associated with one deuterium on the adjacent carbon from an intact acetate unit. Carbon 7 also showed a singly β-shifted peak by –87 ppb in the ^{13}C spectrum. The β-shifted peak of C11 is probably superimposed on the C7 signal because the intensity of C7 should be the same as C11. The β-shifted peak of C15 was observed –246 upfield accompanied with small peaks nearby, which represents a signal shift due to three retained deuteriums in an intact starter acetate unit. Compared with the other labeled carbons, C3 showed a much smaller shifted signal by –23 ppb. If this figure is derived from one deuterium correlated with C3, the shifted signal (–107 upfield) observed from the previous experiment may indicate the retention of three or four deuteriums instead of one deuterium, which was the conclusion in the previous experiment.

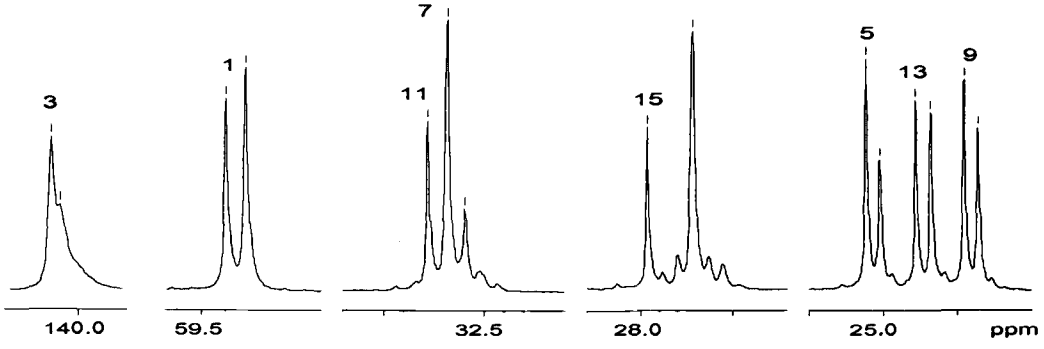

Fig.3.20. Partial spectra for phytol from the incubation experiment using [1-^{13}C-2-$^{2}H_3$]-acetate (supplemented with unlabeled acetate). Bars indicate each peak.

Table 3.2. Differences of the ^{13}C chemical shifts between natural and β-shifted signals from the [1-^{13}C-2-$^{2}H_3$]-acetate incubation experiment (supplemented with unlabeled acetate).

carbon #	1	3	5	7	9	11	13	15
β-shifted peaks (ppb)	−83	−23	−94	−87	−95	−98	−102	−246
attached ^{2}H number	1	1	1	1	1	1	1	3

The number of deuteriums bound to the C16 and the branching methyl carbons was determined by the ^{1}H- and ^{2}H-decoupled ^{13}C-NMR spectrum of phytol derived from the [2-^{13}C-2-$^{2}H_3$]-acetate incubation experiment (Fig.3.21). Although the shifted ^{13}C signals were more complex than expected, C3', C7' and C11' clearly appeared as doubly shifted peaks at 643 ppb upfield for C3' and at 571 ppb upfield for C7' and C11' due to two retained deuteriums (Table 3.3) and the signal of C15' was doubly shifted 748 upfield. These doubly shifted peaks clearly reveal the retention of two deuteriums at the branching methyls. The C16 derived from the starter acetate unit also showed a triply shifted peak 1005 upfield due to three deuteriums.

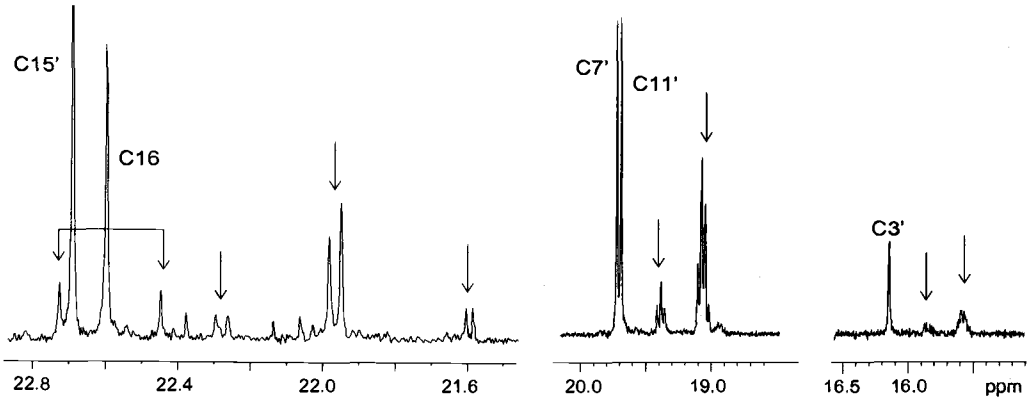

Fig.3.21. Partial spectra for phytol from the incubation experiment using [2-^{13}C-2-$^{2}H_3$]-acetate. Arrows indicate each α-shift peak. Connected arrows indicate ^{13}C-^{13}C coupling.

In the spectrum, the singly shifted peaks were also observed at the branching methyls, which might be attributed to replacement of deuteriums of the acetate unit with hydrogen atoms during the incubation period. The higher intensity of the doubly α-shifted peaks than the singly shifted peaks, however, explicitly revealed the major contribution of doubly ^{2}H-labeled acetate units to the formation of phytol. The carbons C2, C4, C6, C8, C10, C12, and C14 of the linear backbone appeared as singly α-shifted peaks, and all α-shifts are summarized in Table 3.3.

Table 3.3. Differences of the ^{13}C chemical shifts between natural and α-shifted signals from the [2-^{13}C-2-$^{2}H_3$]-acetate incubation experiment.

carbon #	2	4	6	8	10	12	14	16	3'	7' & 11'	15'
α-shifted peaks (ppb)	–345	–[a]	–474	–[a]	–475	–[a]	–526	–320 –634 –1005	–263 –571	–321 –643	–402 –748

[a] Not applicable

In the phytol spectrum, the ^{13}C-^{13}C couplings arising from [1,2-$^{13}C_2$]-acetate were considerably detected in all carbons except for the branching methyls as shown at C16 (Fig.3.21). This finding presumably resulted from introduction of [2-^{13}C-2-$^{2}H_3$]-acetate into the glyoxylate cycle to form the doubly ^{13}C-labeled acetate, which leads to the labeling pattern consistent with the [1,2-$^{13}C_2$]-acetate incubation experiment.[12]

Based on the β-shifts from the incubation experiment using [1-^{13}C-2-$^{2}H_3$]-acetate and unlabeled acetate, we were able to reinterpret the previous phytol spectrum. All labeled carbons from the incubation experiment using [1-^{13}C-2-$^{2}H_3$]-acetate and unlabeled glucose appear to be correlated with deuteriums from the intact acetate, as well as with adjacent deuteriums from other exogenous labeled acetates, which leads to the multiplicity of shifted peaks. For example, the methine

C3 would be correlated with one deuterium at C2, one deuterium at C4, and two deuteriums from the methyl C3'. The β-shifts of C7 and C11 also occur in a similar manner to C3. The terminal methine C15 should be associated with three deuteriums from C16 as the intact starter acetate unit, one deuterium for C14, and two deuteriums of C15'. These overall results clearly show one deuterium attached to the methylene carbons and three deuteriums at C16, which represents that phytol is synthesized via a PK-type pathway.

Additionally, similar correlations between exogenous labeled acetates occurred in α-tocopherol isolated from the incubation experiment using [1-^{13}C-2-^{2}H$_3$]-acetate and unlabeled glucose. The phytyl chain of α-tocopherol appeared as two β-shifted peaks at C5, C9, and C13 and several peaks at C7, C11, and C15 consistent with the phytol pattern (Fig.3.22). Except for the singly β-shifted peak at C1, all enhanced carbons were correlated with more deuteriums than would be explained by incorporation by a singly intact labeled acetate unit.

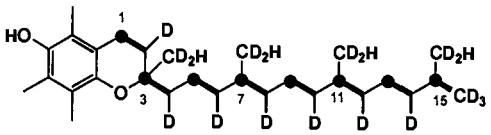

vitamin E

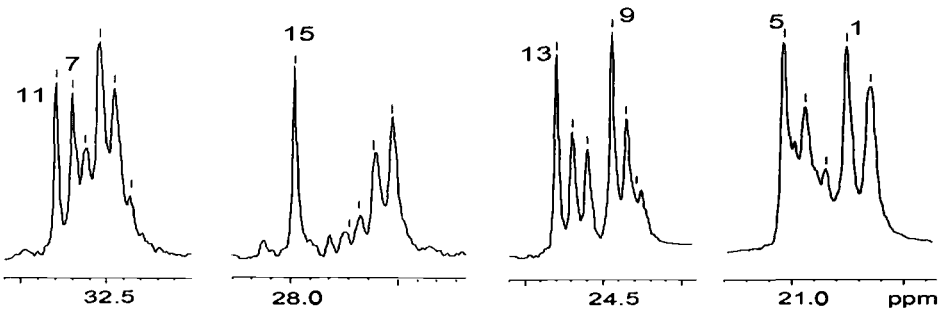

Fig.3.22. Partial spectra for α-tocopherol from the incubation experiment using [1-^{13}C-2-^{2}H$_3$]-acetate and unlabeled glucose. Bars indicate each peak.

Based on the results from the incubation experiments using [2-^{13}C]-malonic acid, [1-^{13}C-2-^{2}H$_3$]-acetate, and [2-^{13}C-2-^{2}H$_3$]-acetate, we propose that phytol biosynthesis occurs by a modified PK pathway in *E. gracilis* (Fig.3.23). The starter acetate unit would be loaded onto the ACP and is then condensed with a malonate

unit to form a diketide (C_4 backbone). Subsequently, the diketide undergoes HMG-CoA synthase-type condensation with an acetate unit (M domain),[27] followed by either decarboxylation (DC) and isomerization (IS) reactions (route a) or dehydration (DH) and decarboxylation (route b) to form the thioester of dimethylacrylate which is reduced by the ER. After a malonate unit is added to the diketide, the triketide would be processed by KR, DH, and ER activities to provide the saturated backbone. These chain elongation steps would continue until the saturated C_{14} backbone with three branching methyls is prepared. After the last malonate unit is assembled with C_{14} backbone, modifications of the octaketide would go through either route a or b without the reduction reaction of the enoyl moiety to produce the unsaturated form. The elongation would be terminated by a thioesterase (TE). In this case, modifications of phytic acid, such as reduction or phosphorylation reactions should be required to form phytyl diphosphate, the precursor of α-tocopherol, phylloquinone, and chlorophylls. Further experiments will be needed to explain the details, including the methylation steps to build the branching methyl carbons and either modifications of phytic acid or possible reductive cleavage for the formation of phytol.

Therefore, the investigation of phytol biosynthesis initiated with the labeling pattern inconsistent with two isoprenoid pathways leads to the distinct finding that *E. gracilis* produces phytol and phytol-related compounds through the PK-type pathway, instead of the isoprenoid pathway.

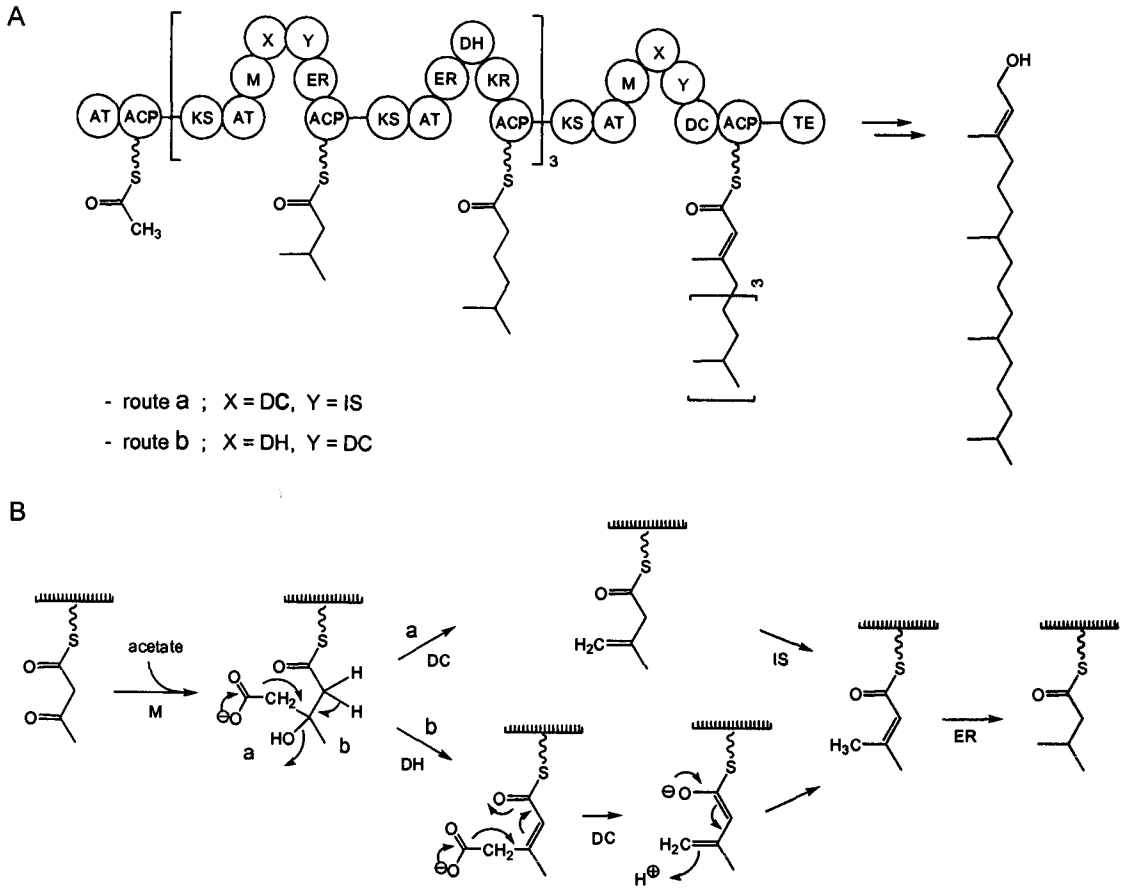

Fig.3.23. A proposed PK-type phytol pathway. The whole pathway (A) and the partial pathway to the ester of dimethylacrylate (B) are shown. Striped bar indicates the PK synthase, and ACP indicates acyl carrier protein. The reaction steps are indicated; AT, acyl transferase; KS, β-ketoacyl synthase; KR, ketoreductase; DH, dehydratase; ER, enoyl reductase; TE, thioesterase; M, HMG-CoA synthase-like enzyme; DC, decarboxylase; IS, isomerase.

Experimental

Instruments

All ^{1}H, ^{2}H, and ^{13}C nuclear magnetic resonance (NMR) spectra were recorded on a Bruker AC 300 spectrometer operating at 300 MHz for ^{1}H and 75 for ^{13}C, and on a Bruker AM 400 spectrometer operating at 400.13 MHz for ^{1}H, 100.13 MHz for ^{13}C, and 61.42 MHz for ^{2}H. Chemical shifts of NMR spectra are shown as δ, and references were based on the NMR solvents as an internal standard ($CHCl_3$ at 7.26 ppm for ^{1}H-NMR and $^{13}CDCl_3$ at 77.0 ppm for the center line of the triplet in ^{13}C-NMR, acetone at 2.08 ppm for ^{1}H-NMR and acetone-d_6 at 30.7 ppm for the center line of the septet in ^{13}C-NMR, CH_3OH at 3.4 ppm for ^{1}H-NMR and CD_3OD at 50.2 ppm for the center line of the septet in ^{13}C-NMR). The inverse-gated decoupled technique is applied for determining ^{13}C isotopic enhancement levels. Incorporation levels for ^{13}C signals of isoprenoids in the incubation experiments using labeled compounds were calculated on the basis of the intensities of the target peak relative to the intensity of an unenriched peak. This ratio was compared with the ratio for the corresponding peaks from the natural abundance ^{13}C-NMR spectrum for unlabeled isoprenoids to determine the relative incorporation level. Absolute ^{13}C enrichments were determined by integration of ^{13}C satellite peaks in the ^{1}H-NMR spectrum. Levels of incorporation from ^{2}H NMR spectra were calculated on the basis of the integration of the target peak relative to the natural abundance of the deuterium signal of $CHCl_3$ (0.5 mL, 0.016 %) and acetone (0.5 mL, 0.016 %) each. Phosphoric acid (85 % in H_2O) was used as an external standard (δ_p 0.0 ppm) for ^{31}P NMR spectra operating at 121.4 MHz of Bruker AC 300 spectrometer. Low and high-resolution chemical ionization mass spectra (CIMS) and fast atom bombardment mass spectra (FABMS) were recorded on a Kratos MS50TC spectrometer. Cultures were grown in a Hoffman illuminated incubator. Harvesting of *Euglena* cells was done with a Beckman J2-HS centrifuge and lyophilization of the cells utilized a Labconco freeze dry system.

Biosynthetic experiments

An axenic culture of *E. gracilis* (*Z* strain, UTEX 753, identical to SAG 1224-25) was purchased from UTEX, The Culture Collection of Algae at the University of Texas at Austin.

For maintenance of the organism, *E. gracilis* was cultivated in modified media containing D-glucose (1.0 g/L), $(NH_4)_2HPO_4$ (1.0 g/L), KH_2PO_4 (1.0 g/L), $MgSO_4 \cdot 7H_2O$ (0.2 g/L), $CaCl_2 \cdot 2H_2O$ (0.02 g/L), sodium citrate·$2H_2O$ (0.5g/L), thiamine·HCl (10 μg/L), vitamin B_{12} (0.5 μg /L) and trace metals.[28] Trace metals were prepared with $FeCl_3 \cdot 6H_2O$ (3.2 mg/L), $MnCl_2 \cdot 4H_2O$ (1.8 mg/L), $CoCl_2 \cdot 6H_2O$ (1.1 mg/L), $ZnSO_4 \cdot 7H_2O$ (0.4 mg/L), $Na_2MoO_4 \cdot 2H_2O$ (0.3 mg/L), $CuSO_4 \cdot 5H_2O$ (0.02 mg/L). Seed cultures were inoculated into medium (200 mL) and were grown at 30 °C for 7-10 days under constant illumination with 40 W cool-white fluorescent lights (200-210 ftc). For mass cultivation, the seed cultures were inoculated into medium (5-6 L), aerated and grown for 7-13 days under the same condition as the seed cultures. For incubation experiments with labeled compounds, the labeled compounds were mixed with unlabeled D-glucose (1 g/L) at a ratio of 1:60 to 1:10 (w/w).

Inorganic salts for the culture media were purchased from Mallinckrodt, and D-glucose, vitamin B_{12}, and thiamine·HCl were from Sigma-Aldrich. Labeled compounds ([1-^{13}C]-acetate, [2-^{13}C]-acetate, [1-^{13}C-2-$^{2}H_3$]-acetate, [2-^{13}C-2-$^{2}H_3$]-acetate, [U-$^{13}C_6$]-glucose, [1-^{13}C]-glucose, [methyl-^{13}C]-methionine, [1,2,3,4-$^{13}C_4$]-acetoacetate, and [2-^{13}C]-malonic acid) were purchased from Cambridge Isotope Laboratories Inc. and Sigma-Aldrich. For the syntheses of [5-$^{2}H_2$]-deoxy-D-xylulose, [1,2,3,4-$^{13}C_4$]-acetoacetyl-*N*-acetylcysteamine, [1,2,3,4-$^{13}C_3$]-dimethyl acrylic acid, 3-[$^{2}H_3$]-methyl-3-butenoic acid, and 3-[$^{2}H_3$]-methyl-3-butenoyl-*N*-acetylcysteamine, $LiAlD_4$, ethyl-[1,2,3,4-$^{13}C_4$]-acetoacetate, and CD_3MgI were purchased from Cambridge Isotope Laboratories Inc. and Sigma-Aldrich and employed as isotope sources. For syntheses, commercial grade reagents and starting materials from Sigma-Aldrich were used without further purification, and most organic solvents were dried before use as recommended.[29] Synthetic reactions were carried out in oven-dried glassware under a positive pressure of argon. Phytol, α-tocopherol, and ergosterol standards were purchased from Sigma-Aldrich. Water was deionized using a Milli Q Millipore system for all experiments. Silica gel (Merck, grade 60, 220-

400 mesh) was used for flash column chromatography.[30] Merck glass-backed TLC plates (silica gel 60 F254) were employed for thin layer chromatography (TLC) and preparative TLC (prep-TLC).

Isolation of Isoprenoids

After cultivation, cells were harvested by centrifugation at 7000 rpm (JA-10 rotor, 8671 *g*) for 10 min and lyophilized to obtain 0.3-0.5 g of dry weight per liter. The lyophilized cells were extracted three times (30 min each) with a mixture of $CHCl_3$ and MeOH (2:1) at room temperature to provide a crude extract, which was applied to a silica gel flash chromatography column. The column was developed with mixtures of 15-50 % EtOAc in hexanes to separate four fractions which were determined by color of pigments. The fractions 1 (orange color) and 2 (yellow color) contain the non-polar compounds (R_f = 0.8-0.9 and 0.7, silica gel TLC plate, 5 % EtOAc in hexanes). Fraction 3 is the chlorophyll-containing fraction (R_f = 0.5-0.6, silica TLC plate, 10 % EtOAc in hexanes). Fraction 4 (orange-red) contains the polar compounds (R_f = 0.2-0.3, silica gel TLC plate, 30 % EtOAc in hexanes). After the organic solvent was evaporated, each fraction was processed to separate the isoprenoids: α-tocopherol, phytol, or ergosterol.

α-Tocopherol (0.2 mg/L, avg. yield) was obtained from silica TLC plates from which fraction 2 was redeveloped three times with 5 % EtOAc in hexanes. The band corresponding to α-tocopherol on the TLC plates was scraped and extracted with $CHCl_3$. The chlorophyll-containing fraction was hydrolyzed in 10 % (w/v) KOH in MeOH overnight, and extracted with ether. The ethereal extract was washed with a saturated NH_4Cl solution and *dd*-H_2O, dried, and concentrated. The extract was applied to a flash chromatography column (silica gel, 15% EtOAc in hexanes) to separate phytol and ergosterol. The isolated phytol was decolorized by passing the phytol solution over a short column of charcoal and Florisil and washing with ether to provide 4 mg/L, avg. yield of pure phytol. Ergosterol was purified by silica prep TLC plates developing three times with 5 % EtOAc in hexanes (0.1 mg/L, avg. yield). α-Tocopherol, phytol, or ergosterol obtained from the *E. gracilis* were analyzed by mass spectrometry and NMR spectroscopy. ^{13}C- and ^{1}H-NMR assignments for α-Tocopherol,[31] phytol,[32,33] and ergosterol[34] were previously published.

Synthesis of [5-$^{2}H_2$]-Deoxy-D-xylulose[35,36]

Details were provided in the experimental section of Chapter Two.

Synthesis of NAC [1,2,3,4-$^{13}C_4$]-acetoacetate[22]

Details were provided in the experimental section of Chapter Two.

Synthesis of [1,2,3,4-$^{13}C_4$]-dimethylacrylic acid[37,38]

Details were provided in the experimental section of Chapter Two.

Syntheses of 3-[$^{2}H_3$]-Methyl-3-butenoic acid and its NAC derivative[22,39]

Details were provided in the experimental section of Chapter Two.

References

(1) Rüdiger, W.; Schoch, S. In *Chlorophylls*; Scheer, H., Ed.; CRC Press: Boca Raton, 1991, pp. 451-464.

(2) Soll, J.; Schultz, G.; Rüdiger, W.; Benz, J. Hydrogenation of Gernylgeraniol. *Plant Physiol.* **1983**, *71*, 849-854.

(3) Schwender, J.; Seemann, M.; Lichtenthaler, H. K.; Rohmer, M. Biosynthesis of isoprenoids (carotenoids, sterol, prenyl side-chains of chlorophylls and plastoquinone) via a novel pyruvate.gylceraldehyde 3-phosphate non-mevalonate pathway in the green alga *Scenedesmus Obliquus. Biochem. J.* **1996**, *316*, 73-80.

(4) Lichtenthaler, H. K.; Schwender, J.; Disch, A.; Rohmer, M. Biosynthesis of isoprenoids in higher plant chloroplasts proceeds via a mevalonate-independent pathway. *FEBS Lett.* **1997**, *400*, 271-274.

(5) Disch, A.; Schwender, J.; Muller, C.; Lichtenthaler, H. K.; Rohmer, M. Distribution of the mevalonate and glyceraldehyde phosphate/pyruvate pathways for isoprenoid biosynthesis in unicellular algae and the cyanobacterium *Synechocystis PCC 6714. Biochem. J.* **1998**, *333*, 381-388.

(6) Müller, C.; Schwender, J.; Disch, A.; Rohmer, M.; Lichtenthaler, F. W.; Lichtenthaler, H. K. Occurence of the 1-deoxy-D-xylulose 5-phosphate pathway of isopentenyl diphosphate biosynthesis in different algae groups. *Adv. Plant Lipid Res.* **1998**, 425-428.

(7) Threlfall, D. R.; Goodwin, T. W. Nature, intracellular distribution and formation of terpenoid quinones in *Euglena gracilis. Biochem. J.* **1967**, *103*, 573-588.

(8) Ahrens, E. H. J.; Williams, D. C.; Battersby, A. R. Biosynthesis of porphyrins and related macrocycles. Part 11. Studies on biosynthesis of the phytyl chain of chlorophyll a by use of carbon-13. *J. Chem. Soc., Perkin Trans. 1* **1977**, *23*, 2540-2545.

(9) Douglas, S. E.; Turner, S. Molecular evidence for the origin of plastids from a cyanobacterium-like ancestor. *J. Mol. Evol.* **1991**, *33*, 267-273.

(10) Seto, H.; Watanabe, H.; Furihata, K. Simultaneous operation of the mevalonate and non-mevalonate pathway in the biosynthesis of isopentenyl diphosphate in *Streptomyces aeriouvifer. Tetrahedron Lett.* **1996**, *37*, 7979-7982.

(11) Duvold, T.; Cali, P.; Bravo, J.-M.; Rohmer, M. Incorporation of 2-C-methyl-D-erythritol, a putative C_5 isoprenoid precursor in the mevelonate-independent pathway, into ubiquinone and menaquinone of *Escherichia coli*. *Tetrahedron Lett.* **1997**, *38*, 6181-6184.

(12) Nabeta, K.; Saitoh, T.; Adachi, K.; Komuro, K. Biosynthesis of phytyl side-chain of chlorophyll a: apparent reutilization of carbon dioxide evolved during acetate assimilation in biosynthesis of chloroplastidic isoprenoid. *Chem. Commun.* **1998**, 671-672.

(13) Koyama, T.; Ogura, K. In *Comprehensive Natural Product Chemistry*; Cane, D. E., Ed.; Elsevier: New York, 1999; Vol. 2, pp. 69-96.

(14) Goodwin, T. W.; Griffiths, L. A. Studies in carotenogenesis. V. Carotene production by various mutants of *Phycomyces blakesleeanus* and by *Phycomyces nitens*. *Biochem. J.* **1952**, *52*, 499-501.

(15) Chichester, C. O.; Yokoyama, H.; Nakayama, T. O.; Lukton, A.; Mackinney, G. Leucine metabolism and carotene biosynthesis. *J. Biol. Chem.* **1959**, *234*, 598-602.

(16) Nes, W. D.; Bach, T. J. Evidence for a mevalonate shunt in a tracheophyte. *Proc. R. Soc. Lond. B* **1985**, *225*, 425-444.

(17) Britton, G. In *Carotenoids*; Britton, G., Liaaen-Jensen, S., Pfander, H., Eds.; Birkhäuser: Basel, 1998; Vol. 3, pp. 13-147.

(18) Ginger, M. L.; Chance, M. L.; Goad, L. J. Elucidation of carbon sources used for the biosynthesis of fatty acids and sterols in the trypanosomatid Leishmanis mexicana. *Biochem. J.* **1999**, *342*, 397-405.

(19) Ginger, M. L.; Prescott, M. C.; Reymonds, D. G.; Chance, M. L.; Goad, L. J. Utilization of leucine and acetate as carbon souces for sterol and fatty acid biosynthesis by old and new world *Leishmanis* species, *Endotrypanum monterogeii* and *Trypanosoma cruzi*. *Eur. J. Biochem.* **2000**, *267*, 2555-2566.

(20) Breckenridge, D. G.; Watanabe, Y.; Greenwood, S. J.; Gray, M. W. U1 small nuclear RNA and spliceosomal introns in Euglena gracilis. *Proc. Natl. Acad. Sci. U S A* **1999**, *96*, 852-856.

(21) Martin, W.; Borst, P. Secondary loss of chloroplasts in trypanosomes. *Proc. Natl. Acad. Sci. U S A* **2003**, *100*, 765-767.

(22) Liu, Y.; Li, Z.; Vederas, J. C. Biosynthetic incorporation of advenced precursors into dehydrocurvularin, a polyketide phytotoxin from *Alternaria cinerariae*. *Tetrahedron* **1998**, *54*, 15937-15958.

(23) Wolpert, J. S.; Ernst-Fonberg, M. L. A Mulitenzyme Complex for CO_2 Fixation. *Biochemistry* **1975**, *14*, 1095-1102.

(24) Wolpert, J. S.; Ernst-Fonberg, M. L. Dissociation and Characterization of Enzyme from a Mulitenzyme Complex involved in CO_2 Fixation. *Biochemistry* **1975**, *14*, 1103-1107.

(25) Simpson, T. J. Application of mutinuclear NMR to structural and biosynthetic studies of polyketide microbial metabolites. *Chem. Soc. Rev.* **1987**, *16*, 123-160.

(26) Jordan, P. M.; Spencer, J. B. Stereospecific manipulation of hydrogen atoms with opposite absolute orientations during the biosynthesis of the polyketide 6-methylsalicylic acid from chiral malonates in penicillium patulum. *J. Chem. Soc., Chem. Commun.* **1990**, 238-242.

(27) El-Sayed, A. K.; Hothersall, J.; Cooper, S. M.; Stephens, E.; Simpson, T. J.; Thomas, C. M. Characterization of the mupirocin biosynthesis gene cluster from *Pseudomonas fluorescens* NCIMB 10586. *Chem. Biol.* **2003**, *10*, 419-430.

(28) Battersby, A. R.; Hodgson, G. L.; Hunt, E.; McDonald, E.; Saunders, J. Biosynthesis of porphyrins and related macrocycles. Part VI. Nature of the rearrangement process leading to the natural type III porphyrins. *J. Chem. Soc., Perkin Trans. 1* **1976**, *3*, 273-282.

(29) Perrin, D. D.; Armarego, W. L. F. *Purification of Laboratory Chemicals*; 3rd ed.; Pergamon Press, New York, 1988.

(30) Still, W. C.; Kahn, M.; Mitra, A. Rapid chromatographic technique for preparative separations with moderate resolution. *J. Org. Chem.* **1978**, *43*, 2923-2925.

(31) Matsuo, M.; Urano, S. Carbon-13 NMR spectra of tocopherols and 2,2-dimethylchromanols. *Tetrahedron* **1976**, *32*, 229-231.

(32) Goodman, R. A.; Oldfield, E.; Allerhand, A. Assignments in the natural-abundance carbon-13 nuclear magnetic resonance spectrum of chlorophyll a and a study of segmental motion in neat phytol. *J. Am. Chem. Soc.* **1973**, *95*, 7553-7558.

(33) Proteau, P. J. Biosynthesis of phytol in the cyanobacterium *Synechocystis sp.* UTEX 2470: utilization of the non-mevalonate pathway. *J. Nat. Prod.* **1998**, *61*, 841-843.

(34) Tsukida, K.; Akutsu, K.; Saiki, K. Carbon-13 nuclear magnetic resonance spectra of vitamins D and related compounds. *J. Nutr. Sci. Vitaminol.* **1975**, *21*, 411-420.

(35) Taylor, S. V., Vu, L. D., and Begley, T. P. Chemical and enzymatic synthesis of 1-deoxy-D-xylulose-5-phosphate. *J. Org. Chem.* **1998**, *63*, 2375-2377.

(36) Kennedy, I. A.; Hemscheidt, T.; Britten, J. F.; Spenser, I. D. 1-Deoxy- D-xylulose. *Can. J. Chem.* **1995**, *73*, 1329-1333.

(37) Winter, R. E. K.; Jian, Z. A Convenient preparation of 3-[$^2H_3$]-methyl-3-buten-1-ol. *J. Labelled Compd. Radiopharm.* **1992**, *31*, 787-791.

(38) Sum, F.-W.; Weiler, L. Stereoselective synthesis of β-substituted α,β-unsaturated esters by dialkylcuprate coupling to the enol phosphate of β-keto esters. *Can. J. Chem.* **1979**, *57*, 1431-1441.

(39) Fujisawa, T.; Sato, T.; Gotoh, Y. Reaction of diketene with grignard reagents in the presence of cobalt catalyst. A convenient method for the synthesis of 3-methylenealkanoic acids leading to terpenoids. *Bull. Chem. Soc. Jpn.* **1982**, *55*, 3555-3559.

CHAPTER FOUR

Studies on Isoprenoid Biosynthesis in Various *Euglena* species

Introduction

The genus *Euglena*, a photosynthetic flagellate group, occupies a branch point between the plant and animal kingdom.[1,2] *Euglena* species are ubiquitously found in nature and are readily cultivated in laboratories. They have been frequently employed for various studies such as phylogenetic investigation, chlorophyll biosynthesis, identification of new carotenoid pigments, or composition of sterols in the cell.[3,4] Studies on isoprenoid biosynthesis in *Euglena* species have been also performed several times over the past 40 years.

Shortly after the mevalonate (MVA) pathway was discovered, carotenoid biosynthesis was investigated in *Euglena gracilis* var. *bacillaris* by Steele *et al.*[5] Potential precursors, such as pyruvate and succinate, for the formation of β-carotene were studied by Cooper *et al.*[6] The biosynthesis and localization of terpenoid quinones were also examined in *Euglena gracilis* strain *Z*, *E. gracilis* var. *bacillaris*, and *E. gracilis* 1224-5g.[7] The pathway to phytol, the side chain of chlorophylls, was studied in *E. gracilis* 1224-5*Z*.[8] These early investigations on isoprenoid biosynthesis in several *E. gracilis* strains reached the conclusion that these organisms incorporate acetate efficiently into isoprenoid compounds via the MVA pathway.

When the 2-*C*-methylerythritol-4-phosphate (MEP) pathway emerged in the early 1990's, the biosynthesis of isoprenoids was extensively reinvestigated in photosynthetic organisms such as cyanobacteria, green algae, red algae, and higher plants.[9-11] These investigations revealed that all of these organisms except for *E. gracilis* 1224-5/9 possessed the MEP pathway in the cells or in chloroplasts. Although *E. gracilis* is a photosynthetic eukaryote which evolutionally acquired chloroplasts from green algae,[12] the labeling patterns for phytol and ergosterol, which are representative metabolites in chloroplasts and in the cytosol, respectively, indicated that *E. gracilis* is an exceptional organism in which the MEP pathway was not detected.[9,11] This result coupled to previous findings in *E. gracilis*, strongly

suggested that isoprenoid biosynthesis in *E. gracilis* strains is accomplished via the MVA pathway. The strain numbers of *E. gracilis* used in previous studies are summarized in Table 4.1.

Table 4.1. Comparison of *Euglena* strains.

Strains	SAG[a]	UTEX[b]	CCAP[c]	ATCC[d]
E. gracilis var. *saccharophila*	1224-5/9[9,11]	752	1224/5T	12893
E. gracilis var. *bacillaris*	1224-5/15	160	1224/7A	10616[5,8]
E. gracilis strain Z	1224-5/25	753	1224/5Z[7]	12894
*E. gracilis*1224/ 5g[7] (= *Astasia longa*)	–[e]	–[e]	1204/17D	–[e]

[a] Sammlung von Algenkulturen Göttingen Culture Collection of Algae at the University Göttingen.
[b] The Culture Collection of Algae at The University of Texas at Austin.
[c] The Culture Collection of Algae and Protozoa.
[d] American Type Culture Collection.
[e] Not available.

However, our recent studies on isoprenoid biosynthesis in *E. gracilis* strain Z described results inconsistent with the already established findings. These investigations suggested that (1) *E. gracilis* strain Z is not a peculiar organism which has only the MVA pathway to isoprenoid compounds, but is able to operate the MEP pathway to carotenoid compounds such as β-carotene and diadinoxanthin, (2) carotenoids and phytol, the plastid isoprenoids, are synthesized via independent pathways, and (3) phytol biosynthesis occurs by an unusual pathway, a modified polyketide-type pathway rather than an isoprenoid pathway, based on incubation experiments with [1-^{13}C-$^{2}H_3$]-acetate and [2-^{13}C]-malonic acid which are the starter and the extender units in polyketide biosynthesis, respectively. These conflicting

results have never been previously reported, so broader investigations were pursued to support our findings.

To expand our findings, several *Euglena* or *Euglena*-related species such as *E. mutabilis, E. viridis, E. anabaena, E. geniculata, E. stellata, E. gracilis* 1224-5/15, *E. gracilis* 1224-5/9, *Colacium sideropus,* and *Phacus similis* were targeted for examination. The main criteria for the selection of organisms were close phylogenetic relationship to *Euglena*, the ability to synthesize phytol (as the side chain of chlorophyll), and availability as an axenic strain from an established culture collection. These organisms were tested in growth media containing glucose or acetate as carbon sources. After examining the growth process of each species, *E. mutabilis*, *E. gracilis* 1224-5/15, and *E. gracilis* 1224-5/9 were employed for the incubation experiment using [U-$^{13}C_6$]-glucose to compare with isoprenoid biosynthesis in *E. gracilis* strain *Z*. The rest of strains did not grow suitably under heterotrophic conditions containing acetate or glucose as a carbon source. *E. mutabilis* is an acidophilic *Euglena* sp. which has been noticed due to its survival in harsh environments such as extremely acidic or metal-polluted conditions. *E. gracilis* 1224-5/9 was used for the study on isoprenoid biosynthesis by Rohmer *et al.*, which led to the conclusion that *E. gracilis* operates the MVA pathway for the formation of phytol and ergosterol.[9,11] *E. gracilis* 1224-5/15 has been used for studies on carotenoid biosynthesis, pigment composition in light and dark grown species, and the role of vitamin B_{12} in metabolism.[5,13,14]

In order to trace the labeling patterns, isoprenoid compounds such as the carotenoid pigments (β-carotene and diadinoxanthin), ergosterol, phytol, and α-tocopherol were examined in these *Euglena* strains in this Chapter (Fig.4.1). An incubation experiment with [U-$^{13}C_6$]-glucose should provide evidence for the presence of the alternate pathway for the formation of phytol, confirming for the previous conclusion.

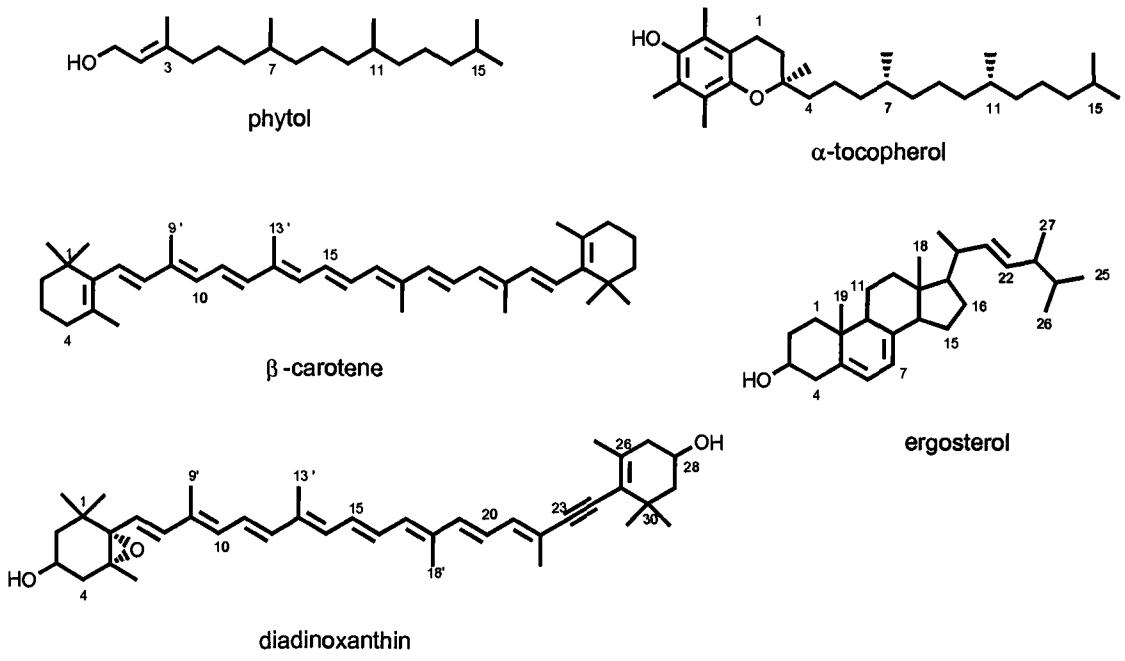

Fig.4.1. Structures of isoprenoids in *E. gracilis*.

Results and Discussion

Because this novel mode of phytol biosynthesis has never been reported, we were curious to find out if this alternate pathway was present in other organisms related to *Euglena*. After examining the growth process of eight *Euglena* or *Euglena*-related species, *E. mutabilis* was chosen for an incubation experiment using [U-$^{13}C_6$]-glucose. Although *E. mutabilis* has a longer doubling time (around 3 days)[15] than *E. gracilis* (8 h)[16], it grew well in medium containing glucose at 23 °C. *E. mutabilis* was incubated with [U-^{13}C]-glucose for 27 days. After incubation, β-carotene, diadinoxanthin, and phytol were isolated from the cells. Unfortunately, neither phytol nor the carotenoids were specifically labeled by [U-$^{13}C_6$]-glucose at all, which suggests that *E. mutabilis* is not an appropriate heterotrophic species for this study.

Because none of the other *Euglena* species or *Phacus* or *Colacium* grew well or readily with acetate or glucose, other strains of *E. gracilis*, such as *E. gracilis* 1224-5/9 and *E. gracilis* 1224-5/15 were next considered for the investigation of phytol biosynthesis. Because *E. gracilis* 1224-5/9 and *E. gracilis* 1244-5/15 had previously been employed for studies of isoprenoid biosynthesis, these organisms are expected to successfully incorporate [U-$^{13}C_6$]-glucose into isoprenoids. In order to grow these *E. gracilis* strains, a modified medium containing DL-malic acid (0.2 g/ 6 L), D-glutamic acid (0.5 g/ 6 L), unlabeled glucose (1 g/L), and labeled glucose (0.4 g/6 L).[14]

In the experiment with *E. gracilis* 1244-5/15, the incorporation levels for phytol and the carotenoids were, on the whole, low (3.6 % by integrating the ^{13}C enrichment at H1 of phytol), but the ^{13}C-NMR spectra of isoprenoids clearly revealed the same unique labeling pattern observed in *E. gracilis Z* . The labeling pattern of phytol from *E. gracilis* 1224-5/15 was characterized by doublets at C1-C2 and C3-C4 and a singlet at C5 of the isoprene unit, while β-carotene and diadinoxanthin appeared as doublets at C1-C2 and C3-C5 and a singlet at C4 of the isoprene unit (Fig.4.2).

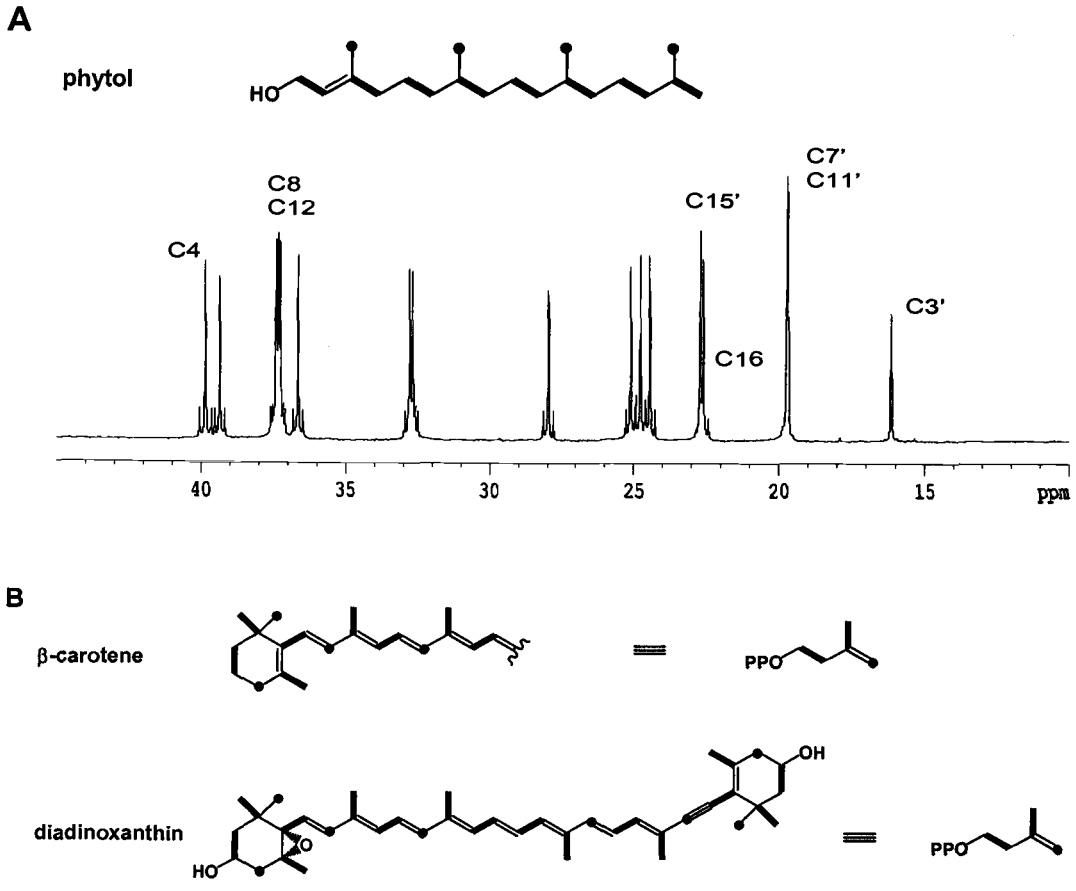

Fig.4.2. Labeling pattern and partial ^{13}C-NMR spectrum for phytol (A) and labeling pattern of carotenoids (B) from the [U-$^{13}C_6$]-glucose incubation experiment in *E. gracilis* 1224-5/15.

In contrast, *E. gracilis* 1224-5/9 grown in the same medium displayed a higher incorporation level (5.6 % by integrating the ^{13}C enrichment at H1 of phytol) than *E. gracilis* 1224-5/15. The labeling pattern for phytol was also consistent with that for *E. gracilis Z*, showing doublets at C1-C2 and C3-C4 and a singlet at C5 of the isoprene unit (Fig.4.3). These results suggest that the unusual pathway of phytol is not limited to *E. gracilis Z*, but appears to be a common feature of heterotrophic *E. gracilis* strains.

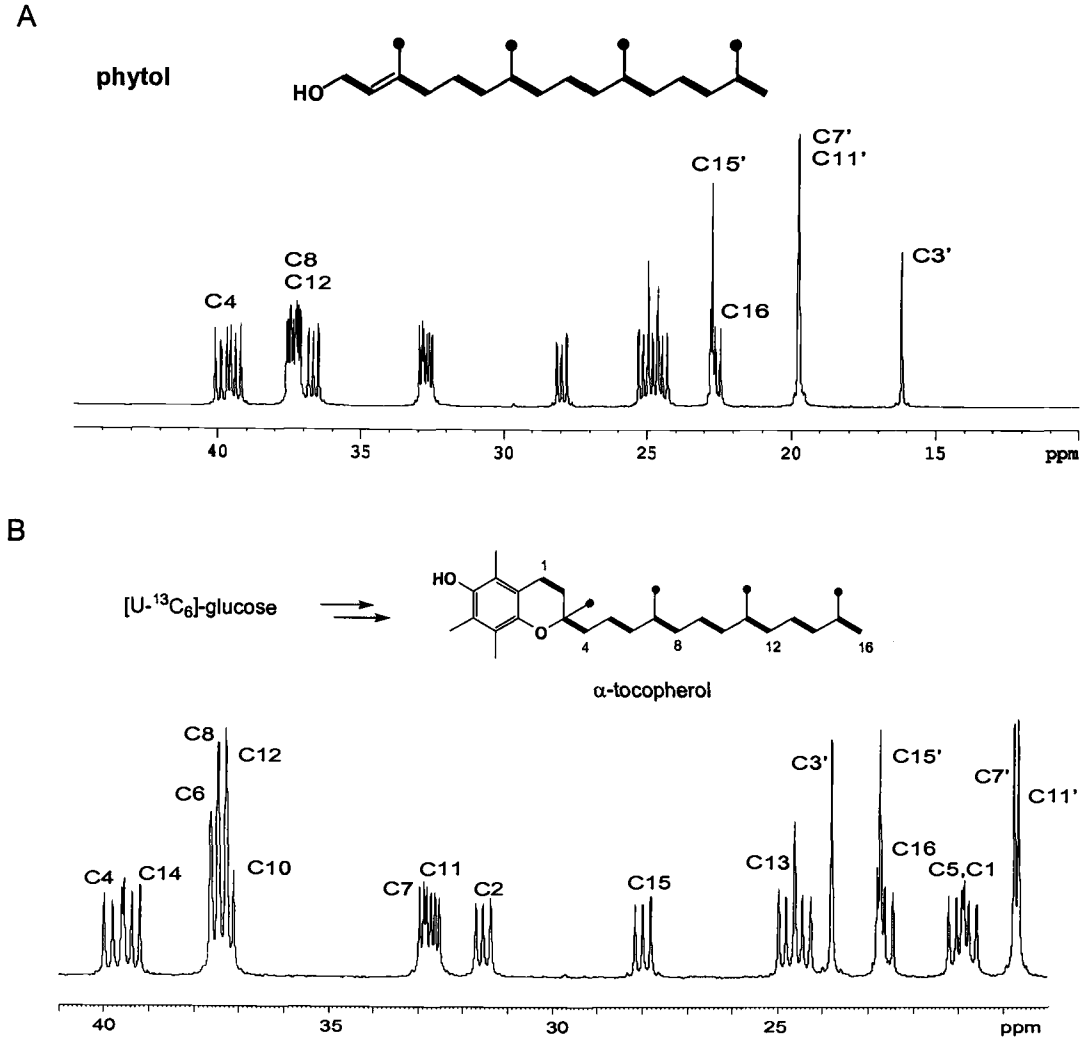

Fig.4.3. Partial ^{13}C-NMR spectra and labeling patterns for phytol (A) and α-tocopherol (B) of *E. gracilis* 1224-5/9 from the [U-$^{13}C_6$]-glucose incubation experiment.

When the incubation experiment with [U-$^{13}C_6$]-glucose in *E. gracilis* 1224-5/9 was carried out, small quantities of α-tocopherol and ergosterol were also isolated to investigate their labeling patterns. The structure of α-tocopherol is known to consist of an aromatic moiety with a phytyl side chain incorporated into a pyran ring. Because the isoprenoid portion of α-tocopherol typically arises from phytyl diphosphate, it also may be formed in *E. gracilis* by the same route as phytol. The result from the incubation experiment using [U-$^{13}C_6$]-glucose indicated that labeled glucose was incorporated into the phytyl-derived moiety of α-tocopherol consistent

with the phytol labeling pattern showing doublets at C1-C2 and C3-C4 and an intense singlet at C4. This represents that this phytol-related metabolite is also produced via the unusual polyketide-like pathway in *Euglena* species (Fig.4.3).

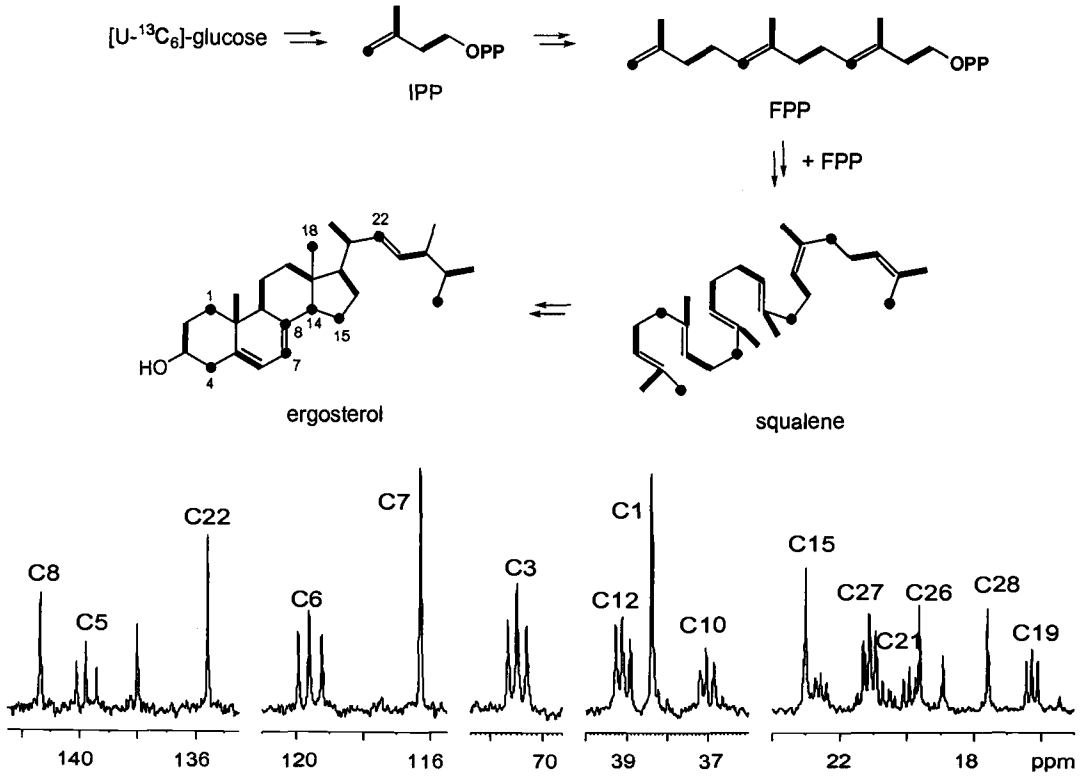

Fig.4.4. Labeling pattern and partial ^{13}C-NMR spectra for ergosterol from the [U-$^{13}C_6$]-glucose incubation experiment.

Ergosterol is regarded as a representative cytosolic isoprenoid which is discriminated from plastidic isoprenoids based on the differential contribution of the MVA and the MEP pathways in each compartment, such as the cytosol and the chloroplasts of photosynthetic eukaryotes.[9-11] Ergosterol biosynthesis has already been concluded to occur by the MVA pathway in photosynthetic eukaryotes, as well as in *E. gracilis*.[9,11] The labeling pattern of ergosterol from the [U-$^{13}C_6$]-glucose incubation experiment is shown in Figure 4.4. Squalene derived from the general precursor farnesyl diphosphate (FPP) undergoes cyclization, methyl migration, demethylation, and methylation reactions, which results in the rearrangement of carbon positions labeled with ^{13}C isotopes. Based on the MVA pathway, C1, C7, C15,

and C22 corresponding to C4 of the isoprene unit appeared as singlets due to the loss of the carboxyl carbon in the decarboxylation reaction to form IPP. Singlets at C4 and C8 arise from demethylation steps. And C14 and C18 also appeared as singlets arising from methyl migration steps, even though they are originated from intact acetate units. The labeling pattern shows no sign of the unique phytol-like labeling pattern. This result, along with the low incorporation of the labeled DX into ergosterol (see Chapter Two), supports the conclusion that ergosterol is synthesized mainly via the MVA pathway as previously determined. [9,11]

Based on the consistent labeling patterns of phytol and α-tocopherol, we suggest that the presence of the alternate polyketide-type pathway operates for the formation of phytol and its related compounds in heterotrophic *Euglena* species. Although more experiments are necessary to fully detail the biosynthetic pathways to sterol and carotenoids in *E. gracilis* strains 5/9 and 5/15, sterols and carotenoid biosyntheses in these strains clearly occur by a different route from phytol biosynthesis and are assumed to follow in the same manner of *E. gracilis* strain Z.

Experimental

Instruments

All ^{1}H and ^{13}C nuclear magnetic resonance (NMR) spectra were recorded on a Bruker AC 300 spectrometer operating at 300 MHz for ^{1}H and 75 for ^{13}C, and on a Bruker AM 400 spectrometer operating at 400.13 MHz for ^{1}H and 100.13 MHz for ^{13}C. Chemical shifts of NMR spectra are shown as δ, and references are based on deuterated NMR solvents as an internal standard ($CHCl_3$ at 7.26 ppm for ^{1}H-NMR and $^{13}CDCl_3$ at 77.0 ppm for the center line of the triplet in ^{13}C-NMR, acetone at 2.08 ppm for ^{1}H-NMR and acetone-d_6 at 30.7 ppm for the center line of the septet in ^{13}C-NMR). Incorporation levels for ^{13}C signals of isoprenoids in the incubation experiments using labeled compounds were calculated on the basis of the intensities of the target peak relative to the intensity of an unenriched peak. This ratio was compared with the ratio for the corresponding peaks from the natural abundance ^{13}C-NMR spectrum for unlabeled isoprenoids to determine the relative incorporation level. Low and high-resolution chemical ionization mass spectra (CIMS) and fast atom bombardment mass spectra (FABMS) were recorded on a Kratos MS50TC spectrometer. Strains were grown in a Hoffman illuminated incubator for mass cultivation. Harvesting of *Euglena* cells was done with a Beckman J2-HS centrifuge and lyophilization of the cells utilized a Labconco freeze dry system.

Biosynthetic experiments

Agar slants of *E. gracilis* (SAG 1224-5/9, formerly *E. gracilis* var. *saccharophila*), *E. gracilis* (SAG 1224-5/15, formerly *E. gracilis* var. *baciilaris*), *E. mutabilis* (SAG 1224-9a), *E. viridis* (SAG 1224-21), *E. anabaena* (SAG 1224-15b), *E. geniculata* (SAG 1224-4C), *E. stellata* (SAG 1224-14), *Phacus similis* (SAG 58.81), *and Colacium sideropus* (SAG 14.90) were obtained from SAG, The Culture Collection of Algae at Göttingen University, Germany.

For maintenance of the organisms, *E. gracilis* 1224-5/9 and *E. gracilis* 1224-5/15 were cultivated in modified media containing D-glucose (1.0 g/L), $(NH_4)_2HPO_4$ (1.0 g/L), KH_2PO_4 (1.0 g/L), $MgSO_4 \cdot 7H_2O$ (0.2 g/L), $CaCl_2 \cdot 2H_2O$ (0.02 g/L), sodium citrate$\cdot 2H_2O$ (0.5g/L), thiamine·HCl (10 μg/L), vitamin B_{12} (0.5 μg /L) and trace metals.[17] Trace metals were prepared with $FeCl_3 \cdot 6H_2O$ (3.2 mg/L), $MnCl_2 \cdot 4H_2O$ (1.8

mg/L), $CoCl_2 \cdot 6H_2O$ (1.1 mg/L), $ZnSO_4 \cdot 7H_2O$ (0.4 mg/L), $Na_2MoO_4 \cdot 2H_2O$ (0.3 mg/L), $CuSO_4 \cdot 5H_2O$ (0.02 mg/L). Seed cultures were inoculated into medium (200 mL) and were grown at 30 °C for 7-14 days under constant illumination with 40 W cool-white fluorescent lights (200-210 ftc). For mass cultivation, the seed cultures were inoculated into medium (6 L), aerated and grown for 7-14 days under the same condition as the seed cultures. For incubation experiments with labeled compounds, the labeled compounds (0.4 g/6L) were mixed with unlabeled D-glucose (1 g/L). When *E. gracilis* 1224-5/9 and *E. gracilis* 1224-5/15 were grown in 6 L media, 0.5 g of D-glutamic acid and 0.2 g of DL-malic acid were added in the media (6 L).[14]

For maintenance as well as for mass cultivation (6 L) of *E. mutabilis*, the medium was prepared with D-glucose (1 g/L), $(NH_4)_2SO_4$ (0.5 g/L), KH_2PO_4 (0.5 g/L), $MgSO_4 \cdot 7H_2O$ (0.5 g/L), sodium citrate$\cdot 2H_2O$ (0.2 g/L), NaCl (30 mg/L), $CaCl_2 \cdot 2H_2O$ (13 mg/L), thiamine·HCl (0.2 mg/L), vitamin B_{12} (4 μg/L), and trace metals and then adjusted to pH 3.6 with 1 N HCl. The solution of trace metals contained $ZnSO_4 \cdot 7H_2O$ (2 mg/L), $FeSO_4 \cdot 7H_2O$ (1.1 mg/L), $MnSO_4 \cdot 4H_2O$ (1.0 mg/L), $CuSO_4 \cdot 5H_2O$ (0.06 mg/L), $Co(NO_3)_2 \cdot 6H_2O$ (0.024 mg/L), H_3BO_3 (0.011 mg/L), and $Na_2Mo_7O_{24} \cdot 4H_2O$ (0.011 mg/L). Cultures were maintained in the medium at room temperature with ambient lighting. Seed cultures were inoculated into medium (200 ml) and were grown at 23 °C for 21 days under constant illumination with 40 W cool-white fluorescent lights (200-210 ftc). For mass cultivation, the seed cultures was inoculated into medium (6 L), aerated and grown for 27 days under the same condition as the seed cultures. For incubation experiments with labeled compounds, the labeled compounds (0.1 g/L) were mixed with unlabeled D-glucose (1 g/L).

For maintenance, *E. geniculata* and *E. stellata* were cultivated in modified BG-11 medium[18] containing sodium acetate (1.0 g/L), $NaNO_3$ (1.5 g/L), KH_2PO_4 (0.4 g/L), $MgSO_4 \cdot 7H_2O$ (0.075 g/L), $CaCl_2 \cdot 2H_2O$ (0.036 g/L), Na_2CO_3 (0.02 g/L), citric acid$\cdot 2H_2O$ (0.006 g/L), EDTA·disodium salt (0.001 g/L), ferric ammonium citrate (6 mg/L), thiamine·HCl (10 μg/L), vitamin B_{12} (0.5 μg /L) and trace metals. Trace metals were prepared with H_3BO_3 (2.86 mg/L), $MnCl_2 \cdot 4H_2O$ (1.81 mg/L), $Na_2MoO_4 \cdot 2H_2O$ (0.39 mg/L), $ZnSO_4 \cdot 7H_2O$ (0.222 mg/L), $CuSO_4 \cdot 5H_2O$ (0.079 mg/L), and $CoCl_2 \cdot 6H_2O$ (0.0494 mg/L). For maintenance, *E. viridis, E. anabaena,* and *Colacium sideropus* were cultivated in modified SAG medium containing sodium acetate (1.0 g/L), beef-extract (1.0 g/L), bacto-tryptone (2.0 g/L), yeast extract (2.0 g/L), KNO_3 (0.2 g/L),

sodium citrate·$2H_2O$ (0.8g/L), $MgSO_4 \cdot 7H_2O$ (0.01 g/L), $CaCl_2 \cdot 2H_2O$ thiamine·HCl (10 μg/L), vitamin B_{12} (0.5 μg /L) and trace metals. Trace metals were prepared with H_3BO_3 (2.86 mg/L), $MnCl_2 \cdot 4H_2O$ (1.81 mg/L), $Na_2MoO_4 \cdot 2H_2O$ (0.39 mg/L), $ZnSO_4 \cdot 7H_2O$ (0.222 mg/L), $CuSO_4 \cdot 5H_2O$ (0.079 mg/L), and $CoCl_2 \cdot 6H_2O$ (0.0494 mg/L). All cultures were maintained in their media at room temperature with ambient lighting.

Inorganic salts for the culture media were purchased from Mallinckrodt, and D-glucose, vitamin B_{12}, and thiamine·HCl were from Sigma-Aldrich. Beef-extract, bacto-tryptone, and yeast extract were obtained from Difco Laboratories. [U-$^{13}C_6$]-Glucose was purchased from Cambridge Isotope Laboratories. Phytol, vitamin E, and β-carotene standards were purchased from Sigma-Aldrich. Water was deionized using a Milli Q Millipore system for all experiments. Silica gel (Merck, grade 60, 220-400 mesh) was used for flash column chromatography.[19] Merck glass-backed TLC plates (silica gel 60 F254) were employed for thin layer chromatography (TLC) and preparative TLC (prep-TLC).

Isolation of Isoprenoids

After cultivation, cells were harvested by centrifugation at 7000 rpm (JA-10 rotor, 8671 *g*) for 10 min and lyophilized to obtain 0.3-0.5 g of dry weight per liter. The lyophilized cells were extracted three times (30 min each) with a mixture of $CHCl_3$ and MeOH (2:1) at room temperature to provide a crude extract, which was applied to a silica gel flash chromatography column. The column was developed with mixtures of 15-50 % EtOAc in hexanes to separate four fractions which were determined by color of pigments. The fractions 1 (orange color) and 2 (yellow color) contain the non-polar compounds (R_f = 0.8-0.9 and 0.7, silica TLC plate, 5 % EtOAc in hexanes). Fraction 3 is the chlorophyll-containing fraction (R_f = 0.5-0.6, silica gel TLC plate, 10 % EtOAc in hexanes). Fraction 4 (orange-red color) contains the polar compounds (R_f = 0.2-0.3, silica gel TLC plate, 30 % EtOAc in hexanes). After the organic solvent was evaporated, each fraction was processed to separate the isoprenoids.

Fraction 1 was applied to a silica prep-TLC plate, which was developed in a mixture of cyclohexane, hexanes, and toluene (4:4:1). An orange band (R_f = 0.4) was carefully scraped from TLC plates and extracted with $CHCl_3$ to provide 1 mg/L (avg.

yield) of β-carotene. α-Tocopherol (0.2 mg/L, avg. yield) was obtained from fraction 2 which was developed on the TLC plates three times with 5 % EtOAc in hexanes. The band corresponding to α-tocopherol on TLC plates was scraped and extracted with $CHCl_3$. The chlorophyll-containing fraction was hydrolyzed in 10 % (w/v) KOH in MeOH overnight, and extracted with ether. The ethereal extract was washed with a saturated NH_4Cl solution and *dd*-H_2O, dried, and concentrated. The extract was applied to a flash chromatography column (silica gel, 15% EtOAc in hexanes) to separate phytol and ergosterol. The isolated phytol was decolorized by passing the phytol solution over a short column of charcoal and Florisil and washing with ether to provide 4 mg/L (avg. yield) of pure phytol. Ergosterol was further purified by silica prep TLC plates developing three times with 5 % EtOAc in hexanes (0.1 mg/L, avg. yield). Diadinoxanthin (2 mg/L, avg. yield) was purified from fraction 4 by using a Sephadex LH-20 column (2.5 × 28 cm) with MeOH as eluent. β-Carotene, α-tocopherol, phytol, ergosterol, and diadinoxanthinobtained from the *Euglena* strains were analyzed by mass spectrometry and NMR spectroscopy. ^{13}C- and ^{1}H-NMR assignments for β-carotene, α-tocopherol, phytol, ergosterol, and diadinoxanthin were previously described in Chapter Two and Three.

References

(1) Johnson, L. P. In *The Biology of Euglena*; Buetow, D. E., Ed.; Academic Press: New York, 1968; Vol. 1, pp. 1-25.

(2) Gojdics, M. *The genus Euglena*; University of Wisconsin Press, Madison, 1953.

(3) Heelis, D. V.; Kernick, W.; Phillips, G. O.; Davies, K. Separation and identification of the carotenoid pigments of stigmata isolated from light-grown cells of *Euglena gracilis* strain *Z. Arch. Microbiol.* **1979**, *121*, 207-211.

(4) Zielinski, J.; Kokke, W. C.; Fenical, W.; Djerassi, C. Sterols of the cultured euglenid *Eutreptia viridis*: a novel delta 23-unsaturated sterol. *Steroids* **1982**, *40*, 403-411.

(5) Steele, W.; Gurin, S. Biosynthesis of β-carotene in *Euglena gracilis*. *J. Biol. Chem.* **1960**, *235*, 2778-2785.

(6) Cooper, C. Z.; Benedict, C. R. *Plant Physiol.* **1967**, *42*, S44-S45.

(7) Threlfall, D. R.; Goodwin, T. W. Nature, intracellular distribution and formation of terpenoid quinones in *Euglena gracilis*. *Biochem. J.* **1967**, *103*, 573-588.

(8) Ahrens, E. H. J.; Williams, D. C.; Battersby, A. R. Biosynthesis of porphyrins and related macrocycles. Part 11. Studies on biosynthesis of the phytyl chain of chlorophyll a by use of carbon-13. *J. Chem. Soc., Perkin Trans. 1* **1977**, *23*, 2540-2545.

(9) Müller, C.; Schwender, J.; Disch, A.; Rohmer, M.; Lichtenthaler, F. W.; Lichtenthaler, H. K. Occurence of the 1-deoxy-D-xylulose 5-phosphate pathway of isopentenyl diphosphate biosynthesis in different algae groups. *Adv. Plant Lipid Res.* **1998**, 425-428.

(10) Lichtenthaler, H. K. The plants' 1-deoxyD-xylulose-5-phosphate pathway for biosynthesis of isoprenoids. *Fett/Lipid* **1998**, *100*, 128-138.

(11) Disch, A.; Schwender, J.; Muller, C.; Lichtenthaler, H. K.; Rohmer, M. Distribution of the mevalonate and glyceraldehyde phosphate/pyruvate pathways for isoprenoid biosynthesis in unicellular algae and the cyanobacterium *Synechocystis PCC 6714*. *Biochem. J.* **1998**, *333*, 381-388.

(12) Douglas, S. E.; Turner, S. Molecular evidence for the origin of plastids from a cyanobacterium-like ancestor. *J. Mol. Evol.* **1991**, *33*, 267-273.

(13) Goodwin, T. W.; Gross, J. A. Carotenoid distribution in bleached substrains of *Euglena gracilis*. *J. Protozool.* **1958**, *5*, 292-295.

(14) Venkataraman, S.; Netrawall, M. S.; Sreenivasan, A. The Role of Vitamin B_{12} in the Metabolism of *Euglena gracilis* var. *bacillaris*. *Biochem. J.* **1965**, *96*, 552-556.

(15) Olaveson, M. M.; Stokes, P. M. Responses of the acidophilic alga *Euglena mutabilis* to carbon enrichment at pH3. *J. Phycol.* **1989**, *25*, 529-539.

(16) Cook, J. R. In *The Biology of Euglena*; Buetow, D. E., Ed.; Academic Press: New York, 1968; Vol. 1, pp. 244-314.

(17) Battersby, A. R.; Hodgson, G. L.; Hunt, E.; McDonald, E.; Saunders, J. Biosynthesis of porphyrins and related macrocycles. Part VI. Nature of the rearrangement process leading to the natural type III porphyrins. *J. Chem. Soc., Perkin Trans. 1* **1976**, *3*, 273-282.

(18) Stanier, R. Y.; Kunisawa, R.; Mandel, M.; Cohen-Bazire, G. Purification and properties of unicellular blue-green algae (order Chroococcales). *Bacteriol. Rev.* **1971**, *35*, 171-205.

(19) Still, W. C.; Kahn, M.; Mitra, A. Rapid chromatographic technique for preparative separations with moderate resolution. *J. Org. Chem.* **1978**, *43*, 2923-2925.

CHAPTER FIVE

General Conclusion

Isoprenoid biosynthesis occurs by two established pathways, the mevalonate (MVA) pathway and the 2-*C*-methyl-D-erythritol-4-phosphate (MEP) pathway in all organisms. Photosynthetic eukaryotes, including higher plants, are known to possess both pathways, with a distinct compartmentation of isoprenoid biosynthesis. They are able to utilize the MVA pathway to produce cytosolic isoprenoids, such as sterols, and the MEP pathway to synthesize phytol and carotenoids in chloroplasts.

To date, however, *Euglena gracilis* has been reported to be the only photosynthetic eukaryote in which the MEP pathway is not detected. In this dissertation, isoprenoid biosynthesis in *E. gracilis* strain *Z* was investigated using incubation experiments with labeled precursors such as [1-^{13}C]-glucose, [5-$^{2}H_2$]-deoxy-D-xylulose, [U-$^{13}C_6$]-glucose, [1,2-$^{13}C_2$]-acetate, [methyl-^{13}C]-methionine, [2-^{13}C]-leucine, [1-^{13}C]-butyric acid, [1,2,3,4-$^{13}C_4$]-acetoacetyl-*N*-acetylcysteamine, [1,2,3,4-$^{13}C_3$]-dimethylacrylic acid, 3-[$^{2}H_3$]-methyl-3-butenoic acid, 3-[$^{2}H_3$]-methyl-3-butenoyl-*N*-acetylcysteamine, [2-^{13}C]-malonic acid, [1-^{13}C-2-$^{2}H_3$]-acetate, and [2-^{13}C-2-$^{2}H_3$]-acetate.

Through the incubation experiments using [1-^{13}C]-glucose and [5-$^{2}H_2$]-DX, differential incorporation of [1-^{13}C]-glucose into each isoprene unit of carotenoids and intact incorporation of [5-$^{2}H_2$]-DX into carotenoids were found, which represents that (1) *E. gracilis* undoubtedly possesses the MEP pathway and utilizes both the MVA and the MEP pathways to produce carotenoids and (2) phytol and ergosterol, however, are not biosynthesized via the MEP pathway, which is consistent with previous results.

Because phytol was not synthesized by the same route as carotenoids in *E. gracilis*, phytol biosynthesis was pursued further. Incubation experiments using [U-$^{13}C_6$]-glucose and [1,2-$^{13}C_2$]-acetate provided labeling patterns inconsistent with either of the isoprenoid pathways. This unusual labeling pattern was also seen in α-tocopherol, which consists of sidechain derived from phytyl diphosphate and an aromatic moiety. The α-tocopherol was isolated from *E. gracilis* strain 1224-5/9.

Because the labeling patterns of phytol and α-tocopherol were consistently reproducible, incubation experiments using [2-^{13}C]-leucine, [1-^{13}C]-butyric acid, [1,2,3,4-$^{13}C_4$]-acetoacetyl-*N*-acetylcysteamine, [1,2,3,4-$^{13}C_3$]-dimethylacrylic acid, 3-[methyl-$^{2}H_3$]-3-butenoic acid, and 3-[methyl-$^{2}H_3$]-3-butenoyl-*N*-acetylcysteamine were examined to further elucidate phytol biosynthesis. Although these experiments did not reveal any specific labeling of phytol, these compounds did provide further clues about the differences in precursors for carotenoids and phytol. Carotenoids were labeled with the intact butyric acid and acetoacetyl-*N*-acetylcysteamine, as well as with metabolized leucine and dimethylacrylic acid. In contrast, leucine, butyric acid, acetoacetyl-*N*-acetylcysteamine, and dimethylacrylic acid all have to be metabolized before they are utilized for phytol biosynthesis.

The lack of incorporation of reasonable isoprenoid precursors into phytol led us to consider a polyketide, rather than an isoprenoid, route to phytol. An incubation experiment using [2-^{13}C]-malonic acid, an extender unit of polyketide biosynthesis, was a first step to elucidate a polyketide route to phytol in *E. gracilis*. The labeled malonate was highly incorporated into the phytol backbone but did not strongly label the branching methyl groups or the starter acetate unit. Based on this finding, incubation experiments using [1-^{13}C-2-$^{2}H_3$]-acetate and [2-^{13}C-2-$^{2}H_3$]-acetate were performed to further discriminate between isoprenoid and polyketide pathways. By assigning the number of deuterium atoms retained at C4, C8, C12, and C15, support could be provided for one or the other pathway. The retention of single deuterium atoms at these positions in phytol was only consistent with a polyketide pathway. Through these results, we propose that phytol biosynthesis occurs by a polyketide-type biosynthetic pathway in *E. gracilis*. This is an unprecedented finding in that phytol is a well-described isoprenoid in all other chloroplast-containing organisms that have been examined. However, It appears that phytol in *E. gracilis* is more accurately described as a polyketide.

Therefore, in this dissertation, the first evidence for the existence of the MEP pathway in *E. gracilis* was revealed, specifically for the synthesis of carotenoids. It was also discovered that phytol and α-tocopherol biosynthesis appears to occur via a polyketide-type pathway instead of by an isoprenoid pathway. Although our data strongly support a polyketide-type route to phytol and α-tocopherol, further work will be necessary to uncover the details of this novel biosynthetic pathway.

Bibliography

Ahrens, E. H. J.; Williams, D. C.; Battersby, A. R. Biosynthesis of porphyrins and related macrocycles. Part 11. Studies on biosynthesis of the phytyl chain of chlorophyll a by use of carbon-13. *J. Chem. Soc., Perkin Trans. 1* **1977**, *23*, 2540-2545.

Alexander, R. W. Teasing apart the taxol pathway. *Trends Biochem. Sci.* **2001**, *26*, 152.

Altincicek, B.; Kollas, A. K.; Sanderbrand, S.; Wiesner, J.; Hintz, M.; Beck, E.; Jomaa, H. GcpE is involved in the 2-C-methyl-D-erythritol 4-phosphate pathway of isoprenoid biosynthesis in Escherichia coli. *J. Bacteriol.* **2001**, *183*, 2411-2416.

Altincicek, B.; Kollas, A.; Eberl, M.; Wiesner, J.; Sanderbrand, S.; Hintz, M.; Beck, E.; Jomaa, H. LytB, a novel gene of the 2-C-methyl-D-erythritol 4-phosphate pathway of isoprenoid biosynthesis in Escherichia coli. *FEBS Lett.* **2001**, *499*, 37-40.

Anderson, M. S.; Muehlbacher, M.; Street, I. P.; Proffitt, J.; Poulter, C. D. Isopentenyl diphosphate:dimethylallyl diphosphate isomerase. An improved purification of the enzyme and isolation of the gene from *Saccharomyces cerevisiae*. *J. Biol. Chem.* **1989**, *264*, 19169-19175.

Anding, C.; Brandt, R. D.; Ourisson, G. Sterol biosynthesis in *Euglena gracilis Z.* Sterol precursors in light- grown and dark-grown *Euglena gracilis Z. Eur. J. Biochem.* **1971**, *24*, 259-263.

Arigoni, D.; Sagner, S.; Latzel, C.; Eisenreich, W.; Bacher, A.; Zenk, M. H. Terpenoid biosynthesis from 1-deoxy-D-xylulose in higher plants by intramolecular skeletal rearrangement. *Proc. Natl. Acad. Sci. U S A* **1997**, *94*, 10600-10605.

Armstrong, G. In *Comprehensive Natural Product Chemistry*; Cane, D. E., Ed.; Elsevier: New York, 1999; Vol. 2, pp. 321-352.

Bach, T. J.; Lichtenthaler, H. K. Plant growth regulation by mevinolin and other sterol biosynthesis inhibitors. *Am. Chem. Soc. Symp. Series* **1987**, *325*, 109-139.

Battersby, A. R.; Hodgson, G. L.; Hunt, E.; McDonald, E.; Saunders, J. Biosynthesis of porphyrins and related macrocycles. Part VI. Nature of the rearrangement process leading to the natural type III porphyrins. *J. Chem. Soc., Perkin Trans. 1* **1976**, *3*, 273-282.

Bently, R.; Meganathan, R. Biosynthesis of vitamin K (menaquinone) in Bacteria. *Microbiol. Rev.* **1982**, *46*, 241-280.

Bloch, K.; Chaykin, S.; Phillips, J. W.; deWaard, A. Mevalonic acid pyrophosphate and isopentenylpyrophosphate. *J. Biol. Chem.* **1959**, *234*, 2595-2604.

Bochar, D. A.; Friesen, J. A.; Stauffacher, C. V.; Rodwell, V. W. In *Comprehensive Natural Product Chemistry*; Cane, D. E., Ed.; Elsevier: New York, 1999; Vol. 2, pp. 15-44.

Boucher, Y.; Doolittle, W. F. The role of lateral gene transfer in the evolution of isoprenoid biosynthesis pathways. *Mol. Microbiol.* **2000**, *37*, 703-716.

Braithwaite, G. D.; Goodwin, T. W. Biosynthesis of β-carotene from DL-β-Hydroxy-β-methyl-γ-[2-14C]valerolactone by Phycomyces blakesleeanus and Carrot Slices. *Biochem. J.* **1957**, *67*, 13p-14p.

Braithwaite, G. D.; Goodwin, T. W. Studies in carotenogenesis. 25. The incorporation of [1-^{14}C] acetate, [2-^{14}C] acetate and ^{14}C-labelled carbon dioxide into lycopene by tomato slices. *Biochem. J.* **1960**, *76*, 1-5.

Braithwaite, G. D.; Goodwin, T. W. Studies in carotenogenesis. 27. Incorporation of [2-^{14}C] acetate, DL-[2-^{14}C] mevalonate and ^{14}C-labelled carbon dioxide into carrotroot preparations. *Biochem. J.* **1960**, *76*, 194-197.

Brandt, R. D.; Pryce, R. J.; Anding, C.; Ourisson, G. Sterol biosynthesis in *Euglena gracilis Z.* Comparative study of free and bound sterols in light and dark grown *Euglena gracilis Z. Eur. J. Biochem.* **1970**, *17*, 344-349.

Breckenridge, D. G.; Watanabe, Y.; Greenwood, S. J.; Gray, M. W. U1 small nuclear RNA and spliceosomal introns in Euglena gracilis. *Proc. Natl. Acad. Sci. U S A* **1999**, *96*, 852-856.

Briton, G. In *Aspects of Terpenoid Chemistry and Biochemistry*; Goodwin, T. W., Ed.; Academic Press: New York, 1971, pp. 255-289.

Britton, G. In *Carotenoids*; Britton, G., Liaaen-Jensen, S., Pfander, H., Eds.; Birkhäuser: Basel, 1998; Vol. 3, pp. 13-147.

Broers, S. T. J. Ph. D. Dissertation, Eidgenössische Technische Hochschule, Zürich, 1994.

Campos, N.; Rodriguez-Concepcion, M.; Seemann, M.; Rohmer, M.; Boronat, A. Identification of gcpE as a novel gene of the 2-C-methyl-D-erythritol 4-phosphate pathway for isoprenoid biosynthesis in Escherichia coli. *FEBS. Lett.* **2001**, *488*, 170-173.

Canback, B.; Andersson, S. G. E.; Kurland, C. G. The global phylogeny of glycolytic enzymes. *Proc. Natl. Acad. Sci. U S A* **2002**, *99*, 6097-6102.

Cane, D. E. In *Comprehensive Natural Product Chemistry*; Cane, D. E., Ed.; Elsevier: New York, 1999; Vol. 2, pp. 1-13.

Cane, D. E.; Rossi, T.; Tillman, A. M.; Pachlatko, J. P. Stereochemical studies of isoprenoid biosynthesis. biosynthesis of pentalenolactone from [U-$^{13}C_6$]glucose and [6-$^{2}H_2$]-glucose. *J. Am. Chem. Soc.* **1981**, *103*, 1838-1843.

Champney, W.; Jensen, R. Molecular events in the growth inhibition of *Bacillus subtilis* by D-tyrosine. *J. Bacteriol.* **1970**, *104*, 351-359.

Chichester, C. O.; Yokoyama, H.; Nakayama, T. O.; Lukton, A.; Mackinney, G. Leucine metabolism and carotene biosynthesis. *J. Biol. Chem.* **1959**, *234*, 598-602.

Cook, J. R. In *The Biology of Euglena*; Buetow, D. E., Ed.; Academic Press: New York, 1968; Vol. 1, pp. 244-314.

Cooper, C. Z.; Benedict, C. R. *Plant Physiol.* **1967**, *42*, S44-S45.

Cornforth, J. W.; Cornforth, R. H.; Popjak, G.; Youhotsky-Gore, I. Biosynthesis of squalene and cholesterol from DL-β-hydroxy-β-methyl-γ-[2-^{14}C]-valerolactone. *Biochem. J.* **1957**, *66*, 10p.

Cox, E. R. *Phytoflagellates*; Elsevier, New York, 1980.

Cunningham, F. X., Jr.; Lafond, T. P.; Gantt, E. Evidence of a role for LytB in the nonmevalonate pathway of isoprenoid biosynthesis. *J. Bacteriol.* **2000**, *182*, 5841-5848.

Disch, A.; Schwender, J.; Muller, C.; Lichtenthaler, H. K.; Rohmer, M. Distribution of the mevalonate and glyceraldehyde phosphate/pyruvate pathways for isoprenoid biosynthesis in unicellular algae and the cyanobacterium *Synechocystis PCC 6714*. *Biochem. J.* **1998**, *333*, 381-388.

Dolphin, W. Photoinduced carotenogenesis in chlorotic *E. gracilis*. *Plant Physiol.* **1970**, *46*, 685-691.

Douglas, S. E.; Turner, S. Molecular evidence for the origin of plastids from a cyanobacterium-like ancestor. *J. Mol. Evol.* **1991**, *33*, 267-273.

Dubey, V. S. Mevalonate-independent pathway of isoprenoids synthesis: A potential target in some human pathogens. *Curr. Sci.* **2002**, *83*, 685-688.

Duvold, T.; Bravo, J.-M.; Pale-Grosdemange, C.; Rohmer, M. Biosynthsis of 2-C-methyl-D-erythritol, a putative C_5 intermediate in the mevelonate independent pathway for isoprenoid bisynthesis. *Tetrahedron Lett.* **1997**, *38*, 4769-4772.

Duvold, T.; Cali, P.; Bravo, J.-M.; Rohmer, M. Incorporation of 2-C-methyl-D-erythritol, a putative C_5 isoprenoid precursor in the mevelonate-independent pathway, into ubiquinone and menaquinone of *Escherichia coli*. *Tetrahedron Lett.* **1997**, *38*, 6181-6184.

Edelman, M.; Kahana, Z. E. In *The Biology of Euglena*; Buetow, D. E., Ed.; Academic Press: New York, 1989; Vol. 4, pp. 335-351.

Eisenreich, W.; Menhard, B.; Hylands, P. J.; Zenk, M. H.; Bacher, A. Studies on the biosynthesis of taxol: the taxane carbon skeleton is not of mevalonoid origin. *Proc. Natl. Acad. Sci. U S A* **1996**, *93*, 6431-6436.

Eisenreich, W.; Rohdich, F.; Bacher, A. Deoxyxyluose phosphate pathway to terpenoids. *Trends Plant Sci.* **2001**, *6*, 78-84.

El-Sayed, A. K.; Hothersall, J.; Cooper, S. M.; Stephens, E.; Simpson, T. J.; Thomas, C. M. Characterization of the mupirocin biosynthesis gene cluster from *Pseudomonas fluorescens* NCIMB 10586. *Chem. Biol.* **2003**, *10*, 419-430.

Endo, A. The discovery and development of HMG-CoA reductase inhibitor. *J. Lipid Res.* **1992**, *33*, 1569-1582.

Flesch, G.; Rohmer, M. Prokaryotic hopanoids: the biosynthesis of the bacteriohopane skeleton. Formation of isoprenic units from two distinct acetate pools and a novel type of carbon/carbon linkage between a triterpene and D-ribose. *Eur. J. Biochem.* **1988**, *175*, 405-411.

Fujisawa, T.; Sato, T.; Gotoh, Y. Reaction of diketene with grignard reagents in the presence of cobalt catalyst. A convenient method for the synthesis of 3-methylenealkanoic acids leading to terpenoids. *Bull. Chem. Soc. Jpn.* **1982**, *55*, 3555-3559.

Giner, J. L.; Jaun, B.; Arigoni, D. Biosynthesis of isoprenoids in *Escherichia coli*: The fate of the 3-H and 4-H atoms of 1-deoxy-d-xyxyluose. *Chem. Commun.* **1998**, 1857-1858.

Ginger, M. L.; Chance, M. L.; Goad, L. J. Elucidation of carbon sources used for the biosynthesis of fatty acids and sterols in the trypanosomatid Leishmanis mexicana. *Biochem. J.* **1999**, *342*, 397-405.

Ginger, M. L.; Chance, M. L.; Sadler, I. H.; Goad, L. J. The biosynthetic incorporation of the intact leucine skeleton into sterol by the trypanosomatid Leishmania mexicana. *J. Biol. Chem.* **2001**, *276*, 11674-11682.

Ginger, M. L.; Prescott, M. C.; Reymonds, D. G.; Chance, M. L.; Goad, L. J. Utilization of leucine and acetate as carbon souces for sterol and fatty acid biosynthesis by old and new world *Leishmanis* species, *Endotrypanum monterogeii* and *Trypanosoma cruzi*. *Eur. J. Biochem.* **2000**, *267*, 2555-2566.

Gojdics, M. *The genus Euglena*; University of Wisconsin Press, Madison, 1953.

Goodman, R. A.; Oldfield, E.; Allerhand, A. Assignments in the natural-abundance carbon-13 nuclear magnetic resonance spectrum of chlorophyll a and a study of segmental motion in neat phytol. *J. Am. Chem. Soc.* **1973**, *95*, 7553-7558

Goodwin, T. W.; Griffiths, L. A. Studies in carotenogenesis. V. Carotene production by various mutants of *Phycomyces blakesleeanus* and by *Phycomyces nitens*. *Biochem. J.* **1952**, *52*, 499-501.

Goodwin, T. W.; Gross, J. A. Carotenoid distribution in bleached substrains of *Euglena gracilis*. *J. Protozool.* **1958**, *5*, 292-295.

Goodwin, T. W.; Jamikorn, M. Carotenoid synthesis in two varieties of Euglena gracilis. *J. Protozool.* **1954**, *1*, 216-219.

Granger, P.; Maudinas, B.; Herber, R.; Villoutreix, J. Proton and carbon-13 NMR spectra of cis- and trans- phytoene isomers. *J. Magn. Res.* **1973**, *10*, 43-50.

Gross, J. A.; Stroz, R. J. Evidence for phytoene in Euglena mutants. *Plant Sci. Lett.* **1974**, *3*, 67-73.

Gross, J. A.; Stroz, R. J.; Britton, G. Carotenoid hydrocarbons of *Euglena gracilis* and derived mutants. *Plant Physiol.* **1975**, *55*, 175-177.

Hamano, Y.; Dairi, T.; Yamamoto, M.; Kuzuyama, T.; Itoh, N.; Seto, H. Growth-phase dependent expression of the mevalonate pathway in a terpenoid antibiotic-producing Streptomyces strain. *Biosci. Biotechnol. Biochem.* **2002**, *66*, 808-819.

Hecht, S.; Eisenreich, W.; Adam, P.; Amslinger, S.; Kis, K.; Bacher, A.; Arigoni, D.; Rohdich, F. Studies on the nonmevalonate pathway to terpenes: the role of the GcpE (IspG) protein. *Proc. Natl. Acad. Sci. U S A* **2001**, *98*, 14837-14842.

Heelis, D. V.; Kernick, W.; Phillips, G. O.; Davies, K. Separation and identification of the carotenoid pigments of stigmata isolated from light-grown cells of *Euglena gracilis* strain *Z. Arch. Microbiol.* **1979**, *121*, 207-211.

Herz, S.; Wungsintaweekul, J.; Schuhr, C. A.; Hecht, S.; Luttgen, H.; Sagner, S.; Fellermeier, M.; Eisenreich, W.; Zenk, M. H.; Bacher, A.; Rohdich, F. Biosynthesis of terpenoids: YgbB protein converts 4-diphosphocytidyl-2-C-methyl-D-erythritol 2-phosphate to 2C-methyl-D-erythritol 2,4-cyclodiphosphate. *Proc. Natl. Acad. Sci. U S A* **2000**, *97*, 2486-2490.

Himmeldirk, K.; Kennedy, I. A.; Hill, R. E.; Sayer, B. G.; Spenser, I. D. Biosynthesis of vitamin B_1 and B_6 in Escherichia coli: consurrent incorporation of 1-deoxy-D-xylulose into thiamin (B_1) and pyridoxol (B_6). *J. Chem. Soc., Chem. Commun.* **1996**, 1187-1188.

Huertas, I. E.; Colman, B.; Espire, G. S. inorganic carbon acquisition and its energization in eustigmatophyte algae. *Funct. Plant Biol.* **2002**, *29*, 271-277.

Itoh, D.; Karunagoda, R. P.; Fushie, T.; Katoh, K.; Nabeta, K. Nonequivalent labeling of the phytyl side chain of chlorophyll *a* in callus of the hornwort *Anthoceros punctatus*. *J. Nat. Prod.* **2000**, *63*, 1090-1093.

Johnson, L. P. In *The Biology of Euglena*; Buetow, D. E., Ed.; Academic Press: New York, 1968; Vol. 1, pp. 1-25.

Jomaa, H.; Wiesner, J.; Sanderbrand, S.; Altincicek, B.; Weidemeyer, C.; Hintz, M.; Turbachova, I.; Eberl, M.; Zeidler, J.; Lichtenthaler, H. K.; Soldati, D.; Beck, E. Inhibitors of the nonmevalonate pathway of isoprenoid biosynthesis as antimalarial drugs. *Science* **1999**, *285*, 1573-1576.

Jordan, P. M.; Spencer, J. B. Stereospecific manipulation of hydrogen atoms with opposite absolute orientations during the biosynthesis of the polyketide 6-methylsalicylic acid from chiral malonates in penicillium patulum. *J. Chem. Soc., Chem. Commun.* **1990**, 238-242.

Kennedy, I. A.; Hemscheidt, T.; Britten, J. F.; Spenser, I. D. 1-Deoxy- D-xylulose. *Can. J. Chem.* **1995**, *73*, 1329-1333.

Kitaoka, S.; Nakano, Y.; Miyatake, K.; Yokota, A. In *The Biology of Euglena*; Buetow, D. E., Ed.; Academic Press: New York, 1989; Vol. 4, pp. 1-137.

Kleinig, H. The role of plastids in isoprenoid biosynthesis. *Annu. Rev. Plant Physiol. Plant Mol. Biol.* **1989**, *40*, 39-59.

Kollas, A. K.; Duin, E. C.; Eberl, M.; Altincicek, B.; Hintz, M.; Reichenberg, A.; Henschker, D.; Henne, A.; Steinbrecher, I.; Ostrovsky, D. N.; Hedderich, R.; Beck, E.; Jomaa, H.; Wiesner, J. Functional characterization of GcpE, an essential enzyme of the non- mevalonate pathway of isoprenoid biosynthesis. *FEBS Lett.* **2002**, *532*, 432-436.

Koyama, T.; Ogura, K. In *Comprehensive Natural Product Chemistry*; Cane, D. E., Ed.; Elsevier: New York, 1999; Vol. 2, pp. 69-96.

Krinsky, N. I.; Goldsmith, T. H. The carotenoids of the flagellated alga, Euglena gracilis. *Arch. Biochem. Biophys.* **1960**, *91*, 271-279.

Kuzuyama, T.; Seto, H. Diversity of the biosynthesis of the isoprene units. *Nat. Prod. Rep.* **2003**, *20*, 171-183.

Kuzuyama, T.; Shimizu, T.; Takahashi, S.; Seto, H. Fosmidomycin, a specific inhibitor of 1-deoxy-D-xylulose 5-phosphate reductoisomerase in the nonmevalonate pathway for terpenoid biosynthesis. *Tetrahedron Lett.* **1998**, *39*, 7913-7916.

Kuzuyama, T.; Takagi, M.; Kaneda, K.; Dairi, T.; Seto, H. Formation of 4-(cytidine 5'-diphospho)-2-C-methyl-D-erythritol from 2-C-methyl-D-erythritol 4-phosphate by 2-C-methyl-D-erythritol 4-phosphate cytidylyltransferase, a new enzyme in the nonmevalonate pathway. *Tetrahedron Lett.* **2000**, *41*, 703-706.

Kuzuyama, T.; Takagi, M.; Kaneda, K.; Watanabe, H.; Dairi, T.; Seto, H. Studies on the nonmevalonate pathway: conversion of 4-(cytidine 5'-diphospho)-2-C-methyl-D-erythritol to its 2-phospho derivative by 4-(cytidine 5'-diphospho)-2-C-methyl-D-erythritol kinase. *Tetrahedron Lett.* **2000**, *41*, 2925-2928.

Kuzuyama, T.; Takahashi, S.; Dairi, T.; Seto, H. Detection of the mevalonate pathway in streptomyces species using the HMG-CoA reductase gene. *J. Antibiot.* **2002**, *10*, 919-923.

Kuzuyama, T.; Takahashi, S.; Watanabe, H.; Seto, H. Direct Formation of 2-C-methyl-D-erythritol 4-phosphate from 1-deoxy-D-xylulose 5-phosphate by 1-deoxy-D-xylulose 5-phosphate reductoisomerase, a new enzyme in the non-mevalonate pathway to isopentenyl diphosphate. *Tetrahedron Lett.* **1998**, *39*, 4509-4512.

Lackey, J. B. In *The Biology of Euglena*; Buetow, D. E., Ed.; Academic Press: New York, 1968; Vol. 1, pp. 27-44.

Lange, B. M.; Rujan, T.; Martin, W.; Croteau, R. Isoprenoid biosynthesis: the evolution of two ancient and distinct pathways across genomes. *Proc. Natl. Acad. Sci. U S A* **2000**, *97*, 13172-13177.

Leedale, G. F. In *The Biology of Euglena*; Buetow, D. E., Ed.; Academic Press: New York, 1968; Vol. 3, pp. 1-27.

Li, S. M.; Henning, S.; Heide, L. Biosynthesis of the dimethylallyl moiety of novobiocin via a non-mevalonate pathway. *Tetrahedron Lett.* **1998**, *39*, 2717-2720.

Lichtenthaler, H. K. The plants' 1-deoxyD-xylulose-5-phosphate pathway for biosynthesis of isoprenoids. *Fett/Lipid* **1998**, *100*, 128-138.

Lichtenthaler, H. K.; Schwender, J.; Disch, A.; Rohmer, M. Biosynthesis of isoprenoids in higher plant chloroplasts proceeds via a mevalonate-independent pathway. *FEBS Lett.* **1997**, *400*, 271-274.

Lichtenthaler, H. K.; Zeidler, J.; Schwender, J.; Muller, C. The non-mevalonate isoprenoid biosynthesis of plants as a test system for new herbicides and drugs against pathogenic bacteria and the malaria parasite. *Z. Naturforsch. [C]* **2000**, *55*, 305-313.

Liu, Y.; Li, Z.; Vederas, J. C. Biosynthetic incorporation of advenced precursors into dehydrocurvularin, a polyketide phytotoxin from *Alternaria cinerariae*. *Tetrahedron* **1998**, *54*, 15937-15958.

Luttgen, H.; Rohdich, F.; Herz, S.; Wungsintaweekul, J.; Hecht, S.; Schuhr, C. A.; Fellermeier, M.; Sagner, S.; Zenk, M. H.; Bacher, A.; Eisenreich, W. Biosynthesis of terpenoids: YchB protein of Escherichia coli phosphorylates the 2-hydroxy group of 4-diphosphocytidyl-2C-methyl-D-erythritol. *Proc. Natl. Acad. Sci. U S A* **2000**, *97*, 1062-1067.

Mann, J. *Chemical Aspects of Biosynthesis*; Oxford University Press, 1994.

Martin, W.; Borst, P. Secondary loss of chloroplasts in trypanosomes. *Proc. Natl. Acad. Sci. U S A* **2003**, *100*, 765-767.

Matsuo, M.; Urano, S. Carbon-13 NMR spectra of tocopherols and 2,2-dimethylchromanols. *Tetrahedron* **1976**, *32*, 229-231.

Müller, C.; Schwender, J.; Disch, A.; Rohmer, M.; Lichtenthaler, F. W.; Lichtenthaler, H. K. Occurence of the 1-deoxy-D-xylulose 5-phosphate pathway of isopentenyl diphosphate biosynthesis in different algae groups. *Adv. Plant Lipid Res.* **1998**, 425-428.

Nabeta, K.; Kawae, T.; Saitoh, T.; Kikuchi, T. Syntheis of chlorophyll a and β-carotene from ^{2}H- and ^{13}C-labelled mevalonates and ^{13}C-labelled glycine in cultured cells of liverworts, *Heteroscyphus planus* and *Lophocoles heterophylla*. *J. Chem. Soc., Perkin Trans. 1* **1997**, 261-267.

Nabeta, K.; Saitoh, T.; Adachi, K.; Komuro, K. Biosynthesis of phytyl side-chain of chlorophyll a: apparent reutilization of carbon dioxide evolved during acetate assimilation in biosynthesis of chloroplastidic isoprenoid. *Chem. Commun.* **1998**, 671-672.

Nes, W. D.; Bach, T. J. Evidence for a mevalonate shunt in a tracheophyte. *Proc. R. Soc. Lond. B* **1985**, *225*, 425-444.

Nitsche, H. Heteroxanthin in *Euglena gracilis*. *Arch. Mikrobiol.* **1973**, *90*, 151-155.

Noggle, J. H.; Schirmer, R. E. *The Nuclear Overhauser Effect-Chemical Application*; Academic Press, New York, 1971.

Okuhara, M.; Kuroda, Y.; Goto, T.; Okamoto, M.; Terano, H.; Kohsaka, M.; Aoki, H.; Imanaka, H. Studies on new phosphonic acid antibiotics. III. Isolation and characterization of FR-31564, FR-32863 and FR-33289. *J. Antibiotics* **1980**, *33*, 24-28.

Olaveson, M. M.; Stokes, P. M. Responses of the acidophilic alga *Euglena mutabilis* to carbon enrichment at pH3. *J. Phycol.* **1989**, *25*, 529-539.

One-dimentional and two-dimentional NMR spectra by modern pulse techniques; Nakanishi, K., Ed.; University Science Books: Mill Valley, 1990.

Orihara, N.; Kuzuyama, T.; Takahashi, S.; Furihata, K.; Seto, H. Studies on the biosynthesis of terpenoid compounds produced by actinomycetes. 3. Biosynthesis of the isoprenoid side chain of novobiocin via the non-mevalonate pathway in Streptomyces niveus. *J. Antibiot.* **1998**, *51*, 676-678.

Packer, L. *Carotenoids*; Academic Press, San Diego, 1992.

Perrin, D. D.; Armarego, W. L. F. *Purification of Laboratory Chemicals*; 3rd ed.; Pergamon Press, New York, 1988.

Piel, J.; Donath, J.; Bandemer, K.; Boland, W. Mevalonate-independent biosynthesis of terpenoid volatiles in plants: induced and constitutive emission of volatiles. *Angew. Chem. Int. Ed.* **1998**, *37*, 2478-2481.

Porter, J. W.; Spurgeon, S. L. *Biosynthesis of Isoprenoid Compounds*; Wiley, New York, 1981.

Proteau, P. J. Biosynthesis of phytol in the cyanobacterium *Synechocystis sp.* UTEX 2470: utilization of the non-mevalonate pathway. *J. Nat. Prod.* **1998**, *61*, 841-843.

Proteau, P. J.; Woo, Y.-H.; Williamson, R. T.; Phaosiri, S. Stereochemistry of the reduction step mediated by recombinant 1-deoxy-D-xylulose 5-phosphate isomeroreductase. *Org. Lett.* **1999**, *1*, 921-923.

Putra, S. R.; Disch, A.; Bravo, J. M.; Rohmer, M. Distribution of mevalonate and glyceraldehyde 3-phosphate/pyruvate routes for isoprenoid biosynthesis in some gram-negative bacteria and mycobacteria. *FEMS. Microbiol. Lett.* **1998**, *164*, 169-175.

Reichenberg; A. Wiesner, J.; Weidemeyer, C.; Dreiseidler, E.; Sanderbrand, S.; Altincicek, B.; Beck, E.; Schlitzer, M. Diaryl ester prodrugs of FR900098 with improved in vivo antimalarial activity. *Bioorg. Med. Chem. Lett.* **2001**, *11*, 833-835.

Reuter, K.; Sanderbrand, S.; Jomaa, H.; Wiesner, J.; Steinbrecher, I.; Beck, E.; Hintz, M.; Klebe, G.; Stubbs, M. T. Crystal structure of 1-deoxy-D-xylulose-5-phosphate reductoisomerase, a crucial enzyme in the non-mevalonate pathway of isoprenoid biosynthesis. *J. Biol. Chem.* **2002**, *277*, 5378-5384.

Richard, S. B.; Ferrer, J. L.; Bowman, M. E.; Lillo, A. M.; Tetzlaff, C. N.; Cane, D. E.; Noel, J. P. Structure and mechanism of 2-C-methyl-D-erythritol 2,4-cyclodiphosphate synthase. An enzyme in the mevalonate-independent isoprenoid biosynthetic pathway. *J. Biol. Chem.* **2002**, *277*, 8667-8672.

Richards, W. R. In *Pigment-Protein Complexes in Plastids: Synthesis and Assembly*; Sundqvist, C., Ryberg, M., Eds.; Academic Press: San Diego, 1993, pp. 91-178.

Rohdich, F.; Wungsintaweekul, J.; Fellermeier, M.; Sagner, S.; Herz, S.; Kis, K.; Eisenreich, W.; Bacher, A.; Zenk, M. H. Cytidine 5'-triphosphate-dependent biosynthesis of isoprenoids: YgbP protein of Escherichia coli catalyzes the formation of 4-diphosphocytidyl-2-C-methylerythritol. *Proc. Natl. Acad. Sci. U S A* **1999**, *96*, 11758-11763.

Rohdich, F.; Zepeck, F.; Adam, P.; Hecht, S.; Kaiser, J.; Laupitz, R.; Grawert, T.; Amslinger, S.; Eisenreich, W.; Bacher, A.; Arigoni, D. The deoxyxylulose phosphate pathway of isoprenoid biosynthesis: studies on the mechanisms of the reactions catalyzed by IspG and IspH protein. *Proc. Natl. Acad. Sci. U S A* **2003**, *100*, 1586-1591.

Rohmer, M. Isoprenoid biosynthesis via the mevalonate-dependent route. *Prog. Drug Res.* **1998**, *50*, 136-154.

Rohmer, M. The discovery of a mevalonate-independent pathway for isoprenoid biosynthesis in bacteria, algae and higher plants. *Nat. Prod. Rep.* **1999**, *16*, 565-574.

Rohmer, M.; Knani, M.; Simonin, P.; Sutter, B.; Sahm, H. Isoprenoid biosynthesis in bacteria: a novel pathway for the early steps leading to isopentenyl diphosphate. *Biochem. J.* **1993**, *295*, 517-524.

Rohmer, M.; Seemann, M.; Horbach, S.; Bringer-Meyer, S.; Sahm, H. Glyceraldehyle 3-phosphate and pyruvate as precursors of isoprenic units in an alternative non-mevalonate pathway for terpenoids biosynthesis. *J. Am. Chem. Soc.* **1996**, *118*, 2564-2566.

Rohmer, M.; Sutter, B.; Sahm, H. Bacterial sterol surrogates. Biosynthesis of the side-chain of bacteriohopanetetrol and of a carbocyclic pseudopentose from ^{13}C-labelled glucose in *Zymomonas mobilis*. *J. Chem. Soc., Chem. Commun.* **1989**, *19*, 1471-1472.

Rüdiger, W.; Schoch, S. In *Chlorophylls*; Scheer, H., Ed.; CRC Press: Boca Raton, 1991, pp. 451-464.

Ruzicka, L. The isoprene rule and the biogenesis of terpenic compounds. *Experientia* **1953**, *9*, 357-367.

Sacchettini, J. C.; Poulter, C. D. Creating isoprenoid diversity. *Science* **1997**, *277*, 1788-1789.

Schuricht, U.; Henning, L.; Findeisen, M.; Welzel, P.; Arigoni, D. The biosynthesis of moenocinol, the lipid part of the moenomycin antibiotics. *Tetrahedron Lett.* **2001**, *42*, 3835-3837.

Schwarz, M. K. Ph.D. Dissertation, Eidgenössische Technische Hochschule, Zürich, 1994.

Schwender, J.; Gemünden, C.; Lichtenthaler, H. K. Chlorophyta exclusively use the 1-deoxyxylulose 5-phosphate/2-C-methylerythritol 4-phosphate pathway for the biosynthesis of isoprenoids. *Planta* **2001**, *212*, 416-423.

Schwender, J.; Seemann, M.; Lichtenthaler, H. K.; Rohmer, M. Biosynthesis of isoprenoids (carotenoids, sterol, prenyl side-chains of chlorophylls and plastoquinone) via a novel pyruvate.gylceraldehyde 3-phosphate non-mevalonate pathway in the green alga *Scenedesmus Obliquus*. *Biochem. J.* **1996**, *316*, 73-80.

Schwender, J.; Zeidler, J.; Groner, R.; Muller, C.; Focke, M.; Braun, S.; Lichtenthaler, F. W.; Lichtenthaler, H. K. Incorporation of 1-deoxy-D-xylulose into isoprene and phytol by higher plants and algae. *FEBS Lett.* **1997**, *414*, 129-134.

Seto, H.; Orihara, N.; Furihata, K. Studies on the biosynthsis of terpenoids produced by Actinomycetes. Part 4. Formation of BE-40644 by the mevelonate and nonmevalonate pathways. *Tetrahedron Lett.* **1998**, *39*, 9497-9500.

Seto, H.; Watanabe, H.; Furihata, K. Simultaneous operation of the mevalonate and non-mevalonate pathway in the biosynthesis of isopentenyl diphosphate in *Streptomyces aeriouvifer*. *Tetrahedron Lett.* **1996**, *37*, 7979-7982.

Shigi, Y. Inhibition of bacterial isoprenoid synthesis by fosmidomycin, a phosphonic acid-containing antibiotic. *J. Antimicrob. Chemother.* **1989**, *24*, 131-145.

Simpson, T. J. Application of mutinuclear NMR to structural and biosynthetic studies of polyketide microbial metabolites. *Chem. Soc. Rev.* **1987**, *16*, 123-160.

Soll, J.; Schultz, G.; Rüdiger, W.; Benz, J. Hydrogenation of Gernylgeraniol. *Plant Physiol.* **1983**, *71*, 849-854.

Sprenger, G. A.; Schörken, U.; Wiegert, T.; Grolle, S.; Graaf, A. A. D.; Taylor, S. V.; Begley, T. P.; Bringer-Meyer, S.; Sahm, H. Identification of a thiamin-dependent synthase in *Escherichia coli* required for the formation of the 1-deoxy-D-xylulose 5-phosphate precursor to isoprenoids, thiamin, and pyridoxaol. *Proc. Natl. Acad. Sci. U S A* **1997**, *94*, 12857-12862.

Stanier, R. Y.; Kunisawa, R.; Mandel, M.; Cohen-Bazire, G. Purification and properties of unicellular blue-green algae (order Chroococcales). *Bacteriol. Rev.* **1971**, *35*, 171-205.

Steele, W.; Gurin, S. Biosynthesis of β-carotene in *Euglena gracilis*. *J. Biol. Chem.* **1960**, *235*, 2778-2785.

Still, W. C.; Kahn, M.; Mitra, A. Rapid chromatographic technique for preparative separations with moderate resolution. *J. Org. Chem.* **1978**, *43*, 2923-2925.

Sum, F.-W.; Weiler, L. Stereoselective synthesis of β-substituted α,β-unsaturated esters by dialkylcuprate coupling to the enol phosphate of β-keto esters. *Can. J. Chem.* **1979**, *57*, 1431-1441.

Taber, H. In *Vitamin K Metabolism and Vitamin K Dependent Proteins*; Suttie, J. W., Ed.; University Park Press: Baltomore, 1980, pp. 177-187.

Taber, H.; Dellers, E. A.; Lombardo, L. R. Menaquinone biosynthesis in *Bacillus subtilis*. *J. Bacteriol.* **1981**, *145*, 321-327.

Takagi, M.; Kuzuyama, T.; Kaneda, K.; Watanabe, H.; Dairi, T.; Seto, H. Studies on the nonmevalonate pathway: formation of 2-C-methyl-D-erythritol 2,4-cyclodiphosphate from 2-phospho-4-(cytidine 5'-diphospho)-2-C-methyl-D-erythritol. *Tetrahedron Lett.* **2000**, *41*, 3395-3398.

Takahashi, S.; Kuzuyama, T.; Watanabe, H.; Seto, H. A 1-deoxy-D-xylulose 5-phosphate reductoisomerase catalyzing the formation of 2-C-methyl-D-erythritol 4-phosphate in an alternative nonmevalonate pathway for terpenoid biosynthesis. *Proc. Natl. Acad. Sci. U S A* **1998**, *95*, 9879-9884.

Tavormina, P. A.; Gibbs, M. H. The metabolism of β,γ-hydroxy-β-methylvaleric acid by liver homogenates. *J. Am. Chem. Soc.* **1956**, *78*, 6210.

Tavormina, P. A.; Gibbs, M. H.; Huff, J. W. The utilization of β-hydroxy-β-methyl-γ-valerolactone in cholesterol biosynthesis. *J. Am. Chem. Soc.* **1956**, *78*, 4498-4499.

Taylor, S. V., Vu, L. D., and Begley, T. P. Chemical and enzymatic synthesis of 1-deoxy-D-xylulose-5-phosphate. *J. Org. Chem.* **1998**, *63*, 2375-2377.

Therisod, M.; Fischer, J. C.; Estramareix, B. The origin of the carbon chain in the thiazole moiety of thiamine in Escherichia coli: incorporation of deuterated 1-deoxy-D-threo-2-pentulose. *Biochem. Biophys. Res. Commun.* **1981**, *98*, 374-379.

Thiel, R.; Adam, K. P. Incorporation of [1-13C]-deoxy-D-xylulose into isoprenoids of the liverwort Conocephalum conicum. *Phytochem.* **2002**, *59*, 269-274.

Threlfall, D. R.; Goodwin, T. W. Nature, intracellular distribution and formation of terpenoid quinones in *Euglena gracilis*. *Biochem. J.* **1967**, *103*, 573-588.

Tsukida, K.; Akutsu, K.; Saiki, K. Carbon-13 nuclear magnetic resonance spectra of vitamins D and related compounds. *J. Nutr. Sci. Vitaminol.* **1975**, *21*, 411-420.

Tsushima, M.; Mune, E.; Maoka, T.; Matsuno, T. Isolation of stereoisomeric epoxy carotenoids and new acetylenic carotenoid from the common freshwater goby *Rhinogobius brunneus*. *J. Nat. Prod.* **2000**, *63*, 960-964.

Van der Auwera, G.; De Wachter, R. Complete large subunit ribosomal RNA sequences from the heterokont algae *Ochromonas danica*, *Nannochloropsis salina*, and *Tribonema aequale*, and phylogenetic analysis. *J. Mol. Evol.* **1997**, *45*, 84-90.

Venkataraman, S.; Netrawall, M. S.; Sreenivasan, A. The Role of Vitamin B_{12} in the Metabolism of *Euglena gracilis* var. *bacillaris*. *Biochem. J.* **1965**, *96*, 552-556.

Wagner, W. P.; Helmig, D.; Fall, R. Isoprene biosynthesis in *Bacillus subtilis* via the methylerythritol phosphate pathway. *J. Nat. Prod.* **2000**, *63*, 37-40.

Wang, D.-Y.; Wu, Y.; Wu, Y.-L.; Li, Y.; Shan, F. Synthesis, iron(II)-induced cleavage and *in vivo* antimalarial efficacy of 10-(2-hydroxy-1-naphthyl)-deoxoqinghaosu. *J. Chem. Soc., Perkin Trans. 1* **1999**, 1827-1831.

White, R. H. Stable isotope studies on the biosynthesis of the thiazole moiety of thiamin in *Escherichia coli*. *Biochemistry* **1978**, *17*, 3833-3840.

Wiesner, J.; Henschker, D.; Hutchinson, D. B.; Beck, E.; Jomaa, H. In vitro and in vivo synergy of fosmidomycin, a novel antimalarial drug, with clindamycin. *Antimicrob. Agents Chemother.* **2002**, *46*, 2889-2894.

Winter, R. E. K.; Jian, Z. A Convenient preparation of 3-[$^2H_3$]-methyl-3-buten-1-ol. *J. Labelled Compd. Radiopharm.* **1992**, *31*, 787-791.

Wise, M. L.; Croteau, R. In *Comprehensive Natural Product Chemistry*; Elsevier: New York, 1999; Vol. 2, pp. 97-153.

Witting, L. A.; Porter, J. W. Intermediates in the conversion of melaonic acid to squalene by a rat liver enzyme system. *J. Biol. Chem.* **1959**, *234*, 2841-2846.

Wolf, D. E.; Hoffman, C. H.; Aldrich, P. E.; Skeggs, H. R.; Wright, L. D.; Folkers, K. Determination of structure of β,γ-dihydroxy-β-methylvaleric acid. *J. Am. Chem. Soc.* **1957**, *79*, 1486-1487.

Wolff, M.; Seemann, M.; Grosdemange-Billiard, C.; Trirsch, D.; Campos, N.; Rodriguez-Concepcion, M.; Boronat, A.; Rohmer, M. Isoprenoid biosynthesis via the methylerythritol phosphate pathway. (E)-4-hydroxy-3-methylbut-2-enyl diphosphate: chemical synthesis and formation from methylerythritol cyclodiphosphate by a cell-free system from Escherichia coli. *Tetrahedron Lett.* **2002**, *43*, 2555-2559.

Wolff, M.; Seemann, M.; Tse Sum Bui, B.; Frapart, Y.; Tritsch, D.; Estrabot, A. G.; Rodriguez-Concepcion, M.; Boronat, A.; Marquet, A.; Rohmer, M. Isoprenoid biosynthesis via the methylerythritol phosphate pathway: the (E)-4-hydroxy-3-methylbut-2-enyl diphosphate reductase (LytB/IspH) from *Escherichia coli* is a [4Fe-4S] protein. *FEBS Lett.* **2003**, *541*, 115-120.

Wolken, J. J. *Euglena; an experimental organism for biochemical and biophysical studies*; 2nd ed.; Appleton-Century-Crofts, New York, 1967.

Wolpert, J. S.; Ernst-Fonberg, M. L. A Mulitenzyme Complex for CO_2 Fixation. *Biochemistry* **1975**, *14*, 1095-1102.

Wolpert, J. S.; Ernst-Fonberg, M. L. Dissociation and Characterization of Enzyme from a Mulitenzyme Complex involved in CO_2 Fixation. *Biochemistry* **1975**, *14*, 1103-1107.

Yajima, S.; Nonaka, T.; Kuzuyama, T.; Seto, H. Crystal structure of 1-deoxy-D-xylulose 5-phosphate reductoisomerase complexed with cofactors: Implications of a flexible loop movement upon substrate binding. *J. Biochem.* **2002**, *131*, 313-317.

Zeidler, J. G.; Lichtenthaler, H. K.; May, H. U.; Lichtenthaler, F. W. Is isoprene emitted by plants synthesized via the novel isopentenyl pyrophosphate pathway? *Z. Naturforsch,* **1997**, *52C*, 15-23.

Zhou, D.; White, R. H. Early steps of isoprenoid biosynthesis in *Escherichia coli*. *Biochem. J.* **1991**, *273*, 627-634.

Zielinski, J.; Kokke, W. C.; Fenical, W.; Djerassi, C. Sterols of the cultured euglenid *Eutreptia viridis*: a novel delta 23-unsaturated sterol. *Steroids* **1982**, *40*, 403-411.

APPENDICES

Appendix A

Investigation of the MEP pathway in *Bacillus subtilis*

Menaquinones (MKs) are lipophilic components found in the cytoplasmic membrane of bacteria.[1,2] They play an important role in bacterial respiration, undergoing reversible oxidation and reduction reactions to interconvert between quinone and hydroquinone. The redox reaction of menaquinones in the respiratory chain is associated with the electron transport process for the formation of ATP and involves the biosynthesis of heme and uracil. The structure of MKs is characterized as the isoprenoid sidechain joined with 2-methyl-1,4-naphthoquinone. By the length of the isoprenoid side chain, various MKs are given their nomenclature as MK-0 to MK-9.

In order to elucidate the biosynthetic pathway of the prenyl sidechain of MKs, *Bacillus subtilis,* a representative species of the *Bacillus* genus, was examined. Unlike other bacteria having several MKs, *B. subtilis* is reported to possess only MK-7 as a redox component of the electron transfer.[3] To differentiate the 2-C-methyl-D-erythritol-4-phosphate pathway (MEP pathway) from the mevalonate pathway (MVA pathway), [6-$^2H_2$]-D-glucose and [1-$^2H_3$]-deoxy-D-xylulose incubation experiments were performed with *B. subtilis*.

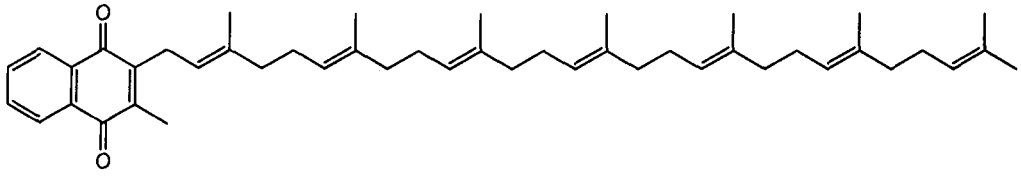

Menaquinone-7

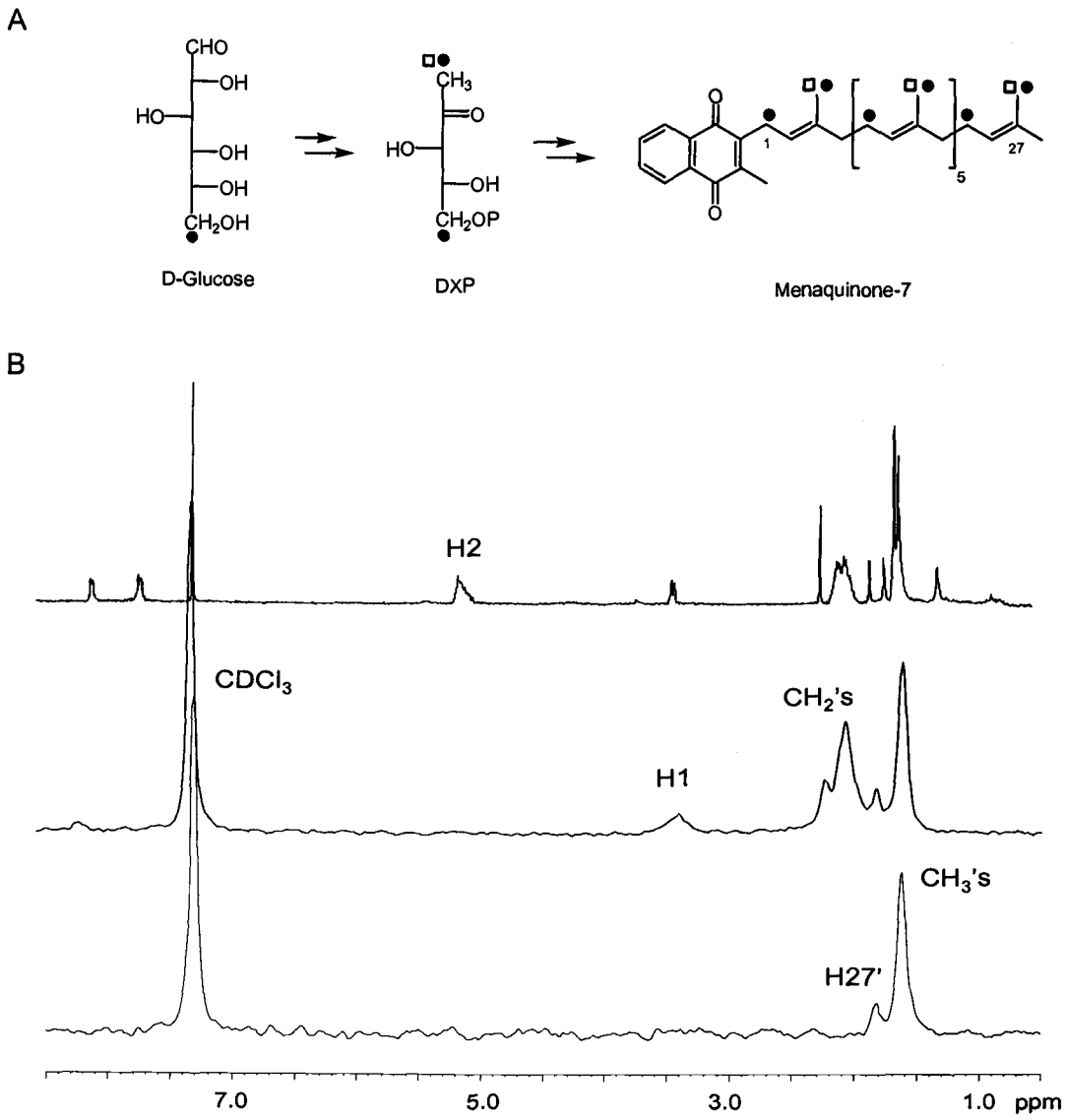

Fig.A.1. Labeling patterns for MK-7 derived from [6-$^2H_2$]-D-glucose (•) and [1-$^2H_3$]-deoxy-D-xylulose (□) incubation experiments (A) and MK-7 spectra (B); upper - ^{1}H-NMR spectrum, middle - ^{2}H-NMR spectrum from [6-$^2H_2$]-D-glucose (•), below - ^{2}H-NMR spectrum from [1-$^2H_3$]-deoxy-D-xylulose (□)).

When [6-$^2H_2$]-D-glucose is used for the formation of the MK-7 sidechain, the key positions for discriminating the MEP pathway from the MVA pathway are H1 of the isoprene unit labeled from the MEP pathway and H2 and H4 of the isoprene unit from the MVA pathway. In contrast, the H5 position of the isoprene unit labeled through both pathways is not diagnostic for either one or the other pathway. On the

basis of the ^{1}H-NMR assignment of MK-7, the peaks at 3.4 ppm for H1 and at ~ 2.1 ppm for the allylic methylenes of MK-7 correspond to H1 of the isoprene unit, and the peaks for vinyl protons derived from H2 of the isoprene unit show at 5.1 ppm. The peaks at ~ 2.1 ppm also represent the H4 position of the isoprene units, so this peak is not diagnostic for either pathway. Therefore, the existence of the peaks at 3.4 ppm or 5.1 ppm in the ^{2}H-NMR spectrum of MK-7 could allow us to distinguish the MEP pathway from the MVA pathway (Fig.A.1).

The ^{2}H-NMR spectrum of MK-7 obtained from the incubation experiment using [6-$^{2}H_{2}$]-D-glucose revealed the peaks at 1.5, 1.8, 2.0, 2.2 and 3.3 ppm. The peaks at 1.5 and 1.8 ppm represent deuteriums of the branching methyls which are incorporated via both pathways. The peak at 2.1 ppm indicates deuteriums of the methylene groups which are not appropriate positions to discriminate the two pathways due to misinterpretation between H1 and H4 via the MEP pathway and the MVA pathway, respectively. Instead, the appearance of the peak at 3.4 ppm is very convincing that MK-7 is produced through the MEP pathway. In addition, the peak at 5.1 ppm corresponding to H2 labeled via the MVA pathway was not observed in the ^{2}H-NMR spectrum. The absence of a deuterium signal at 5.1 ppm along with the existence of the peak at 3.4 ppm suggests that *B. subtilis* synthesizes MK-7 via the MEP pathway (Fig.A.1).

To confirm this result, the incubation experiment using [1-$^{2}H_{3}$]-DX was carried out to see if the intact [1-$^{2}H_{3}$]-DX, a precursor of the MEP pathway, is incorporated into MK-7. If [1-$^{2}H_{3}$]-DX is utilized through the MEP pathway, deuterium peaks should appear at only 1.5 and 1.8 ppm for the branching methyl groups. In contrast, if a catabolized form from [1-$^{2}H_{3}$]-DX is incorporated into MK-7, the ^{2}H-NMR spectrum should appear more complicated.

In the ^{2}H-NMR spectrum of MK-7 from the [1-$^{2}H_{3}$]-DX incubation experiment, only two peaks were seen at 1.8 and 1.6 ppm corresponding to H27' and the other branching methyls, respectively (Fig.A.1). These data clearly demonstrated the use of the MEP pathway in *B. subtilis*. These results were obtained shortly before the genome sequence for *B. subtilis* was published. The genome of *B. subtilis* unquestionably shows only MEP pathway genes, as would be expected from our results. An additional report has described the synthesis of isoprene in *B. subtilis* via the MEP pathway.[4]

Experimental

Instruments

All ^{1}H and ^{13}C nuclear magnetic resonance (NMR) spectra were recorded on a Bruker AC 300 spectrometer operating at 300 MHz for ^{1}H and 75 for ^{13}C, and on a Bruker AM 400 spectrometer operating at 400.13 MHz for ^{1}H, 100.13 MHz for ^{13}C, and 61.42 MHz for ^{2}H. Chemical shifts of NMR spectra are shown as δ, and references are based on deuterated NMR solvents as an internal standard ($CHCl_3$ at 7.26 ppm for ^{1}H-NMR and $^{13}CDCl_3$ at 77.0 ppm for the center line of the triplet in ^{13}C-NMR). Levels of incorporation from ^{2}H NMR spectra were calculated on the basis of the integration of the target peak relative to the natural abundance of the deuterium signal of $CHCl_3$ (0.5 ml, 0.016 %). Low and high-resolution chemical ionization mass spectra (CIMS) and fast atom bombardment mass spectra (FABMS) were recorded on a Kratos MS50TC spectrometer. Strains were grown in an orbital shaker (Forma Scientific) for mass cultivation. Harvesting of *Bacillus* cells was done with a Beckman J2-HS centrifuge and lyophilization of the cells utilized a Labconco freeze dry system.

Biosynthetic experiments

B. subtilis (ATCC #6051) was cultivated on a liquid mineral medium containing D-glucose (1 g/L), K_2HPO_4 (14 g/L), KH_2PO_4 (6 g/L), $MgSO_4$ (0.2 g/L), $(NH_4)_2SO_4$ (2 g/L) and trace elements diluted as 10^{-3} including $ZnSO_4 \cdot 7H_2O$ (1 g), $FeCl_3 \cdot 6H_2O$ (1 g), $CuSO_4 \cdot 5H_2O$ (0.1 g), $MnCl_2 \cdot 4H_2O$ (0.1 g), $(NH_4)_6Mo_7O_{24} \cdot 4H_2O$ (50 mg), $Na_2B_4O_7 \cdot 10H_2O$ (75 mg), $CaCl_2$ (1 g) and $CoCl_2 \cdot 6H_2O$ (25 mg).[5] For incubation experiments with labeled compounds, each labeled compounds ([6-$^{2}H_2$]-D-glucose (0.1 g/L) and [1-$^{2}H_3$]-DX (0.3 g/L)) was mixed with unlabeled D-glucose (1 g/L). The seed cultures of *B. subtilis* (3 mL) grown overnight were used for 750 mL of culture medium, and then cultivated at 30 °C with shaking at 290 rpm for 18-22 h.

Inorganic salts for the culture media were purchased from Mallinckrodt, and D-glucose was from Sigma-Aldrich. [6-$^{2}H_2$]-D-glucose (0.1 g/L) was purchased from Cambridge Isotope Laboratories and [1-$^{2}H_3$]-DX was prepared by Dr. Younhi Woo. Water was deionized using a Milli Q Millipore system for all experiments. Silica gel (Merck, grade 60, 220-400 mesh) was used for flash column chromatography.[6]

Merck glass-backed TLC plates (silica gel 60 F254) were employed for thin layer chromatography (TLC) and preparative TLC (prep-TLC).

Isolation of menaquinone-7

After cultivation, bacteria cells were harvested by centrifugation at 8500 rpm (JA-14 rotor, 11100 *g*) for 10 min and lyophilized. The lyophilized cells (1.27 g / 9 L) were extracted with a mixture of chloroform and methanol (2:1, v/v). This extract was evaporated to dryness, dissolved in hexanes, and applied to a silica gel column chromatography. The column was washed with hexane to remove contaminant lipid, and MK-7 was eluted with 3 % ether in hexanes. After solvent was evaporated, the eluent was dissolved with hexanes and applied on a silica gel prep-TLC plate with chloroform/hexane (2:1 v/v) to separate MK-7 (R_F 0.5). The MK-7 band was scraped from TLC plates and extracted with ethyl acetate (1.2 mg). Purified MK-7 was analyzed by mass spectrometry and NMR spectroscopy.

References

(1) Taber, H. In *Vitamin K Metabolism and Vitamin K Dependent Proteins*; Suttie, J. W., Ed.; University Park Press: Baltomore, 1980, pp. 177-187.

(2) Bently, R.; Meganathan, R. Biosynthesis of vitamin K (menaquinone) in Bacteria. *Microbiol. Rev.* **1982**, *46*, 241-280.

(3) Taber, H.; Dellers, E. A.; Lombardo, L. R. Menaquinone biosynthesis in *Bacillus subtilis*. *J. Bacteriol.* **1981**, *145*, 321-327.

(4) Wagner, W. P.; Helmig, D.; Fall, R. Isoprene biosynthesis in *Bacillus subtilis* via the methylerythritol phosphate pathway. *J. Nat. Prod.* **2000**, *63*, 37-40.

(5) Champney, W.; Jensen, R. Molecular events in the growth inhibition of *Bacillus subtilis* by D-tyrosine. *J. Bacteriol.* **1970**, *104*, 351-359.

(6) Still, W. C.; Kahn, M.; Mitra, A. Rapid chromatographic technique for preparative separations with moderate resolution. *J. Org. Chem.* **1978**, *43*, 2923-2925.

Appendix B

Investigation of the MEP pathway in an Uncharacterized *Eustigmatophyte*

The eustigmatophyte, small unicellular coccoid algae, belongs to the division *Ochrophyta* which is a golden-brown algae group found in both freshwater and in marine environments. The eustigmatophyte is a primarily freshwater plastidic organism and is structurally characterized by a very short flagellum and a large eyespot.[1,2] Although the eustigmatophyte examined in our study was not completely identified, investigation of the MEP pathway was expected to provide preliminary ideas about isoprenoid biosynthesis in ochrophyta species.

In order to determine which isoprenoid pathway is involved in the formation of isoprenoids in this alga, the labeling pattern for phytol was observed from the [6-$^2H_2$]-D-glucose incubation experiment. The deuterium enhancement was clearly present at 4.2 ppm for H1 labeled through the MEP pathway, whereas H2, a representative position derived from the MVA pathway, was not labeled with deuteriums of [6-$^2H_2$]-D-glucose. The ^{2}H-NMR spectrum of phytol, however, indicated a lower enhancement at the positions corresponding to the branching methyls, in contrast with the expected similar levels of labeling for C1 and C5 positions in the isoprene unit. The incorporation ratio between H1 and the other methylene groups, however, was around 1 : 3.3 compatible with the 1 : 3 theoretical ratio. These results may be explained by different pool sizes of glyceradehyde-3-phosphate (GAP) and pyruvate. The [6-$^2H_2$]-D-glucose can be cleaved by aldolase after conversion to fructose-1,6-bisphosphate to labeled GAP and unlabeled dihydroxyacetone-phosphate through the Entner-Doudoroff pathway.[3] Although the labeled GAP can be converted to labeled pyruvate, this conversion takes several steps, with the potential for dilution of label at each step. Further investigation would be required to provide the true explanation for this finding.

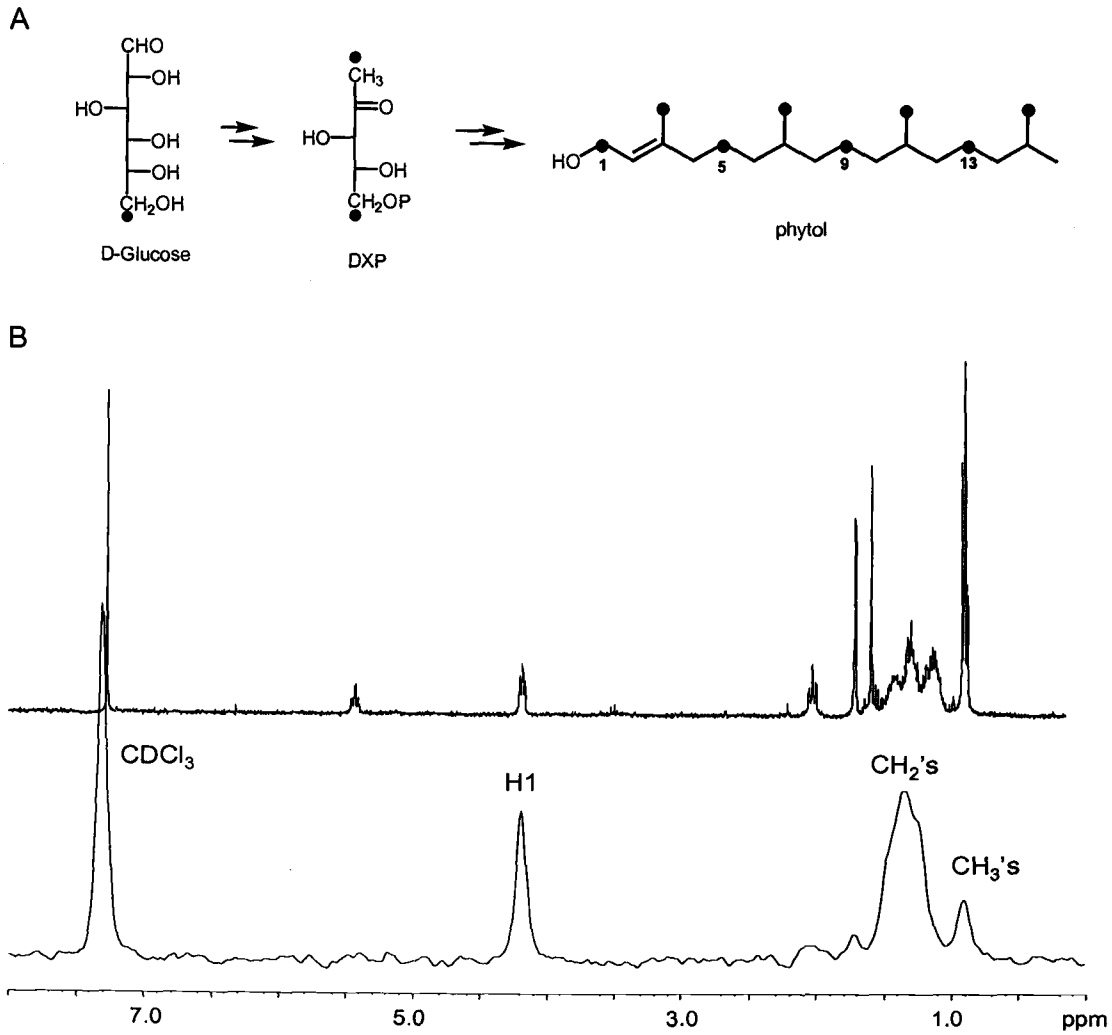

Fig.B.1. Labeling pattern (A) and spectrum (B) for phytol from the [6-$^2H_2$]-D-glucose incubation experiment.

Experimental

Instruments

All ^{1}H and ^{13}C nuclear magnetic resonance (NMR) spectra were recorded on a Bruker AC 300 spectrometer operating at 300 MHz for ^{1}H and 75 for ^{13}C, and on a Bruker AM 400 spectrometer operating at 400.13 MHz for ^{1}H and 100.13 MHz for ^{13}C. Chemical shifts of NMR spectra are shown as δ, and references are based on deuterated NMR solvents as an internal standard ($CHCl_3$ at 7.26 ppm for ^{1}H-NMR and $^{13}CDCl_3$ at 77.0 ppm for the center line of the triplet in ^{13}C-NMR). Low and high-resolution chemical ionization mass spectra (CIMS) and fast atom bombardment mass spectra (FABMS) were recorded on a Kratos MS50TC spectrometer. The cultures were grown in a Hoffman illuminated incubator for mass cultivation. Harvesting of Eustigmatophyte cells was done with a Beckman J2-HS centrifuge and lyophilization of the cells utilized a Labconco freeze dry system.

Biosynthetic experiments

An axenic culture of the uncharacterized eustigmatophyte (Dr. Eric Henry at Oregon State University , College of Science, provided our laboratory with an axenic culture of an alga characterized only as a *Eustigmatophyte*) is maintained in the Proteau laboratory at the Oregon State University, College of Pharmacy. For maintenance and mass cultivation, the eustigmatophyte was cultivated in modified BG-11 medium[4] containing D-glucose (1.0 g/L), $NaNO_3$ (1.5 g/L), KH_2PO_4 (0.4 g/L), $MgSO_4 \cdot 7H_2O$ (0.075 g/L), $CaCl_2 \cdot 2H_2O$ (0.036 g/L), Na_2CO_3 (0.02 g/L), citric acid$\cdot 2H_2O$ (0.006 g/L), EDTA·disodium salt (0.001 g/L), ferric ammonium citrate (6 mg/L), thiamine·HCl (10 μg/L), vitamin B_{12} (0.5 μg /L) and trace metals. Trace metals were prepared with H_3BO_3 (2.86 mg/L), $MnCl_2 \cdot 4H_2O$ (1.81 mg/L), $Na_2MoO_4 \cdot 2H_2O$ (0.39 mg/L), $ZnSO_4 \cdot 7H_2O$ (0.22mg/L), $CuSO_4 \cdot 5H_2O$ (0.08 mg/L), and $CoCl_2 \cdot 6H_2O$ (0.05 mg/L). Seed cultures were inoculated into medium (125 mL) and were grown at 30 °C for 7-14 days under constant illumination with 40 W cool-white fluorescent lights (200-210 ftc). For mass cultivation, the seed culture was inoculated into medium (5 L), aerated and grown for 8 days under the same condition as the seed culture. For the incubation experiment, [6-$^{2}H_2$]-D-glucose (0.1 g/L) was mixed with unlabeled D-glucose (1 g/L). Inorganic salts for the culture media were purchased from

Mallinckrodt, and D-glucose, vitamin B_{12}, and thiamine·HCl were from Sigma-Aldrich. [6-$^2H_2$]-D-glucose was purchased from Cambridge Isotope Laboratories. Phytol standard was purchased from Sigma-Aldrich. Water was deionized using a Milli Q Millipore system for all experiments. Silica gel (Merck, grade 60, 220-400 mesh) was used for flash column chromatography.[5] Merck glass-backed TLC plates (silica gel 60 F254) were employed for thin layer chromatography (TLC).

Isolation of phytol

After cultivation, cells were harvested by centrifugation at 7000 rpm (JA-10 rotor, 8671 *g*) for 5 min and lyophilized to obtain 0.6 g of dry weight per liter. The lyophilized cells were extracted three times (30 min each) with a mixture of $CHCl_3$ and MeOH (2:1) at room temperature to provide a crude extract, which was applied to a silica gel flash chromatography column. The column was developed with mixtures of 15-50 % EtOAc in hexanes to separate several fractions which were determined by color of pigments. The chlorophyll-containing fraction (R_f = 0.5-0.6, silica TLC plate, 10 % EtOAc in hexanes) was collected and the organic solvent was evaporated. The chlorophyll-containing fraction was hydrolyzed in 10 % (w/v) KOH in MeOH overnight, and extracted with ether. The ethereal extract was washed with a saturated NH_4Cl solution and *dd*-H_2O, dried, and concentrated. The extract was applied to a flash chromatography column (silica gel, 15% EtOAc in hexanes) to separate phytol. The isolated phytol was decolorized by passing the phytol solution over a short column of charcoal and washing with acetone to provide 2 mg of pure phytol. Purified phytol was analyzed by mass spectrometry and NMR spectroscopy.

References

(1) Van der Auwera, G.; De Wachter, R. Complete large subunit ribosomal RNA sequences from the heterokont algae *Ochromonas danica*, *Nannochloropsis salina*, and *Tribonema aequale*, and phylogenetic analysis. *J. Mol. Evol.* **1997**, *45*, 84-90.

(2) Huertas, I. E.; Colman, B.; Espire, G. S. inorganic carbon acquisition and its energization in eustigmatophyte algae. *Funct. Plant Biol.* **2002**, *29*, 271-277.

(3) Canback, B.; Andersson, S. G. E.; Kurland, C. G. The global phylogeny of glycolytic enzymes. *Proc. Natl. Acad. Sci. U S A* **2002**, *99*, 6097-6102.

(4) Stanier, R. Y.; Kunisawa, R.; Mandel, M.; Cohen-Bazire, G. Purification and properties of unicellular blue-green algae (order Chroococcales). *Bacteriol. Rev.* **1971**, *35*, 171-205.

(5) Still, W. C.; Kahn, M.; Mitra, A. Rapid chromatographic technique for preparative separations with moderate resolution. *J. Org. Chem.* **1978**, *43*, 2923-2925.